Ph.D Thesis

Techno-Economic Assessment of CO_2 Transport for Carbon Capture and Storage

Advisor: Professor Chonghun Han

BY

Umer Zahid

August 2015

SCHOOL OF CHEMICAL AND BIOLOGICAL ENGINEERING

COLLEGE OF ENGINEERING
SEOUL NATIONAL UNIVERSITY

Techno-economic Assessment of CO_2 Transport for Carbon Capture and Storage

이산화탄소 포집 및 저장 기술을 위한 이산화탄소 수송 및 터미널의 기술-경제적 평가

지도교수 한 종 훈

이 논문을 공학박사학위논문으로 제출함

2015년 7월

서울대학교 대학원

화학생물공학부

Umer Zahid

Umer Zahid의 박사학위논문을 인준함

2015년 7월

위 원 장 金和鉉 (인)

부 위 원 장 韓宗勳 (인)

위 원 尹宣燮 (인)

위 원 李宗珉 (인)

위 원 金勇憲 (인)

Techno-Economic Assessment of CO_2 Transport for Carbon Capture and Storage

Advisor: Professor Chonghun Han

Ph.D Thesis Dissertation by:

Umer Zahid

August 2015

School of Chemical and Biological Engineering
Seoul National University

Submitted to Seoul National University in partial fulfillment of the requirements for the degree of Doctor of Philosophy in

Chemical and Biological Engineering

Approved by:

Chairman:	Prof. Dr. Kim, Hwayong
Vice Chairman:	Prof. Dr. Han, Chonghun
Member:	Prof. Dr. Yoon, En Sup
Member:	Prof. Dr. Lee, Jongmin
Member:	Dr. Kim, Yong Heon

Abstract

Techno-Economic Assessment of CO_2 Transport for Carbon Capture and Storage

Umer Zahid

School of Chemical & Biological Engineering,

Seoul National University.

The continuous rise of CO_2 emissions is a major cause of global climate change. Carbon capture and storage (CCS) is widely seen as a practical technology for reducing CO_2 emissions. CCS is essential if global temperature increase should be limited below two degrees Celsius. CCS mainly consists of capturing CO_2 from large emitting sources and its transportation to a sequestration site where it can be stored safely for a long period of time. Transport links the capture and storage part, so it is a critical component that should not be overlooked.

This research is motivated by the fact that when CCS is to be deployed in full scale, very large quantities of CO_2 will have to be transported from the source to the storage sites. Therefore, this study is focused to investigate the various CO_2 transportation options, technically and economically. Large-scale deployment of CCS will require the development of new infrastructure to transport the captured CO_2 from various sources to the appropriate CO_2 storage sites. Land based transport of CO_2 can be done using pipelines, tanker trucks and/or trains. However, this study is limited to the pipeline and ship

transportation of CO_2 at different thermodynamic conditions. The work is divided in four parts, namely dehydration, CO_2 pipeline transport, CO_2 liquefaction for ship transport and CO_2 terminal design.

a. Dehydration

It is necessary to remove water from the captured CO_2 stream prior to the transportation. Low moisture content is critical in prevention of both corrosion and hydrate formation. The selected dehydration process must be reliable while minimizing the operational issues and ensuring process safety. In this study, traditional glycol process has been simulated to analyze the factors that affect the water removal from the captured CO_2 stream. Using the standard glycol process can easily achieve moisture content of approximately 50 ppmv in the dehydrated CO_2 stream.

b. Pipeline Transport

Currently pipelines are the most economical way of transporting large quantities of CO_2 in the supercritical phase. However, there is a need to compare CO_2 transportation at different thermodynamic operating conditions. A plausible workflow model has been developed that can calculate operational parameters for the CO_2 transportation based on the input variables. This model is useful for performing an economic analysis to check the feasibility of a project. The model is applied to South Korean case to transport captured CO_2 from the power plants to an offshore storage site. Three different sets of temperature-pressure inlet conditions are studied for the CO_2 pipeline transport.

- Temperature = -20 °C; Pressure = 6.50 MPa; Liquid phase
- Temperature = 5 °C; Pressure = 9.30 MPa; Liquid phase
- Temperature = 40 °C; Pressure = 15.00 MPa; Supercritical phase

The transport cost for Korean case varies from 10.9 to 15.5 US$/t$CO_2$ depending on the specific scenario.

c. CO_2 Liquefaction for Ship Transport

Liquefaction is a vital component in ship transportation. A state-of-the-art CO_2 liquefaction processes have been designed by taking CO_2 capture facilities into account. The proposed processes require lower liquefaction energy compared to other processes found in the literature. Different scenarios have been studied in order to explore the effect of thermodynamic conditions on the economics of CO_2 transport. The considered scenarios are categorized on the basis of liquefaction plant location as: (i) the capture site, liquefaction plant and shipping terminal are located close to each other; (ii) the capture site and liquefaction plant are far from shipping terminal; (iii) the capture site is far from liquefaction plant and shipping terminal. The liquefaction energy of 97.3 and 71.89 per kWh tonne of CO_2 is required for post-combustion and pre-combustion facilities, respectively. The basic liquefaction and intermediate storage cost for a post-combustion source varies between 7.00 $ and 7.30 $ per tonne of CO_2 and, a basic cost of 5.28 $ to 5.55 $ per tonne of CO_2 is incurred for a pre-combustion source facility.

d. CO_2 Terminal Design

CO_2 terminal acts as a connecting link between CO_2 liquefaction and the shipping section. Due to the discrete nature of the process, there are number of operational modes which cannot be analyzed using steady-state simulation. Hence, the study is performed using the dynamic simulation for different operational modes of CO_2 terminal. Four scenarios have been developed to define the operational strategy of the terminal: loading case, holding case, unloading case, and emergency shutdown. The results show that boil-off gas (BOG) generation within the CO_2 terminal depends on storage tank size,

operating pressure, ambient conditions, insulation thickness, and the filling level of the vessel.

Keywords: Carbon capture and storage, CO_2 transport, economic analysis, CO_2 liquefaction, CO_2 terminal.

Student ID: 2012-31296

Contents

List of Figures

List of Tables

CHAPTER 1: Introduction

1.1. Research motivation

Global warming is a universal issue due to the continuous rise of greenhouse gases concentration in the atmosphere. Significant efforts are being made to promote renewable energy technologies and improve efficiencies. However, a recent report by the Intergovernmental Panel on Climate Change (IPCC) shows that global emissions of greenhouse gases grew more quickly between 2000 and 2010 than in each of the three previous decades despite a growing number of policies to reduce climate change [1]. Fossil fuels are expected to remain the main source for power generation in the near future. Carbon capture and storage (CCS) is thought to be a key technology which can enable the power sector to keep using fossil fuel resources while minimizing their effect on climate change. It has been estimated that, without CCS in the technology mix, the cost of climate stabilization would increase by 70 % [2]. CCS mainly consists of capturing CO_2 from large emitting sources and its transportation to a sequestration site where it can be stored safely for a long period of time. The transport of captured CO_2 from source site to storage location is a critical component that should not be overlooked. CO_2 can be transported by pipelines, ships, tanker trucks, and trains; depending on region, economics, regulation, location, and type of storage site. Figure 1-1 shows different possible ways to transport CO_2 from the source site to the storage site. Land-based transport of CO_2 can be done using pipelines, tanker trucks and/or trains; while CO_2 transportation to off-shore sites can be done using ships or pipelines.

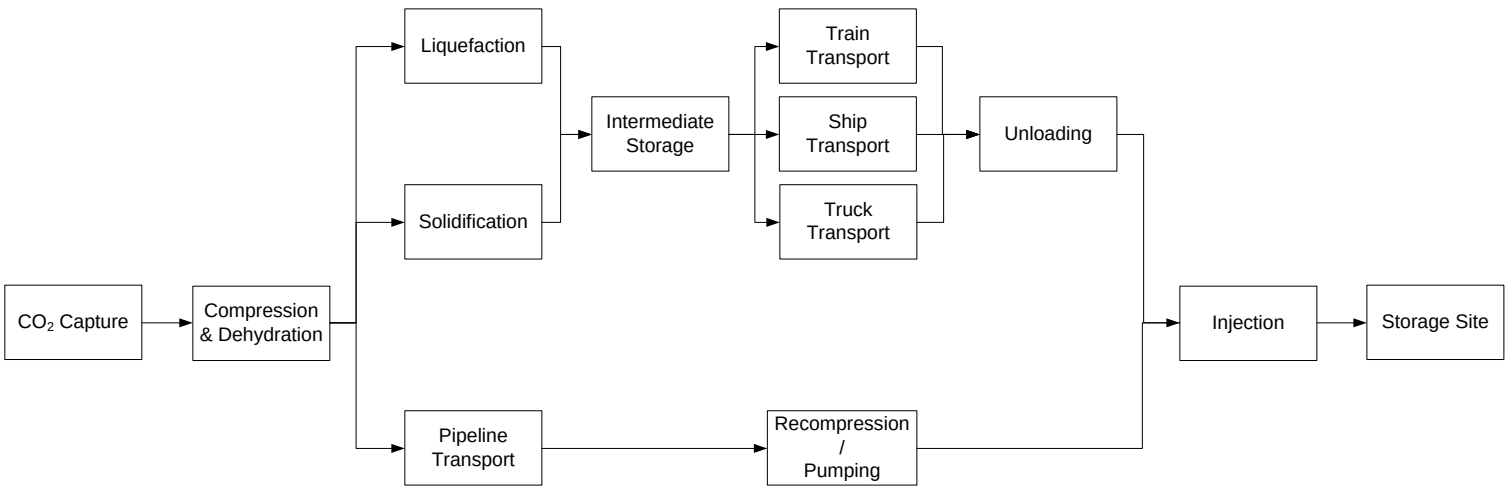

Figure 1-1: CO_2 transport value chain

Among the several approaches to transport CO_2, pipeline transportation is the most economical approach to transport large amounts of CO_2 over long distances. Currently, pipeline networks of about 3100 km are present worldwide, mainly in the US to transport over 50 million tons of CO_2 per year for enhanced oil recovery (EOR) projects [3]. However, no such infrastructure exists in other parts of the world and shall the CCS technology move further towards commercialization, the pipeline network will be required to transport CO_2 from the power plants to the storage sites. Many researchers have done a vast range of studies to address various technical issues related to pipeline transportation. Skovholt [4] presented rules of thumb for the sizing of CO_2 pipelines and also estimated the capital cost of pipeline transport. International Energy Agency Greenhouse Gas (IEAGHG) presented several correlations for the cost of CO_2 pipelines in Europe based on detailed case study designs [5]. More recently, an engineering-economic CO_2 pipeline model was developed at the Massachusetts Institute of Technology (MIT) [6]. Results from these and other similar studies were summarized in a recent Intergovernmental Panel on Climate Change (IPCC) report [7]. All of these studies were focusing on the transport in supercritical condition and none of these studies considered the various transport operational ranges, the realities of available pipeline diameters and costs, or the regional differences affecting design and costs.

Ships can be used for long distance transport of CO_2. Ship transportation becomes important as it offers flexible routes between sources and sink sites. Also, many sources are located along the coasts and storage sites are often off shore. Ships represent a certain residual value, which means that in the event of CCS project failure or cancellation, capital (CAPEX) invested will not be wasted all together and the ship can be employed in alternative trades. Recently many studies have focused on various aspects of CO_2 ship transportation. Yoo *et al*. [8] studied different scenarios for large-scale CO_2

shipping and presented newly developed CO_2 carrier with a capacity of 100,000 m^3 that is currently under research at Daewoo Shipbuilding Ltd. The ship transportation conditions of CO_2 represent a trade-off between temperature and pressure. The lower the design pressure, the thinner the vessel will be, therefore the lower material consumption and costs for transportation. If the pressure is lower, the temperature also has to be lower for CO_2 to be in a state with adequate density for reasonable transport capacities. But the lower the temperature, the more energy for cooling is required [9]. Decarre et al. [10] studied the liquefaction and transport of CO_2 at thermodynamic conditions of (–50 ℃, 7 bar) and (-30 ℃, 15 bar). Currently, small size ships up to 1,500 m^3 are being used for CO_2 transport at (-27 ℃, 16 bar). However, these small ships are not suitable for large-scale ship-based transport of CO_2. Aspelund and Jordal [11] insisted that lower pressure is required for enlarged storage and ship tanks for economical transport of CO_2. Chiyoda Corporation [12] published a report estimating total CO_2 shipping costs for a transportation distance of up to 200 km and a capacity of 1 Mt CO_2 per year. This study also proposed the concept of shuttle ships which are equipped with injection facilities; hence there is no need for injection platform at the injection site. Zero Emission Platform [13] published a report on CO_2 transport, which included six scenarios, out of which costs for CO_2 shipping were calculated for two scenarios. Seo et al. [14] performed an economic analysis for ship transportation of CO_2 based on life-cycle costs and found operational cost (OPEX) of liquefaction unit to be the main cost contributor. Roussanaly et al. [15] compared onshore pipeline and CO_2 shipping between two onshore harbors. Their results showed that for a given CO_2 transport quantity, onshore pipeline should be used for short distances, while shipping between harbors is better for longer distances.

Tanker trucks are mainly used for bulk transportation of CO_2 for retail purposes. Such motor carriers store liquid CO_2 in cryogenic vessels and conditions of liquid CO_2 is typically at 17 bar and –30 ℃ [3]. However, CO_2 transport using tanker trucks is deemed too expensive for CO_2 geological storage purpose.

1.2. Research objectives

Large-scale deployment of CCS will require the development of new infrastructure to transport the captured CO_2 from various sources to the appropriate CO_2 storage sites. Hence, the purpose of this study is to explore various CO_2 transportation methods technically and economically. The specific objectives of this research include:

- Assess the performance of an absorption process for the dehydration of wet CO_2 stream that can satisfy the water content for CO_2 transportation.
- To develop a work-flow model that can calculate operational parameters for the pipeline transport based on the input variables.
- To develop the liquefaction design while taking into account the type of capture facilities (i.e. post-combustion and pre-combustion).
- To decide the optimum location of liquefaction plant based on economic analysis.
- To develop the design of CO_2 terminal and explore its operational issues.

1.3. Organization of the thesis

The thesis mainly consists of following research areas namely, dehydration, CO_2 pipeline transport, ship transportation of CO_2 and CO_2 terminal. Chapter 1 presents the motivation and objective of the research as introduction. Brief

introduction is presented in this chapter about different methods for the transportation of CO_2. Chapter 2 is dedicated to the dehydration of captured CO_2 stream. Physical absorption method (TEG absorption) has been simulated to reduce the water content in the CO_2 stream. A comprehensive system for CO_2 pipeline transport is presented in chapter 3 that can be used over a wide range of operating conditions. This model is then applied to the Korean case for developing an off-shore pipeline model to study the economic feasibility of CO_2 transport in Korea. Chapter 4 is mainly dedicated to CO_2 liquefaction technology which is the most energy intensive section for the CO_2 shipping. Liquefaction processes have been designed by taking account of CO_2 capture facility type (post-combustion and pre-combustion). The proposed processes require lower liquefaction energy compared to other processes found in the literature. Suitable thermodynamic conditions are required for economical transport of CO_2. Therefore, three scenarios each for post-combustion and pre-combustion have been studied in order to explore the effect of thermodynamic conditions on the economics of CO_2 transport. For the case of CO_2 transport using ship, the design and operation of CO_2 terminal is presented in chapter 5. The dynamic simulation is performed for the CO_2 terminal in order to have a more realistic understanding of the process. Different operational modes such as loading case, holding case, unloading case, and emergency shutdown are included to define the operational strategy of the terminal. In chapter 6, the conclusion of this thesis and future work are presented.

CHAPTER 2: Dehydration

2.1. Overview

Dehydration is a system used to control water content in the CO_2 stream. Removal of water is required from the captured CO_2 stream in order to minimize the risk of corrosion and hydrate formation. There is no regulatory standard for the allowable limit of water content in the CO_2 stream. Currently, the water content in the CO_2 stream varies a lot ranging from < 50 ppmv (Snohvit, Kingsnorth, Lacq, OCAP, Weyburn) to 630 ppmv (Central Basin, Sheep Mountain, Mobell, Slaughter, Bairoil, Salt Creek) [16]. The accepted water content after dehydration depends on the downstream processes. Different types of gas dehydration techniques are available and suitable for the CCS application. The simplest dehydration method is by cooling which involves gas cooling (gas expansion, refrigerant or else), water condensation and water separation. However, water removal by cooling can only achieve water contents down to 600 ppmv in the dried gas which is much higher than the required limits. Other dehydration methods include absorption, adsorption or by using membranes.

The most traditional method for large scale dehydration to reasonable water levels is by absorption into glycols. For very low water levels, adsorption processes are necessary [17]. Membrane dehydration is economical only for low gas flow rates but research and development in this area is ongoing. Figure 2-1 shows the different dehydration methods. Triethylene glycol (TEG) has gained universal acceptance as the most cost effective choice in the dehydration process. TEG is easily regenerated to a concentration of 98-99.95 % in an atmospheric stripper because of its high boiling point and decomposition temperature [18]. Vaporization losses are lower than EG or DEG. In addition, capital and operating cost are lower compared to other glycol. There are very

few references in the open literature on the simulation of CO_2 dehydration. In this chapter, a dehydration unit using TEG solvent has been simulated to remove water from the wet CO_2 stream. Various factors such as absorber pressure, inlet wet gas temperature, lean TEG temperature and L/G ratio have been analyzed to see their impact on the water content in the dried CO_2 stream.

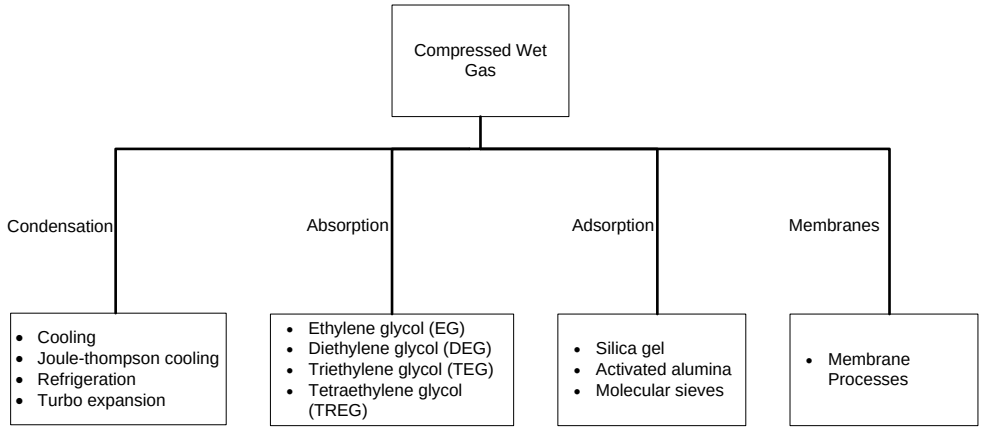

Figure 2-1: Various methods for gas dehydration

2.2. Process Design

2.2.1. Process Description

The dehydration process itself consists of two parts, gas dehydration and solvent regeneration. In gas dehydration, water is removed from the wet CO_2 stream using the solvent in the absorber. The rich solvent is then sent to the solvent regeneration section to strip water out of the solvent. Figure 2-2 shows the process flow diagram of the TEG dehydration process. The wet CO_2 stream saturated with water is first sent to a flash drum where free water is separated. Removing free water in the flash drum decrease the amount of water that has to be removed in the absorption column. In addition, this decreases the size of the column and therefore decrease the TEG needed in the process. The wet gas then enters the bottom of the absorber where it is contacted with the lean TEG solvent fed at the top of the column. The wet gas and TEG flow counter currently in the packed column. Water is absorbed from the gas stream into the TEG. The dried CO_2 stream leaves at the top of the absorber. The rich glycol stream leaving at the bottom of the absorber is passed through an expansion valve to reduce the pressure. Rich TEG is pre-heated through the reflux condenser in the top of the regeneration column. Rich TEG is further heated in the lean/rich heat exchanger before it is fed to the regeneration column. In the regeneration column, water and CO_2 are stripped off from the solvent and leaves at the top of the regenerator column. Whereas, the lean TEG from the bottom of the regenerator is cooled in the lean/rich exchanger with the incoming rich TEG. The lean TEG is further cooled using a cooler before being pumped back to the top of the absorber. Glycol make-up is added to the recycled lean TEG stream to ensure the required glycol recirculation rate.

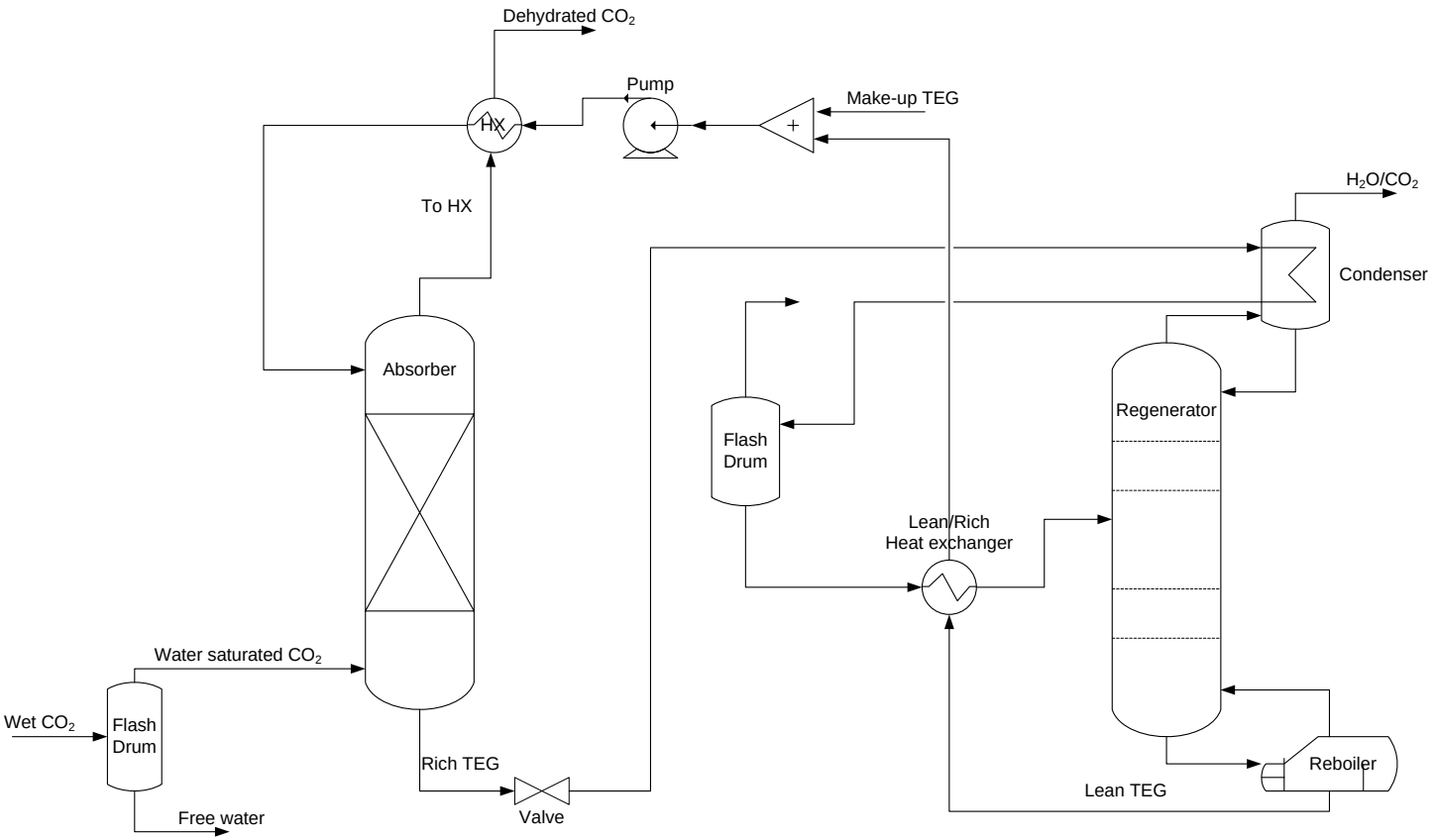

Figure 2-2: TEG absorption and stripping process

2.2.2. Base Case

TEG dehydration process has been simulated using a commercially available software Aspen HYSYS® . The Glycol package with Twu-Sim-Tassone (TST) equation of state is used as a property package. The TST model is a more advanced cubic equation of state with more adjustable parameters. The parameters are especially fitted for the glycol gas dehydration system. The TST model is recommended in the Aspen HYSYS program documentation as the most accurate method for dehydration processes [17]. The specifications for the base case process calculations are given in table 2-1.

Table 2-1: Base case specifications

Inlet Mass Flow rate	26.35 kg/s
Absorber	
Number of stages	3
Stage efficiency	0.5
Absorber pressure	3000 kPa
Regenerator	
Number of stages	3
Stage efficiency	1
Regenerator pressure	101.4 kPa
Condenser type	Full reflux
Reboiler temperature	204 °C
Solvent Specifications (TEG)	
TEG recirculation rate	24 kg/kg H_2O removed
Lean TEG temperature	45 °C
Lean TEG pressure	3000 kPa
Heated rich TEG temperature	150 °C

The absorption column normally converges if the feed streams (wet gas and recycled glycol) are specified, and the number of theoretical stages is limited to 3. The wet gas and lean TEG is fed to absorber counter currently at 3000 kPa. The dried CO_2 stream leaves at the top of the column while rich TEG leaves at the bottom of the absorber. The pressure of rich TEG is reduced to around 180 kPa by expanding it through a control valve. Low pressure TEG is warmed to around 150 °C before entering the regeneration column. The regeneration column consists of three stages including the condenser and reboiler. Manufacturer's literature (Dow Chemical) provides a decomposition temperature of 240 °C for TEG [18]. The required lean TEG concentration dictates the reboiler temperature. Higher reboiler temperatures yield leaner glycol. The maximum reboiler temperature is set as 204 °C, which is the recommended maximum regeneration temperature. It is not recommended to increase the reboiler temperature, because the glycol will start to degenerate above this temperature. The regeneration pressure is set to 101.4 kPa. Lower regeneration pressures favor for the leaner TEG, however, it is not advisable to operate the regeneration column below atmospheric pressure as oxygen leakage into the system can cause explosion hazard. The lean TEG after exchanging heat with rich TEG is pumped back to the top of absorber. The recommended TEG recirculation rate is 17- 42 L per kg of H_2O removed [18]. The glycol recirculation rate in the base case has been set as 21 L per kg of H_2O removed from the wet CO_2 stream [19]. For normal operating plant, Engineering Data Book estimates TEG losses of about 13 L/10^6 Sm^3. Other losses range between 7 L/ 10^6 Sm^3 and 40 L/ 10^6 Sm^3 for high pressure and low temperature dehydration processes respectively [18]. TEG make up is added to the lean TEG to maintain the required recirculation rate. The recycled TEG back to absorber is cooled to 45 °C.

2.2.3. Stripping Gas to Reboiler

It is possible to improve the performance of the process by adding stripping gas to the reboiler or the bottom of the regeneration column. The main effect of adding stripping gas is that the partial pressure of water in the gas phase is reduced so that more water will evaporate and increase the wt% concentration of lean TEG [17]. The stripping gas can come from an external source (usually N_2) or CO_2 from the dehydrated gas can be used. The vent of the flash drum located after the absorber column can also be used for the purpose of stripping in the reboiler. In this study, the flash gas available after the absorber is used as a stripping source in the reboiler of the regeneration column. Figure 2-3 shows the flash gas available at 26 °C and 103.4 kPa that is added to the reboiler.

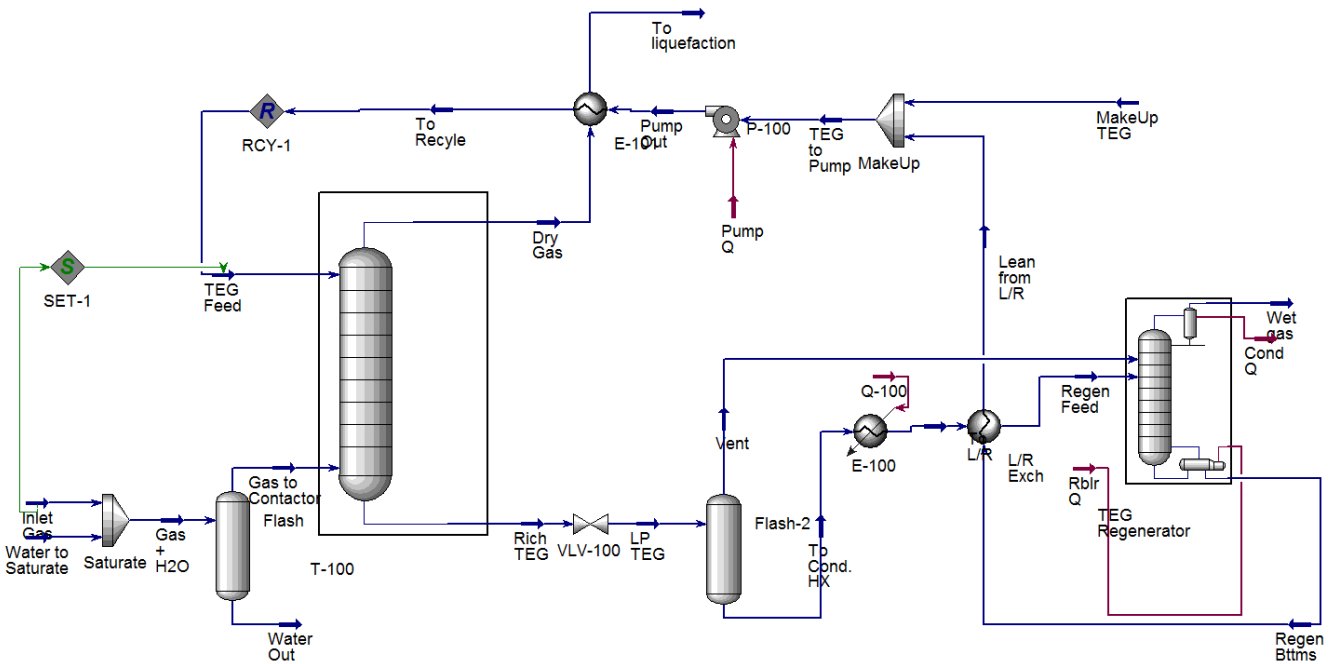

Figure 2-3: HYSYS flow sheet of dehydration process with stripping gas to the reboiler

2.3. Results and Discussion

Operating conditions for the dehydration units are governed by the degree of dehydration required. However, there is a limit on the level of dehydration that can be achieved with the standard operational procedures. The base case results show that water content of 73 ppmv is achieved in the dehydrated gas. Lean TEG leaving at the bottom of the regeneration column has the concentration of 99 wt%. However, in the case of stripping gas addition to the regeneration reboiler, the water content can be reduced to 57 ppmv in the dehydrated CO_2 stream. The lean TEG concentration increased to 99.5 wt% at the bottom of the regeneration column. All the other operational parameters are kept same as that of the base case. The reboiler duty increased slightly with the addition of stripping gas from 119.3 kW to 121.8 kW.

TEG purity of 99.9 wt% can be achieved by using an advanced dehydration process scheme such as Coldfinger, Drizo and Read cycle [20].

2.3.1. Wet Gas Inlet Temperature

The flow rate of gas is much greater than the flow rate of TEG, and the gas temperature will therefore govern the process temperature. Wet gas inlet temperature to the absorber is set as 30 °C. Figure 2-4 shows the water content in the dried CO_2 stream with varying wet gas inlet temperature. Lower absorption temperatures improve the efficiency of dehydration process. However, as the temperature of wet gas is lowered, the viscosity of TEG is sufficiently high to reduce the stage efficiency and increase pumping costs. Absorber inlet temperatures can be as high as 66 °C, however temperatures above 38 °C may result in unacceptable vaporization losses of TEG [18].

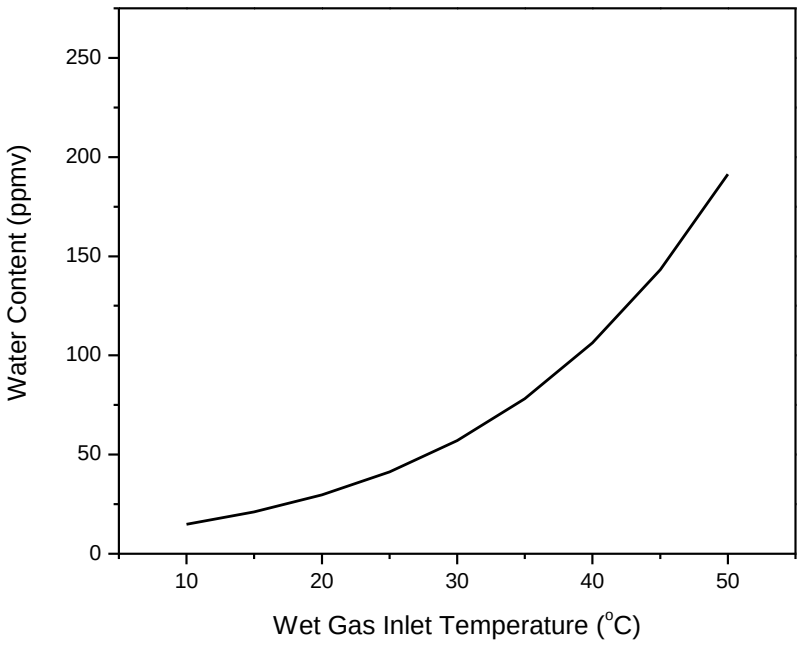

Figure 2-4: Water content in dehydrated gas as a function of wet gas inlet temperature

2.3.2. Absorption Pressure

Sensitivity analysis has been performed on the absorber pressure to analyze its effect on the dehydration. Figure 2-5 shows the content water content in the dried CO_2 stream with varying absorber pressure for the case when stripping gas is added to the reboiler. The calculated water content for different absorption pressures indicates that a maximum dehydration efficiency is best achieved at the pressures above 3000 kPa. The absorber pressure for the base case has been set at 3000 kPa. The water content in the dehydrated stream decreases as the absorber pressure increase up to 6000 kPa. However, any further increase above 6000 kPa in absorber pressure increases the water content in the dried CO_2 stream.

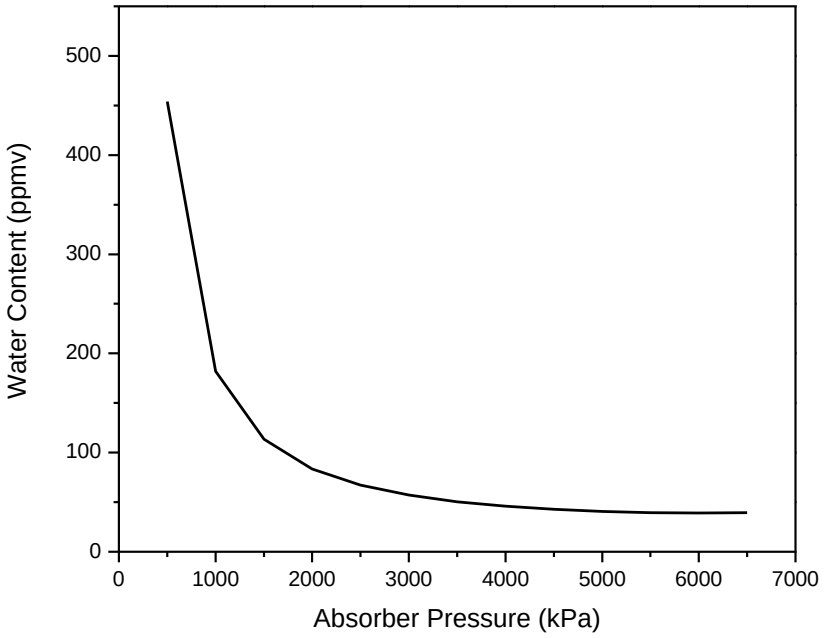

Figure 2-5: Water content in dehydrated gas as a function of absorber pressure

2.3.3. TEG Recirculation Rate

The recommended TEG recirculation rate is 17- 42 L per kg of H_2O removed [18]. Figure 2-6 shows the water content in the dried CO_2 stream with varying TEG recirculation flow rate. An increase in the TEG recirculation rate reduces the water content in the dried CO_2 stream. However, the decrease in the water content becomes less as the TEG recirculation rate surpasses a certain range. Hence, the glycol recirculation rate in the base case has been set as 21 L per kg of H_2O removed from the wet CO_2 stream. It is important to note that as the TEG recirculation rate increases, the reboiler duty also increase linearly.

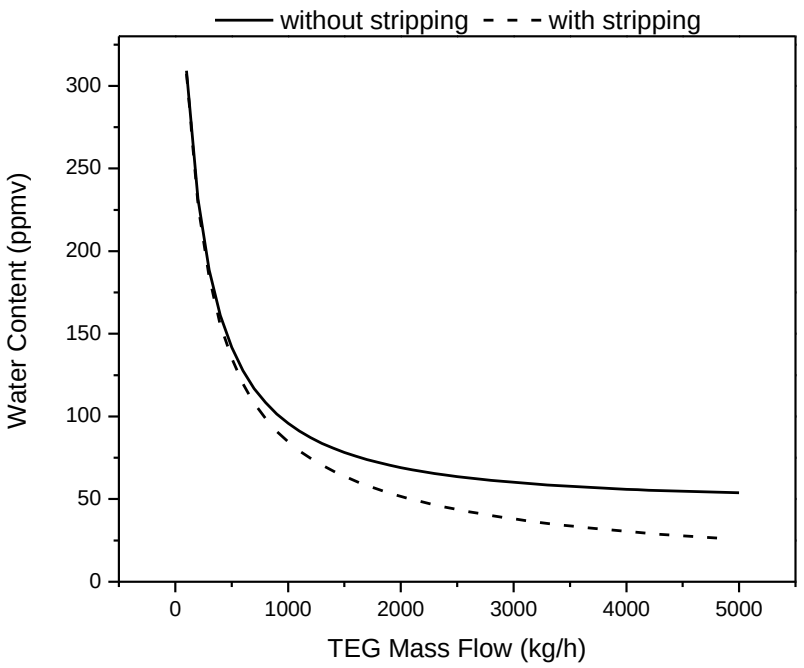

Figure 2-6: Water content in dehydrated gas as a function of TEG recirculation rate

Water content in the dried CO_2 stream was also simulated by varying number of absorber stages and lean TEG inlet temperature to the absorber. The results showed only minor improvement in achieved water content in the dehydrated CO_2 stream.

2.3.4. Heat Integration

Heat integration has been done between the hot and cold streams to reduce the utilities load and make the process more energy efficient. In the base case, around 7 kW of regeneration column condenser cooling duty can be saved. This is done by heating the rich TEG stream using the regeneration condenser energy. The temperature of the rich TEG is increased by 4.5 ^{o}C before it is sent to lean/rich heat exchanger for further heating. The lean TEG leaving at

the bottom of the regeneration column is at 204 °C which needs to be cooled before it is sent back to the absorber. This is done by exchanging heat between lean and rich TEG stream. The rich TEG stream is heated from 31 °C to 150 °C, while the lean TEG stream is cooled down from 204 °C to 75 °C. The lean TEG at 75 °C is further cooled down to 45 °C by exchanging heat with the dehydrated CO_2 stream.

2.3.5. Stripping Gas Flow rate

Simulations were performed to analyze the effect of variation in stripping gas flow rate on the water content in the dehydrated CO_2 stream. This case is studied by the addition of N_2 from an external source and CO_2 from the dehydrated stream as the stripping gas sources. Both N_2 and CO_2 show similar effect on the water content in the dehydrated stream. Figure 2-7 shows the water content in the dried CO_2 stream with varying stripping gas flow rate. The results show that an introduction of stripping gas into the reboiler sharply reduces the water content in the dried stream. However, after a certain flow rate, any further increase in the flow rate of the stripping gas don't reduce the water content in the dehydrated stream.

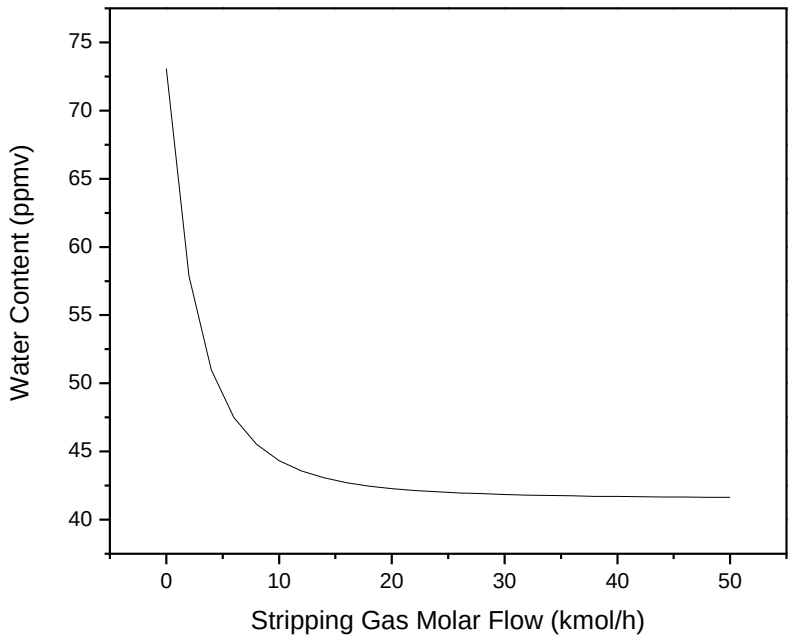

Figure 2-7: Water content in dehydrated gas as a function of stripping gas flow rate

2.4. Summary

In this chapter, dehydration process has been simulated using TEG as a physical absorbent. The base case process is a traditional water removal process, and shows good results in terms of process efficiency. Water content in the CO_2 stream can be reduced to 73 ppmv, while generating 99.03 wt% lean TEG at the bottom of the reboiler. To further improve the efficiency of the dehydration process, stripping gas has been added to the reboiler of the regeneration column. By using the stripping gas, water content in the CO_2 stream can be further reduced to 57 ppmv, while generating 99.5 wt% lean TEG at the bottom of the reboiler.

CHAPTER 3: Pipeline Transport of CO_2

3.1. Overview

The characteristics of the substance transported inside the pipeline will affect the way the pipeline is designed and installed. High pressure pipeline transport is a mature industry and the most relevant example is the use of pipelines for transport of hydrocarbons. This applies to both on- and offshore pipelines. The energy industry has extensive experience with natural gas in all parts of the process chain. A CO_2 transport pipeline can, to a large extent, be planned and constructed in the same way as natural gas transmission pipelines. However, CO_2 has different thermodynamic properties compared to natural gas. For example, natural gas is always transported in its gaseous state in high-pressure pipelines. Design pressures of up to 100 barg are generally allowed for onshore gas transmission systems, while offshore transmission pipelines may have an operational pressure up to, or even beyond, 200 barg [13]. By contrast, when CO_2 is transported, the CO_2 may be in gaseous, liquid or supercritical state – depending on the operating pressure. If pressure inside the pipeline is reduced, the liquid phase CO_2 will start to go into gaseous phase, resulting in mechanical challenges to the pipeline and reducing the transport capacity. Thus, the transport pressure and temperature conditions need to be planned to ensure single (dense, liquid) phase transport from inlet to outlet of the pipeline. In this chapter, a plausible transport model scheme has been developed and then employed to study different offshore CO_2 transportation cases for South Korea.

3.2. Operational range of pipeline

The design of compressor and pipelines rely mainly on the physical properties of the fluid, which is no less true for CO_2. The behavior of CO_2 in various phases has been frequently studied and is well understood but the range of

temperature and pressure makes them unusual. Therefore it is highly necessary to design a pipeline system that it offers not only low cost and a maximum performance but also safety. Normally, it is recommended that the pipeline should be operated at high pressure (usually higher than the critical pressure of CO_2) to increase the transport capability and reduce capital cost of the pipeline system [21-23]. Nimtz et al. [24] modeled a CO_2 transport and storage system in supercritical phase above 8.5 MPa, McCoy [25] recommended a CO_2 pipeline operating pressure of greater than 8.5 MPa, and Mazzoldi et al. [22] recommended CO_2 transport at pressure of around 10 MPa. Many authors mainly referred to high pressure CO_2 transport because of two existing CO_2 injection sites Snohvit and Sleipner which had been developed for pipeline transport at supercritical conditions. Nevertheless, it is still a controversial argument since some researchers reported the transport of sub-cooled liquid CO_2 to be more advantageous. Zhang et al. [26] studied CO_2 transport schemes and showed 16 % reduction in the capital cost over long distance transport. Zhang et al. [21] also studied about the transport system of CO_2 for China and showed similar results consistent with Zhang et al. [26]. Since the temperature, density, viscosity and velocity are interrelated through mass conservation and equation of state, pressure drop along the pipeline is dominantly caused by the frictional forces which are mainly a function of both CO_2 viscosity and flow velocity. Figure 3-1 shows the density variation with the change in temperature for different pressure values. It can be seen that at low temperatures the CO_2 density becomes a function of temperature mainly and pressure has little impact on the density. The pressure drop of pipeline increases with the increase in the inlet temperature of CO_2 stream. Figure 3-2 shows that although CO_2 viscosity decreases when temperature increases, which can help to reduce the pressure drop. However, with the increase in temperature, the volume of CO_2 also increases which in turn increases the flow

velocity, hence pressure drop increases ultimately. A similar conclusion was drawn by Zhang et al. [21] that the pressure drop is proportional to the square of logarithm of viscosity, as well as the square of flow velocity, which causes the velocity to have a bigger impact.

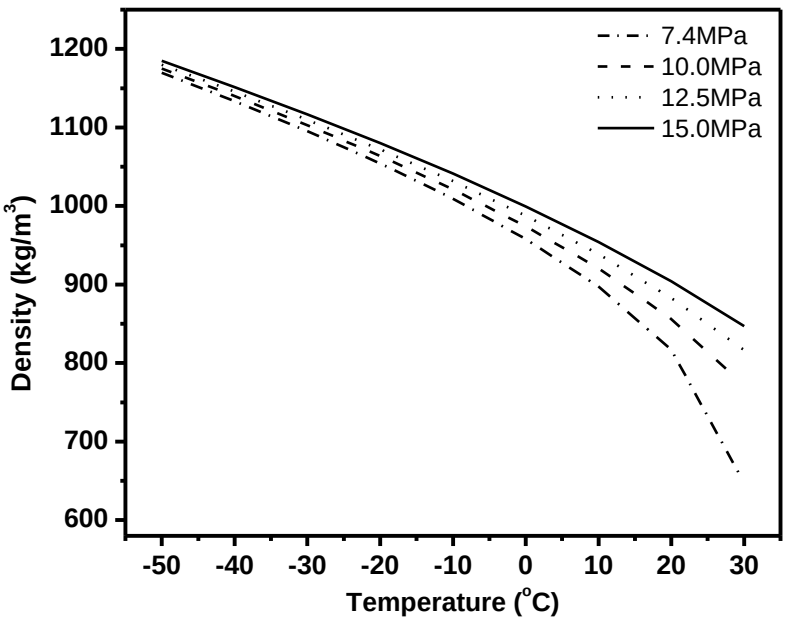

Figure 3-1: Variation in CO_2 density with change in temperature at different pressures (MPa)

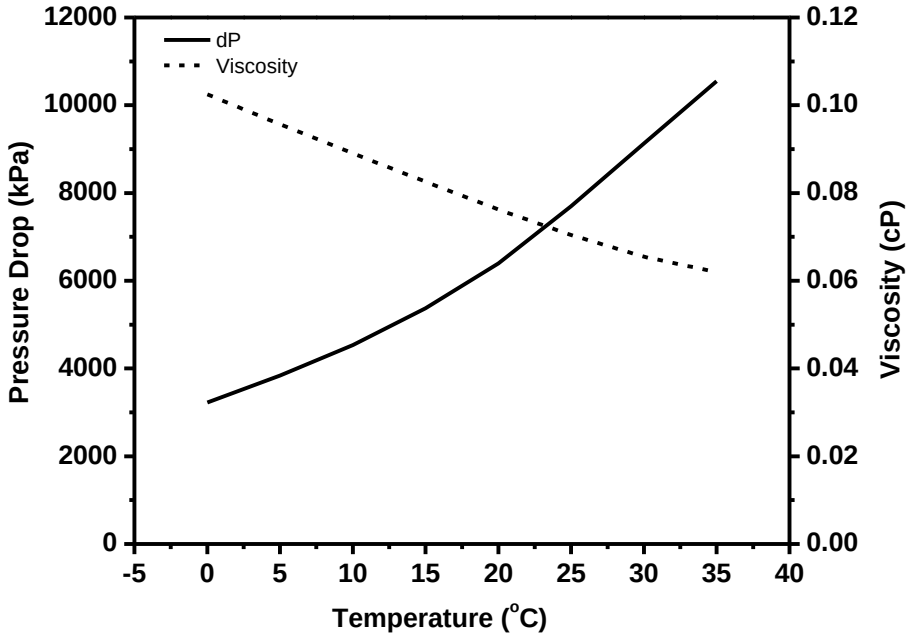

Figure 3-2: Variation in pressure drop and viscosity with change in inlet temperature across 150 km long pipeline

Many previous CO_2 pipeline transport studies focused on how pressure drop in pipelines can be reduced in order to minimize operating costs. Nimtz et al. [24] choose an internal pipeline diameter of 0.5 m so that the flow velocity is not too high (< 2 m/s) and to keep pressure losses to minimal. Increasing pipeline diameter to have low pressure drop will result in lower compression power, however it increases capital cost on the other hand. Haugen et al. [27] studied options for alternative CO_2 transport schemes for Denmark case. In their study, high inlet pressure was used which means the pressure drop in the pipeline must be compensated for by the CO_2 compressor by keeping higher pressure at the pipeline inlet. Another way to keep low pressure drop in pipelines is to transport CO_2 at low temperatures (-40 °C to -20 °C) and an

operating pressure of 6.5 MPa. At this low temperature and pressure condition, CO_2 density becomes above 1,100 kg/m^3 and the pressure drop is reduced as compared to CO_2 transportation at high temperatures as shown in Figure 3-3. However, in order to overcome the reservoir pressure and avoid hydrate and wax formation, the inlet temperature to the storage site well head should be 10 ^oC to 20 ^oC [28].

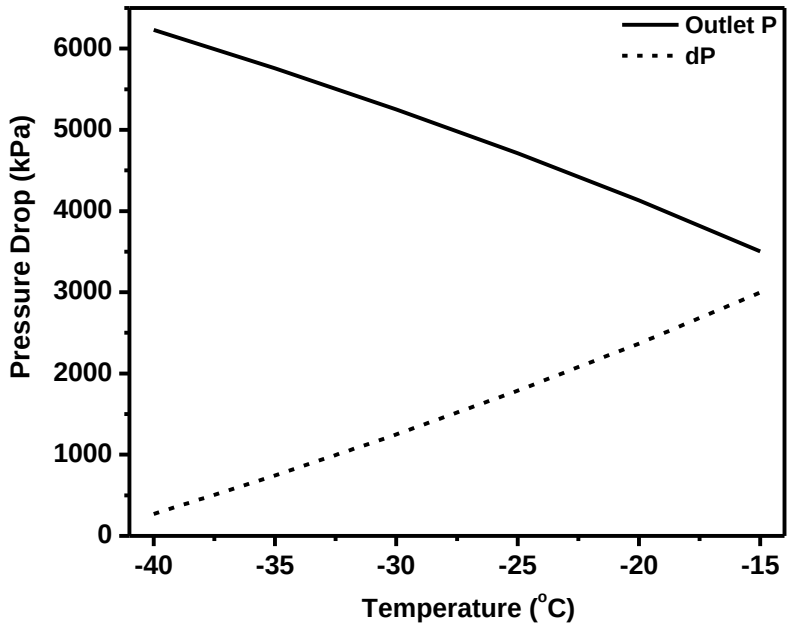

Figure 3-3: Variation in pressure drop across 150km pipeline at different inlet temperature and 6.50MPa

In this case, CO_2 must be heated up before it is injected into the storage injection well. If the pipeline is unburied and icing on the pipe outer wall can be handled, along pipeline can act as a heat exchanger, increasing the retention time of the CO_2 in the pipeline and heating towards the sea water temperature

before it enters the well. This can be used to avoid or decrease the risk of hydrate formation in the well and may be a cheaper and more practical solution than installing heater topside for this purpose [29]. Another economical solution can be to transport low temperature CO_2 to enhanced bed methane recovery sites. CO_2 can be heated up by heat exchanger with natural gas coming out of the well. In this way, energy costs can be reduced on both sides of the process while CO_2 can be stored at the same site.

3.3. Pipeline Transport for Korea

The average CO_2 emission growth rate of Korea is 1.0 % which is the second highest among the Organization for Economic Co-operation and Development (OECD) countries. It becomes even more challenging when CO_2 is transported to an offshore storage since there is little experience with subsea pipelines for CO_2 transportation. This makes it especially important in the case of Korea where emissions are high and the storage sites are offshore. Therefore, in order to analyze the hydrodynamic performances of CO_2 flow in the pipeline, optimize the CO_2 pipeline accordingly, and to estimate the unit cost of CO_2 transport are of great importance for the large scale implementation of CCS. The presence of existing infrastructure can be useful especially during the early demonstration and deployment of CCS. The existing infrastructure can be useful in terms of physical usage or routing of new pipelines. Existing structure can be useful for transporting CO_2 provided that use with CO_2 meets the appropriate design code. For example, Scotland has an existing offshore and onshore pipeline network of approximately 11,000 km for the transportation of oil and gas. A study conducted in 2007 identified 28 existing pipelines with a capacity in the range of 10 to 50 Mt CO_2/year that can be reused for the development of CCS transport infrastructure [30]. The Longannet demonstration project in Scotland is planning the use of a 284 km long onshore and 100 km long offshore existing pipeline network [30]. In case,

the existing pipeline structure cannot be used due to technical, safety, logistics, policy and regulation, or other reasons, it will still be useful for the new pipeline routes to follow the existing layouts as topographic studies have already been done. Korea has an extensive network of natural gas distribution pipeline that can be useful for transporting CO_2 either practically or for mapping routes of new pipelines. The rights-of-way have already been established, which is also valuable for cost reduction. However, it is yet not assessed that how much length of existing pipeline structure can be useful for the transport of CO_2 in South Korea. Since all the storage sites are located offshore and the existing available natural gas pipeline network is located on the mainland, therefore this chapter focuses on the design and modeling of offshore pipeline. However, shall the CCS technology move further towards commercialization, the pipeline network will be required to transport CO_2 from the power plants located at the West and South coast to the storage sites. In that case, the existing pipeline network can play an important role for reducing the time and costs to deploy CCS in Korea.

Donghae and Yongdong coal fired power plants are located in the East of Korea and have a power generation capacity of 400 MW and 325 MW respectively which corresponds to around 4.50 Mt of CO_2 emissions per year. After the CO_2 has been captured at these power plants, it is transported to 150 km offshore Ulleung storage site. The pipeline is assumed to be routed along the floor of the seabed as experienced from the existing offshore oil and gas industry practice. The average depth of the East Sea is approximately 1368 m. Care is required in such design of the pipeline, since the elevation is constantly changing along the horizontal axis. It means that there is a constant change in pressure and hence density of the fluid inside the pipeline. To account for the hydrostatic head due to the elevation related change, a linear increase of 0.912 m depression per 100 m of horizontal axis is assumed on the basis of average

depth of the sea. The transport model has been developed using 4.5 Mt of captured CO_2 per year as the base case. Assuming the CO_2 is dry, which is a common requirement for CCS, material requirements for all the three cases is same. Figure 3-4 shows the scheme for pipeline diameter calculation and how various parameters interact to give the energy and cost optimum calculations. The CO_2 compression has been included as a part of transport in this study.

3.3.1 Transport scenario

The large volumes of CO_2 needs to be transported in dense or liquid phase. In gaseous phase, the volume would require unrealistic pipeline dimensions, increasing costs by an order of magnitude. Then the pressure within the pipeline should be kept so that it is well above the bubbling line. Keeping the phase diagram of CO_2 in view, this means that the minimum operating pressure during summer temperatures should be in the range of 65 bar for buried pipelines. In this study, three different sets of temperature-pressure inlet conditions are studied for CO_2 pipeline transport as shown in table 3-1.

Table 3-1: Operating conditions for case studies

	Temperature (°C)	Pressure (MPa)	Phase
Case 1	-20	6.50	Liquid
Case 2	5	9.30	Liquid
Case 3	40	15.00	Supercritical

3.4. Transport model

3.4.1. Diameter calculation

The pipeline diameter is an important parameter in order to have an accurate look at the economical aspect of transport project. As shown in Figure 3-4, many parameters such as flow rate, inlet P and T, pressure drop, topographic

differences play an important role in the calculation of proper diameter size. Pipeline diameter calculation method can be divided in two main classes [31] :

- Calculations based on hydraulic laws for turbulent flow in circular-shaped pipelines
- Calculations based on economics-related optimal design

Table 3-2 shows (Eqs. 1–4) formula for pipe diameter calculation along with calculated pipeline diameters for Cases 1, 2, and 3 to have a comparison of diameter results. IEAGHG [32] used Eq. 1 to calculate pipeline diameter. This formula gives a quick and rough estimate of the pipeline diameter but does not take pressure drop into account. Also assumed average velocity has been used for the calculation of pipeline diameter.

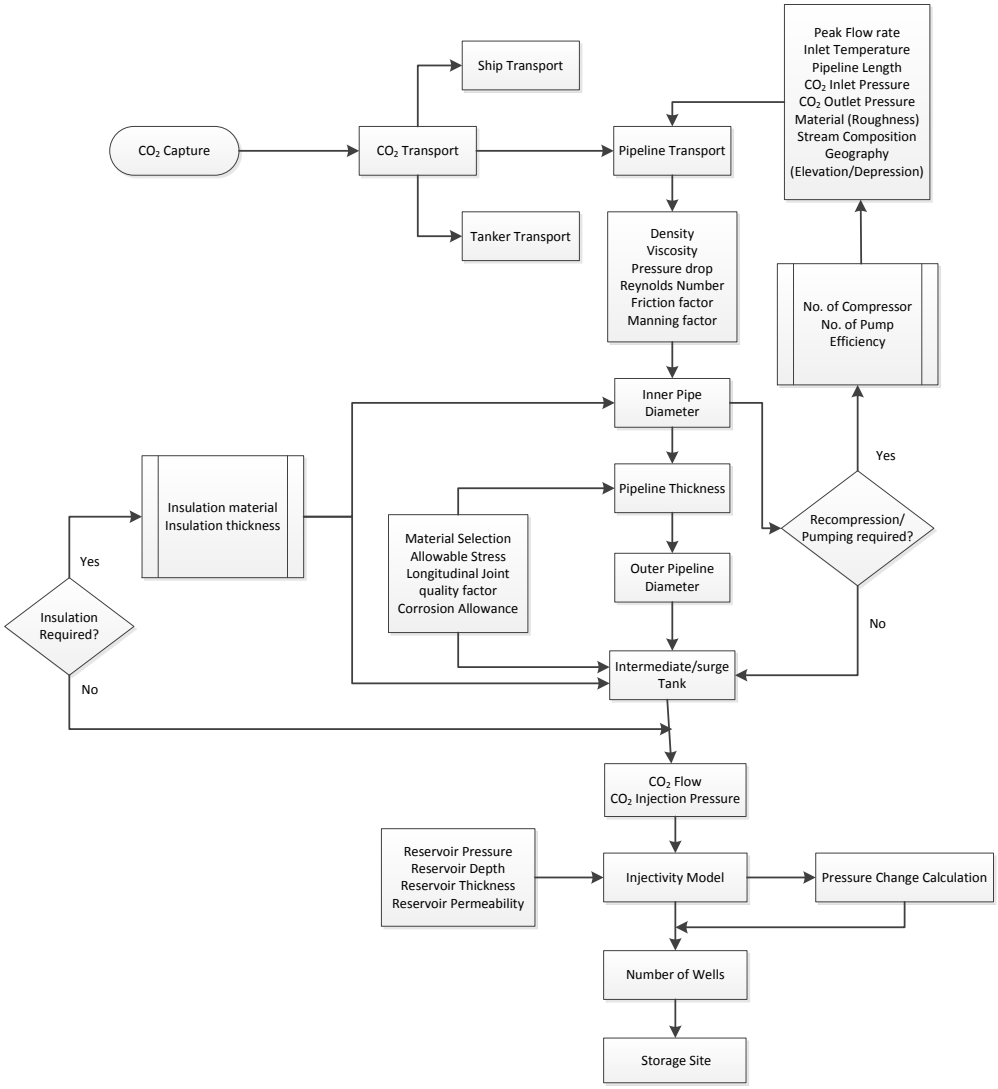

Figure 3-4: CO_2 pipeline transport and storage model

Equation 2 based on basic Bernoulli law was used by Hamelinck et al. [33] and Haeddle et al. [6] to calculate the diameter of pipeline for CO_2 transport, but this equation does not account for topographic differences. During this study, it has been found that Eq. 2 fails to calculate an accurate diameter when ΔP is small. As already shown in Figure 3-3, ΔP is much smaller during low temperature transportation (Case 1), so in that case Eq. 2 cannot calculate pipeline diameter correctly. Figure 3-5 shows the difference in diameter calculated using Eqs. 2 and 3. It can be seen that the difference in diameter calculation using different formulas decreases as pressure drop across the pipeline increases. Vandeginste and Piessens [34] derived Eq. 3 for calculation of pipeline diameter based on Bernoulli law by taking topographic differences into account. Zhang et al. [26] and Lee et al. [35] used Eq. 4 which is based on optimal design. This equation was originally derived by Peters [36] for the calculation of economic pipe diameter assuming average numerical values for some of the less critical parameters and has been used for further calculations in this model. Case 1 and Case 2 have a positive ΔP of 833 kPa and 2056 kPa respectively, whereas Case 3 has a negative ΔP of 2280 kPa across the pipeline. Since the pipeline inlet temperature in Case 3 was 40 °C which eventually decreased to 5 °C, it helped to increase the outlet pipeline pressure of CO_2 along with the hydrostatic pressure increase. The variation of pipeline diameter along the pipe length for Case 1 and Case 2 is not significant because of minor change in density; however the diameter for Case 3 showed a variation of up to 1 inch. The results reported in Table 3-2 show the largest diameters required for all the cases in order to account flow fluctuations for the purpose of safety.

Table 3-2: Comparison of diameter calculation using different methods

	$D = \sqrt{\frac{4Qm}{v\pi\rho}}$ (Equation 1) (26)	$D^5 = \frac{32\, f_F Qm^2}{\pi^2 \rho \left(\frac{\Delta p}{L}\right)}$ (Equation 2) (7, 26)	$D = \left(\frac{4^{10/3}\, n^2\, Qm^2\, L}{\pi^2 \rho^2 (z_1 - z_2 + \left(\frac{p_1 - p_2}{\rho g}\right))} \right)^{3/16}$ (Equation 3) (28)	$D_{opt} = 0.363 \left(\frac{Qm}{\rho}\right)^{0.45} \rho^{0.13} \mu^{0.025}$ (Equation 4) (21)
Case 1 (inches)	11.62	29.72	11.90	11.57
Case 2 (inches)	12.26	15.21	11.87	11.86
Case 3 (inches)	13.48	15.91	12.67	12.47

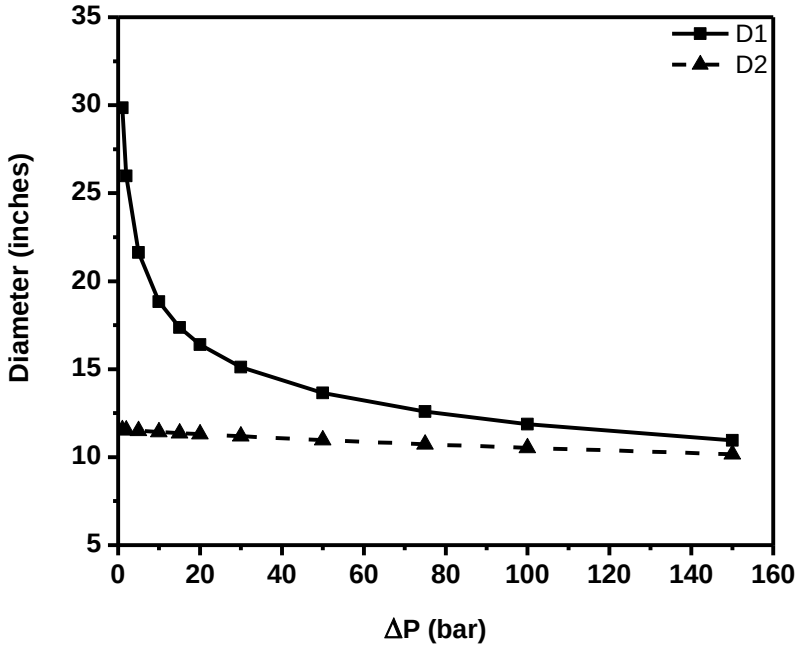

Figure 3-5: Difference in diameter calculation with change in pressure drop using different equations

3.4.2. Pipeline thickness

The pipeline thickness has been calculated by following the ASME B31 standards of pressure piping in order to ensure safe operation. Equation 3.1 has been used to calculate the pipeline thickness (t_{pipe}) for all three cases.

$$t_{pipe} = \frac{P_p \, D_{in,pipe}}{2\,(S\,E + P_p\,Y)} \qquad \text{….. Eq. 3.1}$$

P_p is the maximum internal design pressure, $D_{in,pipe}$ is the internal diameter of pipeline, S is the allowable stress in tension which is taken as 129.9 MPa for stainless steel at room temperature or lower temperatures [37]. E is the longitudinal joint quality factor set to 1.0 assuming that pipes are seamless; Y is the wall thickness correction factor based on the type of steel and design temperature which is set to 0.4 [38]. Corrosion allowance is an additional

thickness that is added to account for wall thinning and wear that can occur in service. Liquid water is undesirable because it can cause corrosion. Removing water from a gas stream is a well-established technology as experienced from natural gas industry and CO_2 pipeline operating between Dakota and Weyburn oilfield in USA. Therefore, this study assumes that the CO_2 is effectively free of water. A corrosion allowance of 3 mm is assumed in this study.

3.4.3. Heat flux

The total heat flux (dQ) is calculated over the pipeline and intermediate surge tank using equation 3b. The overall heat transfer coefficient (U_o) is calculated using equation 3c and 3d for both pipe and tank respectively.

$$dQ = U_o \Delta T \, dA \qquad \text{.....Eq. 3.2}$$

$$U_{o,pipe} = \frac{1}{r_o\left(\frac{1}{r_o h_o} + \frac{\ln\left(r_1/r_o\right)}{k_{01}} + \frac{\ln\left(r_2/r_1\right)}{k_{12}} + \frac{1}{r_1 h_1}\right)} \qquad \text{..... Eq. 3.3}$$

$$U_{o,tank} = \frac{1}{{r_o}^2\left(\frac{1}{{r_o}^2 h_o} + \frac{(r_1 - r_o)}{k_{01} r_1 r_o} + \frac{(r_2 - r_1)}{k_{12} r_2 r_1} + \frac{1}{{r_1}^2 h_1}\right)} \qquad \text{..... Eq. 3.4}$$

Where U, h, and k represent the overall heat transfer coefficient, convective heat transfer coefficient and thermal conductivity respectively; and r_0, r_1 and r_2 represent the internal radius, external radius and outside radius of insulation for pipeline and tank in equations 3-3 and 3-4 respectively. The heat flux across the tank can be calculated by simple integration using the overall heat transfer coefficient. However, the heat flux across the pipeline cannot be simply calculated because the temperature gradient gradually decreases as the pipe length increases. In order to have correct heat flux, the pipeline is segmented and the new temperature gradient reflecting the temperature increase due to the heat influx is used for the contiguous segment heat flux calculation. The ambient temperature of the East Sea water is assumed as 5 °C.

Average speed of the sea water is set to 0.02m/s at the bed of sea [39]. For the case 1, where the operation temperature of pipeline is -20 °C, insulation is required for both the pipeline and tank. Polyurethane is selected as an insulating material for pipeline and tank. Thermal conductivity of polyurethane was set to 0.018 W/m-K which resulted in insulation thickness of 101.6mm ensuring no vapor formation. In case of the tank, the heat transfer coefficient of ambient air is 40W/m^2-K which increases with wind velocity. Hence, heat transfer coefficient for air is taken as 50W/m^2-K for the wind speed of up to 15mph.

3.5. Cost of transport

The cost of transporting CO_2 through pipeline has been calculated by using information on both the capital investment and operation cost from a number of references. The cost of pipeline has been calculated by using relations presented in table 3-3 (equations 11-14) which were taken from regression analysis performed by the University of California [40]. Materials costs account for approximately 26 % of the total construction costs on average. Labor, right of way, and miscellaneous costs make up 45 %, 22 %, and 7 % of the total cost on average respectively. Miscellaneous costs are all costs not included in labor, material, or right of way cost. They generally include surveying, engineering, supervision, contingencies, allowances, overhead, and filing fees [40]. It is important to note that in this study carbon steel was used as the pipeline material. The cost multiplier factor for terrain is set to 2.7 for offshore transport greater than 500m depth [41]. Cost of compressor, cooler, surge tank and insulation has been calculated using mathematical relations provided in the literature [42-44]. It is important to note that insulation and refrigeration is used in case 1 only where CO_2 is transported at -20 °C. The price of electricity was taken as 0.06$/KWh, price of refrigeration (for case 1)

was taken as 1.5 c/MJ and cooling water price was taken as 1c/ton from the literature [36, 42]. Insulation cost has been calculated using rule of thumb by assuming it as 7.5 % (material cost: 3 % and labor cost: 4.5 %) of capital cost [43]. The economic depreciation was assumed to be 5 % over a project of 30 years. The total cost of CO_2 transport can be calculated using equation 3.5.

$$\text{Cost of Transport } \left(\frac{\$}{\text{tonne}} \text{of } CO_2\right) = \left(\frac{\text{Annualized CAPEX+OPEX}}{CO_2 \text{Transported Annually}}\right) \quad \text{….. Eq. 3.5}$$

Table 3-3: Pipeline Cost Breakdown [45]

Cost Type	**Unit**	**Cost Relation**
Materials (Equation 11)	$ Diameter (inches) Length (miles)	$64632+$1.85*L*(330.5*D^2 + 686.7 ∗ D + 26960)
Labor (Equation 12)	$ Diameter (inches) Length (miles)	$341627+$1.85*L*(343.2*D^2 + 2074 ∗ D + 170013)
Miscellaneous (Equation 13)	$ Diameter (inches) Length (miles)	$150166+$1.58*L*(8417*D+7234)
Right of Way (Equation 14)	$ Diameter (inches) Length (miles)	$48037+$1.20*L*(577*D+29788)

The breakdown of major equipment and services capital costs have been shown in table 3-4. The cost of pipeline material increases in the order of Case 3 > Case 2 > Case 1 cost. This is mainly due to the effect of pipeline operating conditions on the calculated pipeline diameter. The capital cost of compressors is mainly dependent on the required outlet pressure; hence the cost of the compressor for case 3 is the highest where outlet pressure is assumed at 15.00 MPa. Since the compressor is the most power consuming equipment, compression energy requirement per ton of CO_2 compressed for case 1, 2 and 3 was consequently 96.20, 99.75 and 118.26 KWh respectively. Case 1 transport costs an additional 6.63M$ for insulation of pipeline and intermediate tank where operating temperature is -20 ℃ during transport. Figure 3-6 shows the breakdown of cost for the three cases. Case 1 offers low pipeline and compressor cost, however demands an additional cost for an insulation material. Case 2 and 3 have higher pipeline and compressor costs compared to case 1 but do not need insulation material. The annualized CAPEX of case 2 offers the lowest cost of 7.45 M$ among the three cases, however it is similar to the annualized CAPEX of case 1 and 3. The main cost difference comes from OPEX which is the highest in case 1. OPEX of case 1 is 32.9 % and 24.8 % higher as compared to case 2 and case 3 respectively. The pipeline diameter for case 1 is smaller compared to other cases causing low pipeline capital cost, also the compression system cost is lower for case 1 due to the transport at 6.4 MPa but use of refrigeration system for transporting CO_2 at -20 ℃ counter effects and makes the total cost higher for case 1 transport. Figure 3-7 shows the OPEX break down for the three transport scenarios. It can be seen that for case 1, compression cost contributes around 50 % of the OPEX, while refrigeration adds up around 34 % of the OPEX. In case 2, since transport is done at 5 ℃, therefore, chilled water at 0℃ is used

for the liquefaction of compressed CO_2. Case 3 is transport in supercritical phase which with most of the OPEX contribution from the compression energy.

Table 3-4: Breakdown of capital investment for major equipment/services

	Pipeline (M$)	**Compressor (M$)**	**Tank (M$)**	**Insulation (M$)**
Case 1	202.81	3.25	13.34	6.63
Case 2	206.43	3.76	13.34	-
Case 3	214.02	4.15	13.34	-

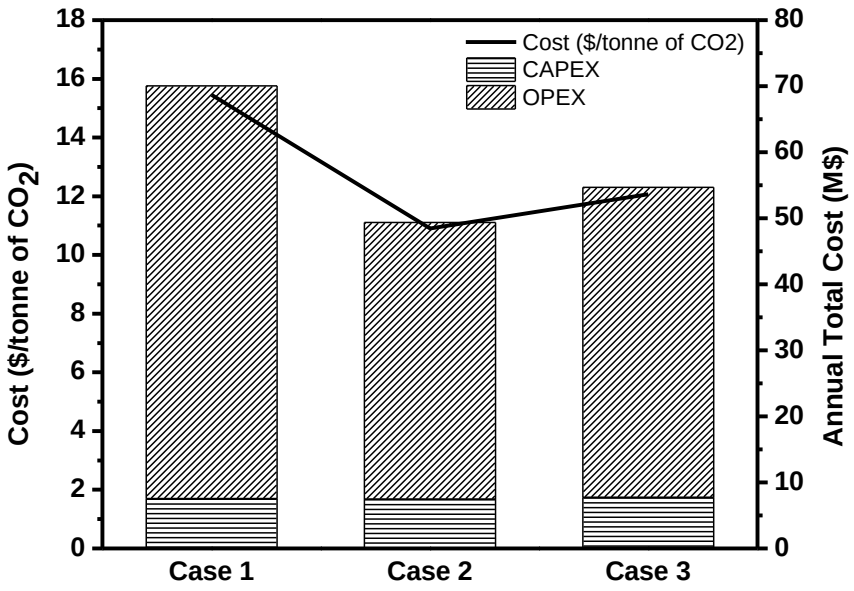

Figure 3-6: Breakdown of total cost for the CO_2 transport

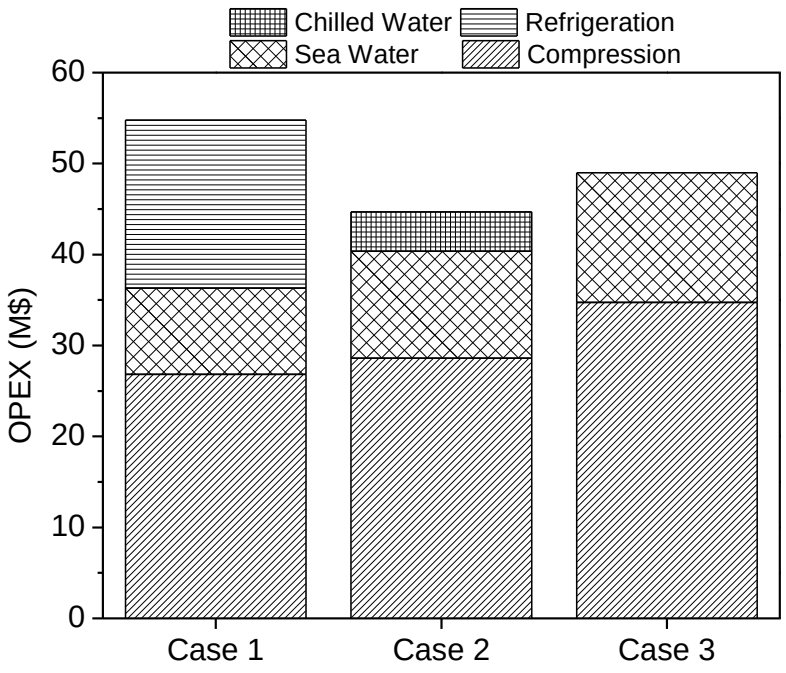

Figure 3-7: Breakdown of OPEX for the CO_2 transport

3.6. Uncertainty in CO_2 Pipeline Transport

There exists a significant level of risks and uncertainty in regard to the implementation of CCS. While doing an economic assessment, a number of uncertainties are involved. This may affect to drive the calculated capacities and hence costs to be different than in the real situations. Therefore, a brief discussion on uncertainties involved in the economic analysis of transport is presented here.

The first uncertainty is the cost of pipeline materials and energy. The cost of pipeline depends mainly on the materials used. Pipelines made of carbon steel can account for as much as 15 to 35 percent of the pipeline cost. Construction and materials cost escalated dramatically in the last decade mainly because of drastic increase in fuel prices. The price of a large-diameter pipe was generally around $500 per ton in 2000. By late 2008, just prior to the start of the global economic crisis, the price of pipe exceeded $2,000 per ton. Most prices then stabilized or receded during the subsequent economic recession in the U.S. and many other countries. However, uncertainty about future trends in material and labor costs cast one of the major insecurity in economic analysis. The second uncertainty is the terrain and topography where the pipeline is installed. Experience with EOR pipelines in the US will not be same for the commercial CCS deployment. CO_2 pipelines used for EOR generally do not pass through urban regions, however it may be difficult to avoid if CCS will be established on a commercial scale. This may add an additional safety cost for the pipelines passing through highly populated areas. Also, some of the terrains may present more challenging situations compared to the others area. For example, pumping booster stations may be required in case of hilly areas which will increase the operational cost of transport. The third uncertainty is the pipeline inlet CO_2 specification including pressure, temperature and composition. In this study, CO_2 from two sources was transported via pipeline

to the storage site. However, in case of multiple CO_2 sources connecting to the big pipeline can cause operational issues. The pressure in CO_2 pipelines is substantially high which on depressurization due to variable CO_2 inlet flow streams can cause very low temperatures and ultimately fracturing. The presence of water content coming from all CO_2 capture sites should be less than 500 ppm, otherwise water dissolved in CO_2 will form carbonic acid which is a serious corrosion threat. The only economic solution is to remove the water from the CO_2 before it enters the pipeline. Most authorities suggest that the impact of drying the CO_2 on the costs of transportation is relatively small. These are some of the basic uncertainties involved in the economic assessment of any CCS project at preliminary stage. However, certainly at this point, when CCS is still in the demonstration and development phase, these economic analyses form the basis to decide the fate of a project.

3.7. Summary

A transport model was defined and then implemented for the Korea case to see the economics of different scenarios. The model was helpful in assessing relationships between various parameters and hence searching low cost transport and storage case. Two coal fired power plants having cumulative power of 725 MW were considered for transport of CO_2 to an offshore storage site 150 km away. Three cases were studied for transport with different operating conditions and case 2 was found to be the most economical at 10.90 US$/t of CO_2 transported. Case 1 offers 15.45 US$/t of CO_2 transported due to use of refrigeration and insulation services but this case may be viable for CO_2 storage at ECBM site. Case 3 transport costs about 12.10 US$/t of CO_2 because of higher operating pressure and hence higher capital and operating cost for the compressors.

CHAPTER 4: CO_2 Liquefaction for Ship Transportation

4.1. Overview

The practice of transporting liquefied and pressurized gases by ship dates back more than 70 years. The regulations for ship transportation, known as the International Gas Code industry (IGO) has been regulated by a United Nations subsidiary, the International Maritime Organization (IMO) since the 1960s [13]. Ship transportation of CO_2 has been taking place for nearly 20 years. The existing fleet of four CO_2 carriers are around 1,000 m^3 each. CO_2 has to be carried at above 5.2 bara to avoid solidification into dry ice. The existing ships carry the cargo at 15-20 bara and around –30°C. For the larger volumes required for CCS purposes it is likely that the CO_2 will be carried at 7-9 bara and down to around –52 °C. This is practically the same cargo condition as that of the significant fleet of semi-ref LPG carriers currently in operation. In fact, six such LPG/ethylene carriers of 8,000 10,000 m^3 in the ownership of IM Skaugen of Norway are approved for the carriage of CO_2 [13]. Most of the recent studies were focused on transportation for specific vessels without taking into account the preceding pipeline transportation and the liquefaction process. Some of the studies included CO_2 liquefaction plants but resulted in high liquefaction energy resulting in high costs. For example, Yoo et al. [8] results correspond to liquefaction energy requirements of 115 kWh per tonne of CO_2; Aspelund and Jordal [11] simulated the CO_2 liquefaction design resulting in liquefaction energy of 105 kWh per tonne of CO_2. Also, most of the reference studies considered CO_2 source sites near the loading terminal, which do not show the complete picture for large scale CO_2 transportation networks. Previous studies assumed CO_2 source to be the post-combustion capture facilities and none of the researches considered the effect of pre-combustion capture facility on the design, operation and cost of transport. In this chapter, liquefaction designs are developed while taking the type of

capture facility into account. Three different scenarios for post-combustion and pre-combustion each have been studied on the basis of location of the liquefaction plant. Therefore, depending on the type of capture facility, quantity of CO_2 to be transported and distance to loading terminal, the right thermodynamic conditions for the transportation of CO_2 to the ship loading terminal and the location of the liquefaction plant can be decided. Finally, an economic analysis is performed for various scenarios in order to evaluate the feasibility of CO_2 transport from source sites to the ship loading terminal including liquefaction plant.

4.2. Liquefaction system

Liquefaction is a vital component for ship transportation of CO_2. There are basically two processes in practice to compress and liquefy CO_2 commercially. The first one is the low pressure process making use of an external refrigeration system to achieve the required cooling for condensation of the gaseous CO_2 after it is dried and compressed to about 17 bar. The choice of refrigerant for this process is mostly ammonia because of its efficient performance, easy availability and environment friendly characteristics compared to other refrigerants. Figure 4-1 shows a simple flow diagram for this process. The low pressure captured CO_2 stream is compressed using two stage compressor with inter-cooling to remove any water present in the stream. The CO_2 is then fed to adsorption dryer to remove most of the water which couldn't be separated during compressor inter-cooling. The water free CO_2 stream then enters the CO_2 condenser where it is liquefied using ammonia refrigeration system and finally stored in the storage tank. Duan et al. [46] proposed a method to liquefy CO_2 using ammonia refrigeration driven by exhaust heat and then making use of pump to raise the CO_2 stream pressure to transport pressure. Alabdulkarem et al. [47] simulated CO_2 liquefaction cycles making use of different refrigerants including R134a, CO_2, NH_3 and

C_3H_8. They found C_3H_8-NH_3 cascade cycle to be the least power consuming. Dopazo et al. [48] developed CO_2-NH_3 cascade refrigeration system and validated it against experimental data. Raja et al. [49] proposed the CO_2 liquefaction by making use of air separation unit (ASU). This work suggested the use of cryogenic cooling system employed in ASU to achieve partial liquefaction of CO_2. Compressors may be used prior to cryogenic cooling system to further facilitate the liquefaction process. However, this study didn't make any comparison with conventional CO_2 liquefaction processes with respect to energy and cost savings.

The second method to liquefy CO_2 is high pressure compression with free liquid expansion. This process uses self-refrigeration to liquefy the CO_2 that is compressed beyond the critical point. Figure 4-2 shows the simple flow diagram of the high pressure compression and adiabatic expansion process. Once the CO_2 reaches the critical pressure (73.8 bar), it is cooled below its critical temperature (31.1 °C). It is then expanded adiabatically where approximately 50 % of the total expanded flow is liquefied, while the cold CO_2 vapor is returned back to the 3rd stage of compression and is maintained in a closed, recycle loop. The low pressure CO_2 stream enters the three stage compressor where it is compressed along with inter-cooling using cooling water to reduce moisture content. After the 2nd stage of compressor, the CO_2 stream is sent to adsorption dryer section to remove any excess moisture. It is then compressed in the 3rd stage to a pressure of 73.8 bar before it is expanded using a Joule-Thompson expansion valve. The liquid CO_2 is produced at approximately 17 bar and -22 °C. The flashed cold CO_2 vapor is recycled back to 3rd stage of compressor.

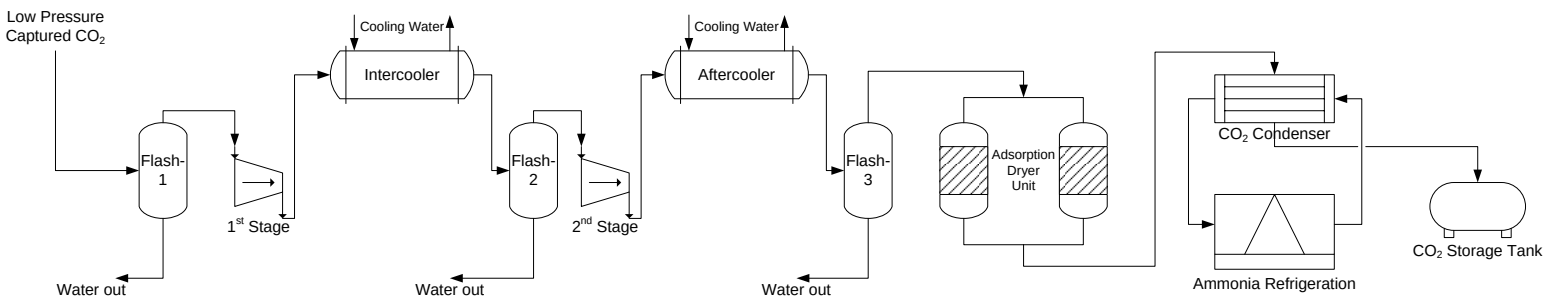

Figure 4-1: Process flow for CO_2 Liquefaction Using Ammonia Refrigeration

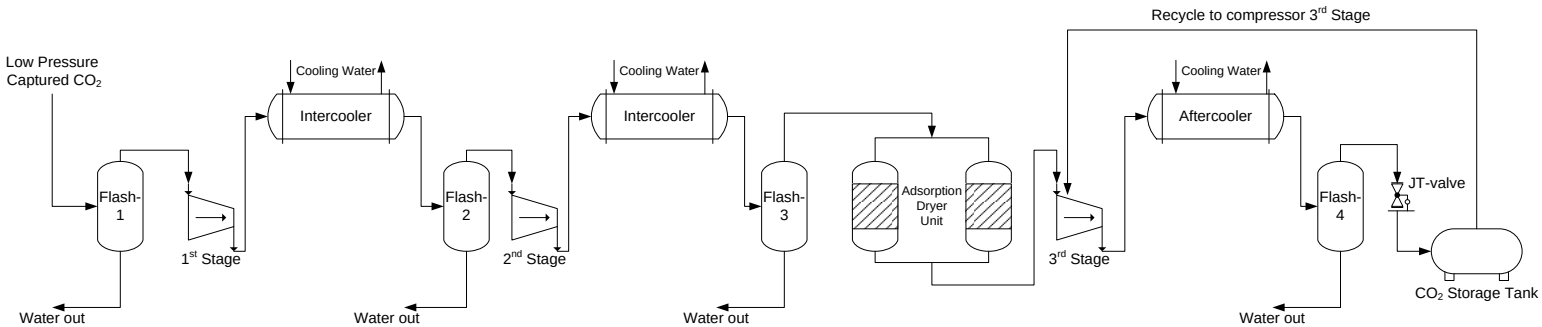

Figure 4-2: Process flow for CO_2 Liquefaction Using Self-Refrigeration

Each of the CO_2 liquefaction method has its cons and pros. Current industrial practices favor CO_2 liquefaction using external refrigerant process because of lower unit operating energy cost. However, with the desired design specifications (i.e. -52 °C, 6.5 bar) for large scale commercial ship transport, external refrigerant process will require much lower temperatures to achieve CO_2 liquefaction than the currently employed industrial process. Therefore, this chapter will stay focused on high compression with free liquid expansion process. Also, CO_2 liquefaction using free liquid expansion does not employ any external refrigerant, hence a more environment friendly method. Many researchers have recently developed CO_2 liquefaction process using free liquid expansion. Barrio et al. [28] studied ship based transport of CO_2 and reported liquefaction energy of 110 kWh per tonne of CO_2; Aspelund and Jordal [11] proposed liquefaction process design for ship transport with liquefaction energy of 105 kWh per tonne of CO_2. They also performed sensitivity analysis by varying nitrogen content in the feed and reported a linear energy requirement increase of 6 kWh per mol of nitrogen. Yoo et al. [8] studied four scenarios for CO_2 transport and simulated CO_2 liquefaction process using free expansion. Their results showed a liquefaction energy requirement of 115 kWh per tonne of CO_2. Lee et al. [50] modified the basic design proposed by Aspelund and Jordal [11] and suggested two alternative designs. This was done by making use of cold energy from flashed CO_2 streams and optimization of compression ratio. The results showed reduced liquefaction energy consumption of 98.9 kWh per tonne of CO_2.

The liquefaction processes in this study has been simulated by using the Aspen Plus® software. Soave Redlich Kwong (SRK) equation of state is used as a property method. The sea water used for cooling compressed CO_2 streams is assumed to be at 10 °C. A minimum temperature approach of 5 °C is assumed

for both the sea water and process heat exchangers. Compressors are assumed to have an isentropic efficiency of 82 %. Flash drums are assumed to have no pressure drop with operational efficiency of 100 %. Final liquid CO_2 specifications are set at -52 °C and 6.5 bar.

4.3. Liquefaction system for post-combustion capture facility

The base design studied in this work for CO_2 liquefaction from post-combustion capture facility was proposed by Lee et al. [50] which is a modified design proposed by Aspelund and Jordal [11]. However, the design proposed by Lee et al. [50] can be further modified and optimized in order to improve the liquefaction energy requirement. To do so, there are two major approaches that can be applied to reduce the operating energy of the original design. First, pressure energy from the cold CO_2 vapor produced during the last stage of expansion can be extracted by using a turbo expander. The expansion through an expansion valve does not remove energy from the gas but moves the molecules father apart under the influence of intermolecular forces. On the other hand, expansion through an expansion turbine can remove energy from the gas in the form of external work. Also, an isentropic expansion through an expander would always be the most effective means of lowering the temperature of a gas. Between any two given pressures, an isentropic expansion will always result in lower final temperature than will an isenthalpic expansion from the same temperature [37]. Although, an expansion turbine effectively reduces the temperature of a gas compared to an expansion valve, it is accompanied by some practical issues. The biggest disadvantage of a turbo expander is the cost. It is a piece of rotating equipment, and as such is much more complex and costly compared to an expansion valve. Also, the operation of an expansion turbine is limited by the critical control of operating conditions, as liquid may form and cause erosion to turbo expander leading to mechanical failures along with production losses.

Second, the process heat exchangers employed to exchange cold energy available from flashed CO_2 vapor can be optimized to improve the overall energy consumption of liquefaction process. The work input to compressor basically depends on two parameters, the compression ratio and the inlet temperature of the compressor. The higher the inlet temperature of gas to compressor, the more work input is required. Therefore, it is necessary to utilize the cold energy available from the flashed CO_2 vapor at the right place in order to attain the least compressors work requirements. In order to assess the process improvement, all the input parameters are kept consistent with the study of Lee et al [50]. Table 4-1 shows the flue gas composition used in this study same as used by Lee et al [50]. The gaseous CO_2 feed stream is compressed using four stage compressor with intercoolers using sea water to cool down the compressed streams. The flash drums are placed strategically to remove any excess water content in the CO_2 stream. Flash drums are widely used in industry for the separation of vapor-liquid mixtures in terms of cost and energy efficiency. The main purpose of flash drum in this study is to separate liquid from vapors in order to ensure compressor safety. Most of the water is removed in the first flash drums before compression and cooling. As the gas is compressed and cooled, most of the remaining water is condensed and removed in the flash drums prior to the compressors. The recovered water is subsequently sent to flash drum before first compression stage to recover the CO_2 dissolved in the water at high pressure. Based on the industrial experience and previous research studies, it is assumed that CO_2 product can contain maximum 50 ppm water content.

Figure 4-3 shows the process flow diagram for the modified design in this study. The pressurized CO_2 stream *13* after fourth compression stage is sent to condenser for the removal of any remaining water and volatile gases. It is important to remove volatiles in order to avoid dry ice formation, since the

CO_2 transport in ship is done near triple point. The pressurized CO_2 stream *15* at 52 bar, free from water and volatile gases, is expanded in three stages using a Joule-Thompson (J-T) valve. In the first expansion stage, the pressure of CO_2 is reduced to 29.2 bar. A mixture of CO_2 liquid and gas is produced at -7.4 °C which is separated using a *flash-6* drum. The cold CO_2 vapors produced from first expansion are sent to *process HX-2* where it cools down the incoming gaseous CO_2 feed. The stream after exchanging heat is sent to *flash-4* prior to input of fourth compressor stage. The liquid CO_2 produced from first expansion (stream *18*) is subjected to a second expansion stage through J-T valve to further lower the temperature. A mixture of CO_2 liquid and gas produced at -34.2 °C is separated in *flash-7* where cold CO_2 vapors are first sent to *process HX-1* for exchanging cold energy with incoming CO_2 stream *5* and then passed through *process HX-1* to exchange heat with incoming CO_2 stream *1*. The flashed CO_2 vapors after passing through both process heat exchangers is sent to the third compressor stage. The liquid CO_2 stream *21* produced from second expansion is sent to third expansion valve where liquid CO_2 is produced at -52 °C. The flashed CO_2 vapors from third expansion are passed through a turbo expander to extract some of the work and further lower the temperature. The cold CO_2 vapors stream *24* then exchanges heat through *process HX-1* and is sent to second compressor stage.

The amount of heat exchanged through process heat exchangers is an important variable in determining the work input required for compressor. The cold vapors stream *17* exchanges heat through *process HX-2* and then sent to fourth compressor stage. There is a trade-off to be made between inlet temperature to first compressor stage and inlet temperature to fourth compressor stage. If more cold energy is sent to inlet of fourth compressor stage, the inlet temperature of first stage compressor increases or vice versa.

The work input to the compressors is minimized by setting the *process HX-2* outlet streams (*27*and *28)* temperatures at 15 °C. Similarly, the flashed CO_2 cold vapor in stream *20* is first sent to *process HX-1,* then passed through *process HX-2* and finally sent to inlet of third compressor stage. If the incoming CO_2 stream *5* is given more cold energy then the temperature at inlet of first compressor stage increases or vice versa. The work input to compressor stages is minimized by setting the temperature of stream *6* to 6 °C. The result shows that in contrast to the base design liquefaction energy of 98.9 kWh per tonne of CO_2, the modified design has lower liquefaction energy requirement of 97.3 kWh per tonne of CO_2. This energy saving has a great impact on the operating costs since the liquefaction process constitutes most of the total cost as will be discussed in the results section.

Table 4-1: Input Stream Specification of CO_2 Liquefaction for Post-Combustion Source Facility

Component (mol%)	
CO_2	94.39
H_2O	5.61
Volatiles	Traces
Pressure (bar)	1.01
Temperature (°C)	35.0

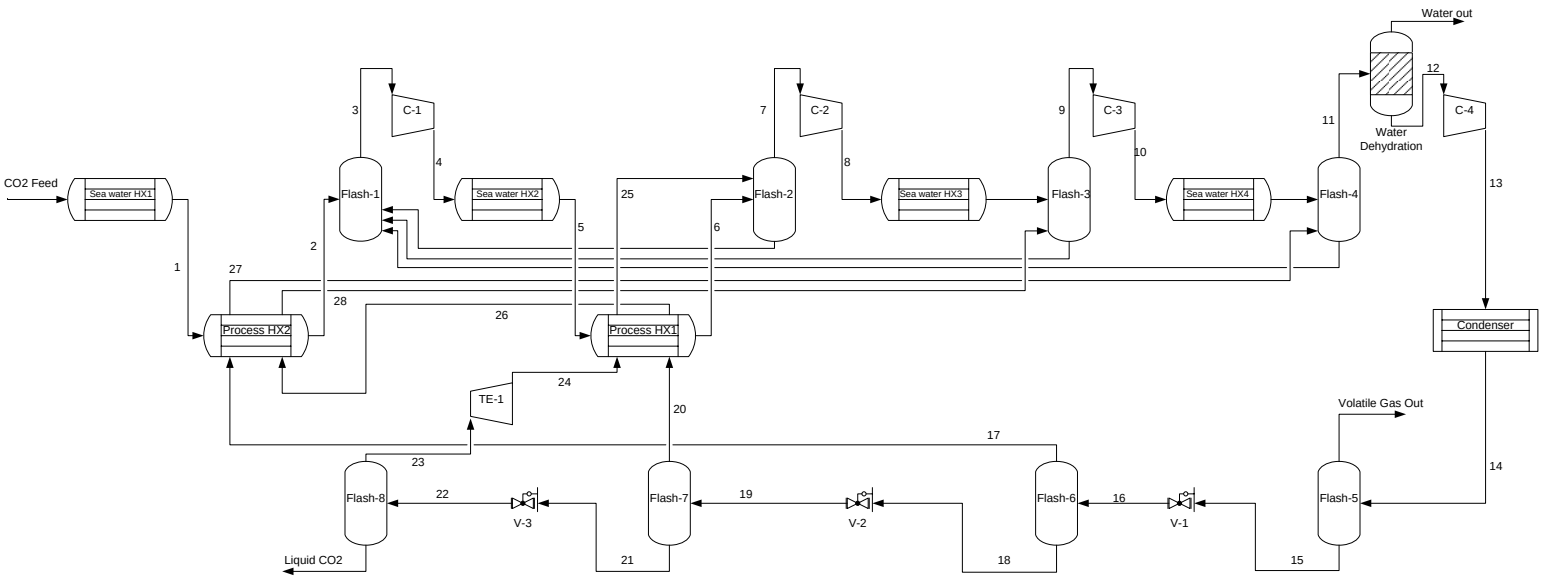

Figure 4-3: Process flow of CO_2 Liquefaction for Post-combustion Source

4.4. Liquefaction system for pre-combustion capture facility

The temperature, pressure and composition of flue gas from the pre-combustion capture facility differs that of post-combustion flue gas conditions the way CO_2 is captured. The capture of CO_2 at the pre-combustion plant often employs physical solvent which on multiple recovery stages produces CO_2 streams at different pressure and temperature. Hence, a new liquefaction process for a pre-combustion capture facility is proposed in this study. The temperature, pressure and composition of CO_2 feed streams are taken from the KRW gasification process. The KRW gasification process employs glycol as a physical solvent for the removal of CO_2 from the flue gas. CO_2 can be recovered by flashing the rich solvent in three stages. The details of the process can be found in the report by Doctor et al. [51]. Since the rich solvent is flashed in three stages for CO_2 recovery, the input to liquefaction system consists of three CO_2 streams at different thermodynamic conditions. A summary of CO_2 feed streams used in this process are presented in table 4-2.

The process flow diagram of liquefaction system for pre-combustion capture facility is shown in figure 4-4. One of the CO_2 feed stream namely CO_2-*1* enters the flash drum before the first compression stage, while the other two CO_2 streams namely CO_2-*2* and CO_2-*3* enter the flash drum before the start of the second compression stage. In this way the captured CO_2 stream from pre-combustion capture facility gets the advantage of utilizing less work for compression because part of it is already at higher pressure. The compressed CO_2 stream free from water and volatile gases is then subjected to three stage expansion using Joule-Thompson valves. The compressed CO_2 stream *18* at 52 bars is expanded through J-T valve at first stage and pressure is reduced to 29.2 bar. The expanded CO_2 stream is then sent to a flash drum, where CO_2 vapor stream *20* is separated from liquid CO_2. The cold vapor stream (*20*) is used to cool down the incoming compressed CO_2 stream *9* from second

compression stage. The streams exchange heat using *process HX-3* and then it is sent to fourth compression stage. Liquid CO_2 from first expansion stage is then sent to second expansion J-T valve where its pressure is reduced to 12.9 bar. After the second stage expansion, more CO_2 cold vapors are produced which are separated from liquid CO_2 using flash drum. The cold CO_2 vapor stream *23* produced from second stage expansion is used to decrease the temperature of incoming CO_2 stream *1* and finally sent to third compression stage. Liquid CO_2 from second expansion stage is then subjected to third and final expansion where its pressure is reduced to 6.5 bar. The pressure of vapor stream *26* produced during third expansion stage is further reduced to 3.5 bar by allowing it to flow through a turbo expander where some of the work is extracted. The temperature of the flashed vapor CO_2 stream *26* after passing through expander is at -77.7 ^{o}C which then exchanges cold energy with incoming CO_2 stream *4* using *process HX-2* and is finally sent to second compression stage. Approximately 59.5 % of the expanded CO_2 flow is converted to liquid CO_2 at -52 ^{o}C and 6.5 bar which is sent to the storage tank. The result shows that liquefaction energy of 71.89 kWh per tonne of CO_2 is required for pre-combustion source facility. The liquefaction energy requirement for pre-combustion source facility is 25.41 kWh per tonne of CO_2 lower than that of post-combustion source mainly because of two reasons. Firstly, a part of CO_2 feed stream in case of pre-combustion capture facility is available at higher pressure which result in overall less compression work requirement. Secondly, the temperature of CO_2 feed streams from pre-combustion capture process is low compared to that of CO_2 stream captured from post-combustion process which leads to a lower compression energy consumption.

Table 4-2: Input Stream Specification of CO_2 Liquefaction for Pre-Combustion Source Facility

Component (mol%)	**CO2-1**	**CO2-2**	**CO2-3**
CO_2	0.973	0.984	0.926
CO	0.000	0.000	0.001
H_2	0.019	0.010	0.010
H_2O	0.000	0.000	0.017
CH_4	0.006	0.006	0.034
O_2	Traces		
Pressure (bar)	1.01	3.50	6.89
Temperature (^oC)	0.00	2.90	5.80

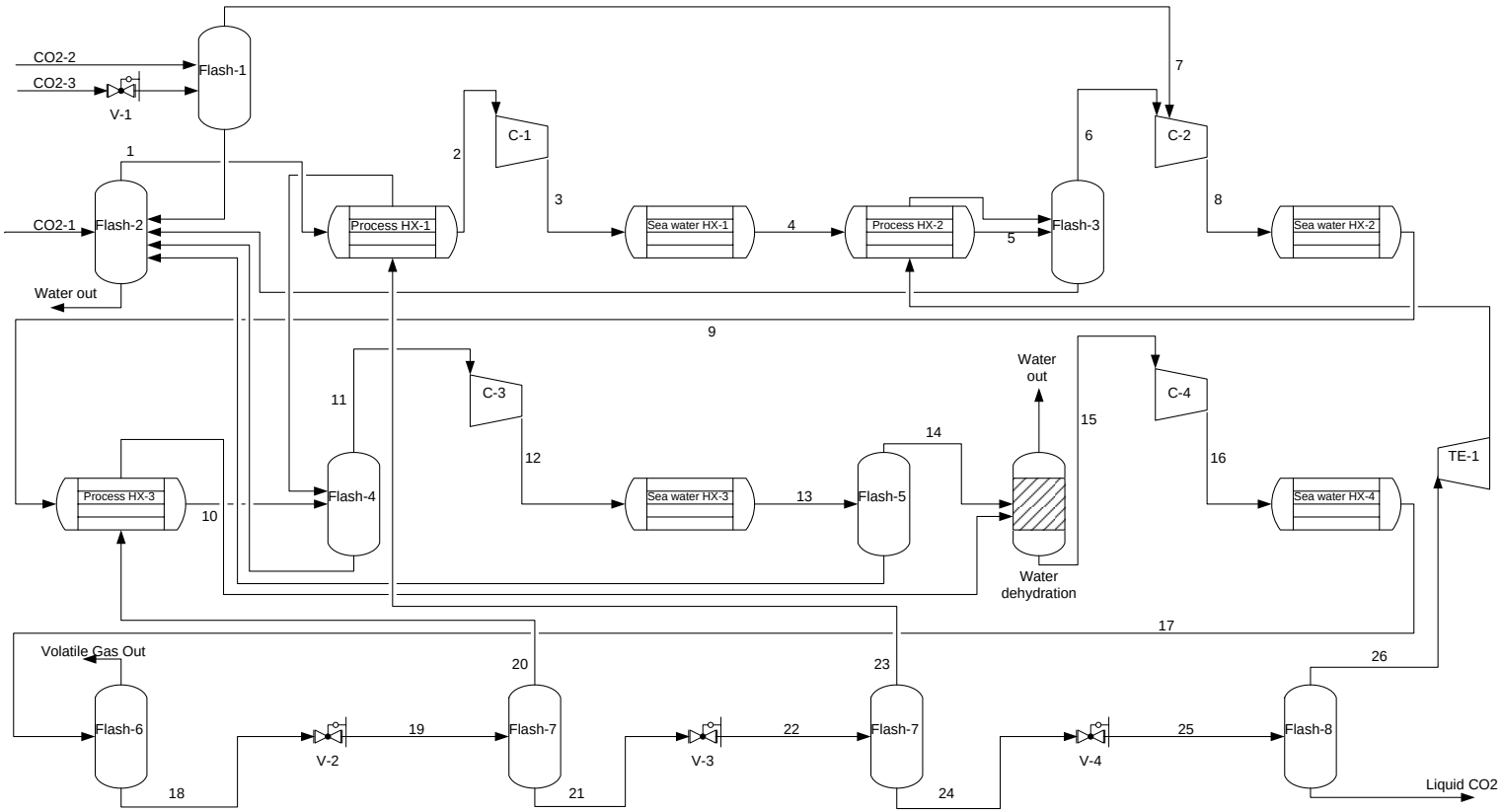

Figure 4-4: Process flow of CO_2 Liquefaction for Pre-combustion Source

4.5. Liquefaction plant location decision

The CO_2 transport scenarios in this chapter are based on the type of CO_2 capture facility and location of the liquefaction plant. The types of CO_2 capture facilities in this study is limited to post-combustion and pre-combustion type. The location of liquefaction plant is categorized accordingly to three different cases:

4.5.1. Case 1

In this case the capture plant, liquefaction plant and intermediate storage are located near the ship loading terminal. This case assumes all the above mentioned facilities are located near the sea shore where loading terminal is located as shown in figure 4-5(a). CO_2 is captured at the source site and then sent to the liquefaction plant present in the same location. Depending on the type of capture facility (post-combustion or pre-combustion), CO_2 is liquefied following the process detailed earlier. It is then sent to storage tanks at the loading terminal site where liquefied CO_2 is stored until it is loaded on the ships. Power plants or large CO_2 sources located along the coastal areas have the advantage that they are able to ship liquefied CO_2 more easily compared to sources located in the mainland areas. Also in the real world, most power plants are preferably located near the coastal areas because of cheap water availability.

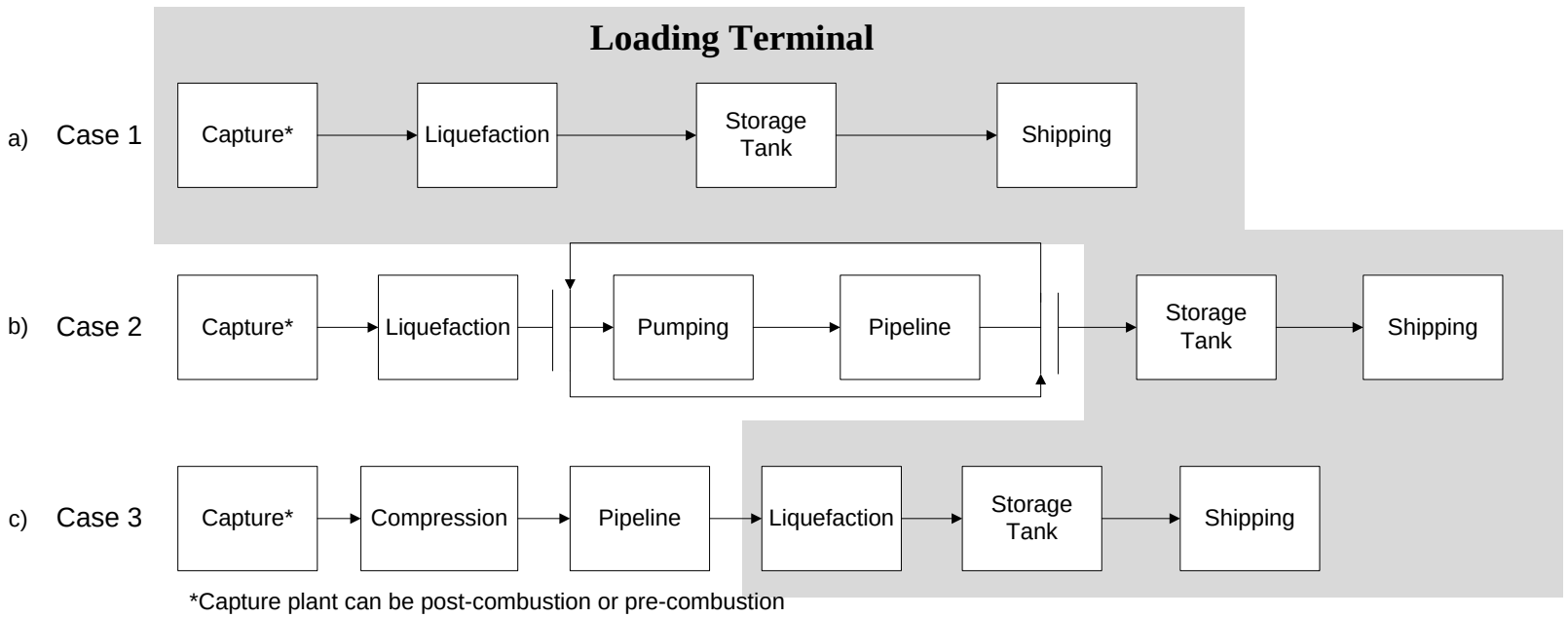

Figure 4-5: Transport Scenarios Based on the Liquefaction Plant Location

4.5.2. Case 2

In this case the capture and liquefaction plant are located far from the intermediate storage and ship loading terminal. This case assumes the capture unit and liquefaction plant are close to each other but far from the loading terminal as shown in figure 4-5(b). CO_2 captured at the source site is first liquefied using the process previously detailed. The liquefied CO_2 at -52 °C and 6.5 bar is then transported via insulated pipeline to the loading terminal where it is stored in the intermediate storage tanks. Contrary to the supercritical pipeline transport, in this case the CO_2 does not need to be compressed to a very high pressure. Once liquefied, pumps can be used to transport liquid CO_2 through the pipeline to the loading terminal site. However, CO_2 pipeline transportation in liquid phase requires pipelines to be insulated and operating conditions should be well controlled in order to ensure safe pipeline operation. Although the pipelines are insulated, some heat influx leaks into the pipeline from the surroundings can cause an increase in CO_2 temperature. The increase in liquid CO_2 temperature due to heat leak and pressure drop due to frictional forces across the pipeline length can cause the formation of CO_2 vapor after a certain distance. In order to ensure no vapor formation and safe pipeline operation, a concept of re-chilling and pumping has been evaluated in this study for the transport of CO_2 in liquid phase. Re-chilling and pumping is a simple concept employing intermediate chilling stations to decrease the temperature of CO_2 stream before any vapor is formed and then pumping it again towards the loading terminal. A similar concept has been also employed in other cryogenic and food chain logistics. Figure 4-6(a) represents the temperature variation along the 500 km long pipeline, whereas figure 4-6(b) shows the operating pressure for a specific distance along the pipe length. The location of chilling and pumping stations along the pipeline can be seen in figure 4-6 for the annual transport capacities of 1 Mt, 5 Mt and

10 Mt of CO_2. The transport distance assumed in this case is 500 km. For 1 Mt of CO_2 transport capacity, chilling and pumping station is required after 260 km, while for transport capacity of 5 Mt CO_2 chilling and pumping station should be located after 455 km. However, no chilling and pumping station is required for 10 Mt transport capacity for the total transport distance of 500 km. This means that with increasing pipeline diameter for larger CO_2 transport capacities, the degree of temperature rise due to heat leaks into liquid CO_2 and pressure drop along the pipeline are not as drastic as for the smaller CO_2 transport volumes. Once the liquid CO_2 reaches the loading terminal site, it is stored in the insulated intermediate storage tanks. Due to some small unavoidable heat leaks into storage tank, boil-off gas (BOG) is generated which must be dealt with. A re-liquefaction plant is therefore installed at the loading terminal site to re-liquefy BOG generated from the intermediate storage tanks.

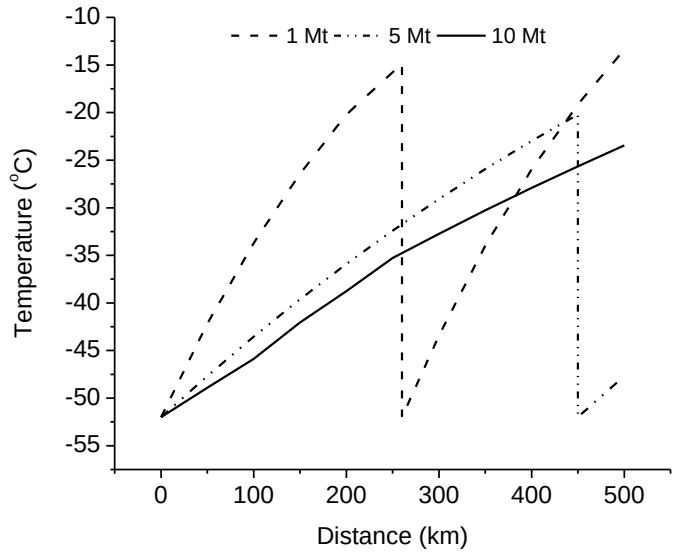

(a) Temperature Change along the Pipeline

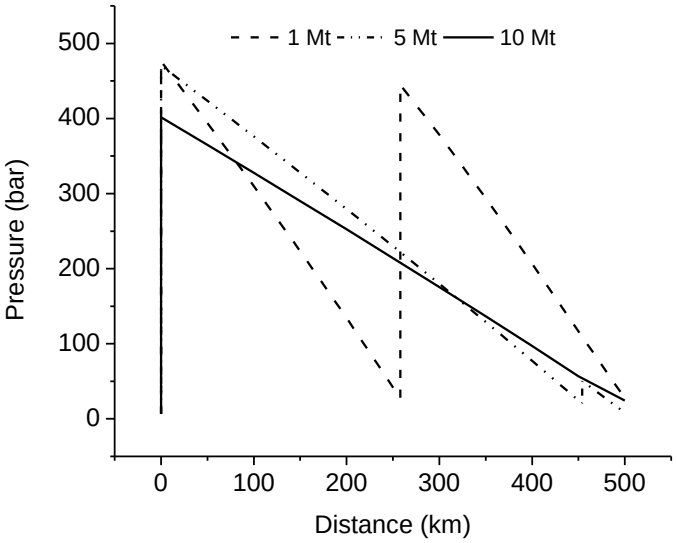

(b) Pressure Change along the Pipeline

Figure 4-6: Location of Chilling and Pumping Stations along the Pipeline for Case 2

4.5.3. Case 3

In this case the capture plant is located far from the ship loading terminal, while liquefaction plant is located at the ship loading terminal. In this case, CO_2 transport from capture plant to loading terminal site is done in supercritical phase. Captured CO_2 is compressed using multistage compressor to a pressure higher than 73.8 bar across supercritical region and then transported through a pipeline as shown in figure 4-5(c). Depending on the total transport distance, supercritical CO_2 pumps may be used in conjunction with compression system to reduce overall power load of compressors. In this study, the compressed CO_2 is assumed to be delivered at liquefaction plant at 52 bar and 15 °C. The high pressure CO_2 can then be liquefied by expansion in three stages. The CO_2 vapor produced at each expansion stage is sent for recompression at the appropriate pressure. However, there is one basic difference with the liquefaction system described earlier compared with this type of system configuration. Since the inlet CO_2 is available at high pressure, three compression stages will meet the needs of the liquefaction system. This case requires setup of CO_2 compressors at two locations (i.e. at capture site and liquefaction site) which increase the capital cost. An alternative scenario is to compress the CO_2 at the capture site, to transport it in supercritical phase through the pipeline and then to decrease the temperature of the high pressure CO_2 using an external refrigeration unit at the liquefaction plant in order to avoid the installation of CO_2 compressors at two different locations. The high pressure and low temperature CO_2 (say 100 bar, -45 ^{0}C) can then be expanded to 6.5 bar pressure into product tank to produce liquid CO_2. However, such process will produce CO_2 boil-off gas which cannot be processed at the facility and may pose safety threat in case of emission to the atmosphere. Approximately 4 % of the total CO_2 mass flow is converted to vapors if the compressed CO_2 at 100 bar and -45 °C is expanded to 6.5 bar. In this study,

CO_2 compressors at dual location and liquefaction plant using multistage expansion process have been assumed for the purpose of economic analysis.

All of the above three cases have been investigated together with each type of capture facility i.e., post-combustion and pre-combustion. The intermediate storage is assumed to be present at the ship loading terminal in all three cases.

4.6. CO_2 Terminal

Regardless of the type of transport, intermediate storage is a vital component of CO_2 transport chain. Intermediate storage for CO_2 transportation becomes particularly important in cases where CO_2 from multiple sources is transported to either a single storage site or multiple storage sites. There are two advantages for intermediate storage tank. Firstly, a steady CO_2 flow can be provided to the storage site which is important for a safe transmission and uninterrupted safe operation of the storage site. Secondly, in case of regular or unforeseen maintenance at the storage site, an intermediate tank will provide a buffer between CO_2 capture and storage process. This kind of buffer is especially important if the non-operational time of injection at the storage site is short, usually less than 24 hours. In this study, the tank capacity selected to hold liquid CO_2 is equivalent to 24 hrs of liquefied CO_2 product.

Liquid CO_2 exists in equilibrium with its vapor inside the tank with the tank pressure being dependent solely on the temperature. The liquid CO_2 can coexist with its vapor and solid at -56.6 °C and 5.2 bar known as the triple point of CO_2. Below triple point condition, there can be an equilibrium between vapor and solid dry ice. However, liquid CO_2 does not exist below the triple point. In fact, it is impossible to have liquid CO_2 at an atmospheric pressure. In an event of some malfunctioning if the tank is vented to atmospheric pressure, the temperature inside the tank will be that of the dry ice (-78.3 °C). It will cause the storage tank to be subjected to extreme stresses

and may suffer a fracture failure during or after this exposure to such a low temperature. The same phase change in CO_2 is seen when a portable CO_2 fire extinguisher is used. The high pressure liquid CO_2 expands adiabatically and converts itself to dry ice at -78.3 °C. In order to ensure safe operation of this critical section, the tank is designed at the operating pressure of 6.5 bar for which the corresponding design temperature is -52 °C. Also, a well-defined operational strategy is important for the safe operation of tank during different stages. The tank operation can be defined in three modes, i.e. loading mode, filled idle mode and unloading mode. During the loading mode, a continuous liquefied CO_2 stream from the liquefaction section is entering the storage tank. The liquid transferred to the tank results in a level built up in the storage vessel and compression of the vapor phase above the liquid. This vapor has to be removed from the tanks to prevent excessive pressure built up in the tanks. A continuous vapor stream is removed from the storage tank and returned to the liquefaction plant during filling of the tanks. Once the tank is filled with liquid CO_2, it is considered to be in filled idle mode until the tank is unloaded. The safe liquid CO_2 hold up during filled idle mode depends on ambient temperature, tank insulation material, insulation thickness and filling level of the tank. Depending on the shipping schedule, the tank is under unloading mode when liquid CO_2 is filled from the storage tank to the ship. The removal of liquid CO_2 from the storage tank will reduce the pressure which can eventually result in solidification of the tank content. Hence, there is a need to compensate the tank pressure by feeding CO_2 vapor. For this purpose, the vapor generated by CO_2 loading in the ship will be returned from the ship into the storage tanks. This will prevent pressure reduction in the tank and pressure built up in the ship [52]. The operational dynamics of the CO_2 terminal are discussed further in chapter 5.

4.7. Results and Discussion

4.7.1. Liquefaction Energy

Liquefaction plant is the most energy consuming section in CO_2 transport chain. On an amortized scale, liquefaction energy can contribute up to 85 % of the total cost and 90 % of the OPEX. Figure 4-7(a) and 4-7(b) show the cost break down in terms of CAPEX and OPEX for post-combustion and pre-combustion capture facilities respectively. For a project life of 30 years, annual operational expense constitutes more than 95 % of the total cost. The liquefaction process for post-combustion capture facility studied in this work offers a lower liquefaction energy requirement compared with other studies found in literature. For CO_2 liquefaction from pre-combustion capture facility, a new process has been proposed which makes use of high pressure energy available in the feed stream. Figure 4-8 shows the liquefaction energy comparison for post-combustion and pre-combustion capture facilities. The liquefaction process for pre-combustion capture facility has 26 % lower energy requirement compared to that of post-combustion capture facility. However, it is important to mention that the lower energy requirement for pre-combustion capture facility is based on the liquefaction process only and does not take account of capture process performance. In order to analyze the bigger picture, the comparison should be done for the cost and performance of not only the liquefaction plant but also the capture plant. During the recent years, many researchers have done studies on various capture systems and analyzed them technically and economically. A report issued by Zero Emissions Platform (ZEP) [13] compared costs of CO_2 capture from different technologies for different coal qualities. According to this report, CO_2 capture cost for hard coal with post-combustion is approximately 47 US$/t$CO_2$, while the capture cost for hard coal with pre-combustion capture is around 56 US$/t$CO_2$. Another report issued by International Energy Agency (IEA) [53]

also compared cost and performance of various CO_2 capture systems from power generation. This report estimated an average capture cost of 58 US$/t$CO_2$ and 43 US$/t$CO_2$ for post-combustion and pre-combustion capture systems. It means that the performance of the two capture technologies is not consistent as reported by different studies as shown in table 4-3 [13, 53]. The reason being is that comparing the cost and performance of capture systems is not straightforward as the boundary conditions are frequently different. However, the general conclusion that emerges from recent studies is that, for coal based power plants, post-combustion capture tend to have lower capital costs and cost of electricity without capture. On the other hand, pre-combustion capture plants tend to be less expensive when current CO_2 capture systems are added. This analysis suggests that pre-combustion plants can be an attractive option for the power generation if CCS technology is implemented on a large scale. In that scenario, lower liquefaction energy for pre-combustion capture facility can be an additional cost reducing element. Today, however, pre-combustion technology (IGCC plants) is still in the early stages of commercialization and lack reliability compared to conventional post-combustion plants.

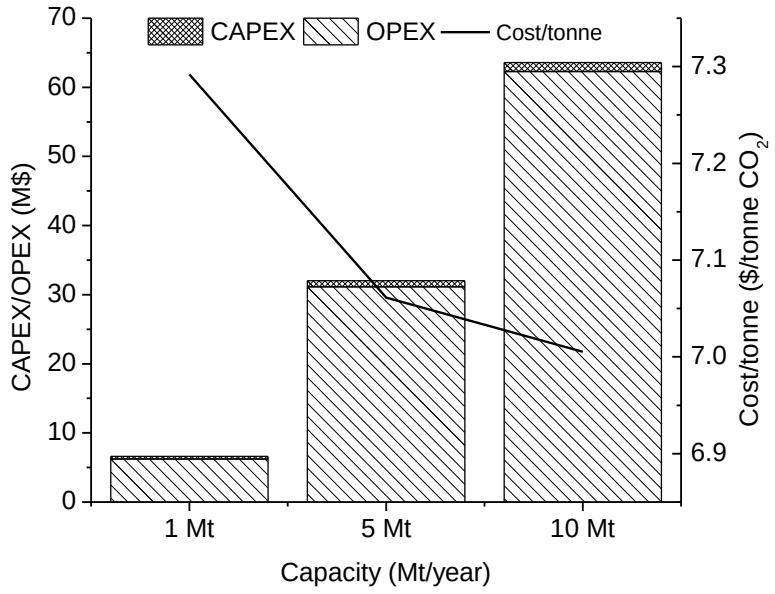

(a) Post-Combustion Source Facility

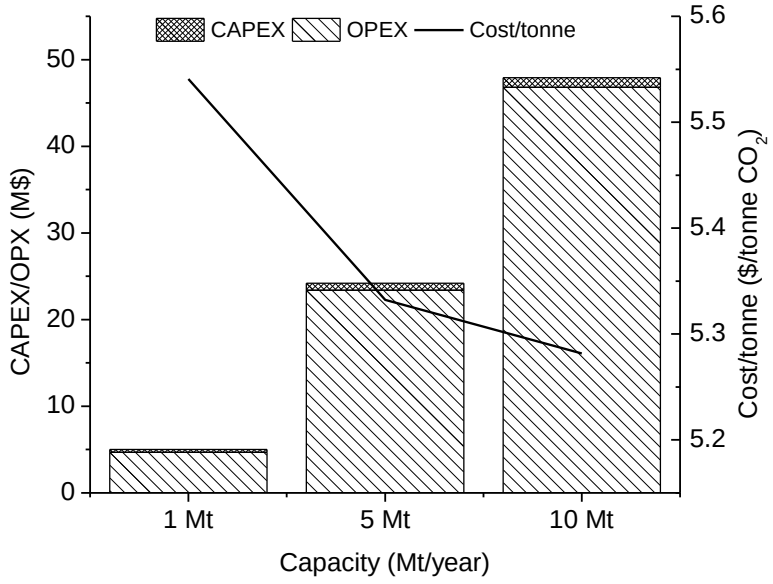

(b) Pre-Combustion Source Facility

Figure 4-7: Cost Break Down in terms of CAPEX, OPEX and Unit Cost

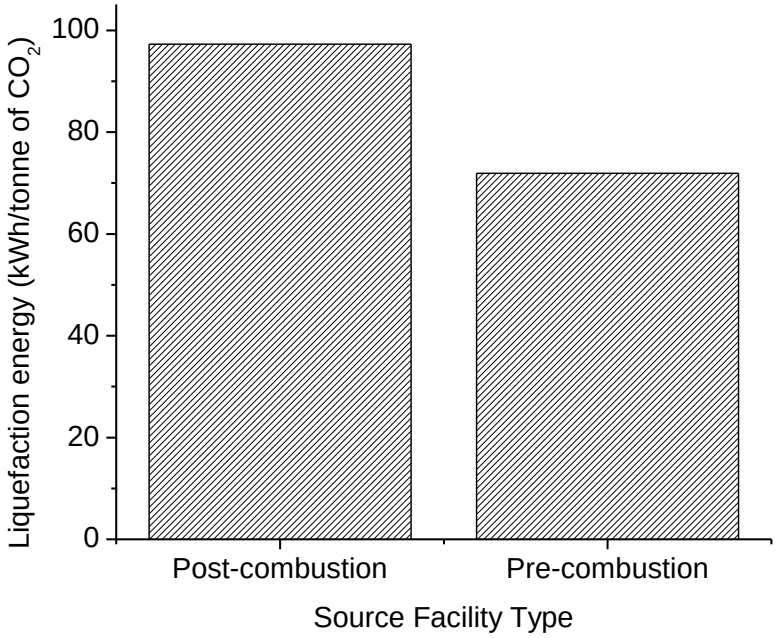

Figure 4-8: Liquefaction Energy Requirement Based on Source Facility Type

Table 4-3: Summary of Reported CO_2 Capture Cost for Post and Pre-combustion Capture Technology

Report	Year	CO_2 Capture Cost (US$/t$CO_2$)	
		Post-Combustion Capture	Pre-Combustion Capture
IEA	2011	58.0	43.0
ZEP	2009	46.3	55.3
Global CCSI	2009	74.0	41.0
Rubin	2008	46.3	21.0
McKinsey	2008	29- 44	35- 44
MIT	2007	40.0	29.0
NETL/DOE	2007	63.3	35.7
EPRI	2007	51.8	35.74
ZEP	2006	41.8	38.3

*Exchange Rate: 1 US$= 0.72 €

4.7.2. Economics

The cost of transporting CO_2 for different cases has been calculated by using information on both the capital investment and operation cost from a number of references available in literature. Three different transport capacities of 1 Mt, 5 Mt and 10 Mt have been selected for the transport distance of up to 500 km. The capital cost includes the costs for compressor, pipeline, pump, turbine, insulation and storage tank. The pipeline cost is mainly influenced by pipeline diameter. The pipeline diameter is an important parameter in order to have an accurate look at the economical aspect of CO_2 transport. Therefore, pipeline diameter is calculated based on economics-related optimal design using equation 4.1 which was originally derived by Peters [36] for the calculation of economic pipe diameter assuming average numerical values for some of the less critical parameters.

$$D_{opt} = 0.363 \left(\frac{Qm}{\rho}\right)^{0.45} \rho^{0.13} \mu^{0.025} \qquad \ldots\ldots \text{Eq. } 4.1$$

Where D_{opt} is the optimal pipeline diameter, Q_m is mass flow rate, ρ is CO_2 density and μ is CO_2 viscosity. The cost calculation method for the pipeline and other utilities is same as outlined earlier in section 3.5.

Figure 4-9 (a-d) shows the cost results for different scenarios based on the type of capture facility and liquefaction plant location for different cases as described earlier. A distance of zero along the horizontal axis represents the case 1 result in which capture facility and liquefaction plant are located near the loading terminal site. As the transport distance increases, the transport cost for smaller capacities increase significantly compared to larger capacities. This means that the collection of CO_2 from several sources into a single pipeline will be cheaper than transporting smaller amounts separately. The results showed that increasing transport capacity for a certain distance

decreases the unit cost. However, increasing the distance for certain capacity increases the unit cost.

The results presented in figure 4-9 (a-d) also show the importance of economies of scale during the transportation of CO_2. Among technical, safety, legal, policy and regulation barriers for commercialization of CCS, one of the primary barrier is the absence of economically viable commercial case. One of the ways to reduce costs is by exploring the economies of scale by having large capacity sharing infrastructure. Results show that a larger capacity decreases per unit cost, thus operating a single large capacity system is cheaper than the aggregate cost of developing and operating separate smaller capacity systems which collectively provide the same total capacity as the single large system. The interception point in figure 4-9 (a-d) where the graph corresponds the vertical axis represents the base cost of developing the liquefaction and intermediate storage system. When calculating the cost per unit capacity, the fixed cost is divided across the total capacity of the system. Therefore, the larger the capacity of the system, the smaller the amount of fixed costs that will be allocated to each unit of capacity. Thus, the cost for systems with a smaller capacity is larger than the cost for systems with a large capacity.

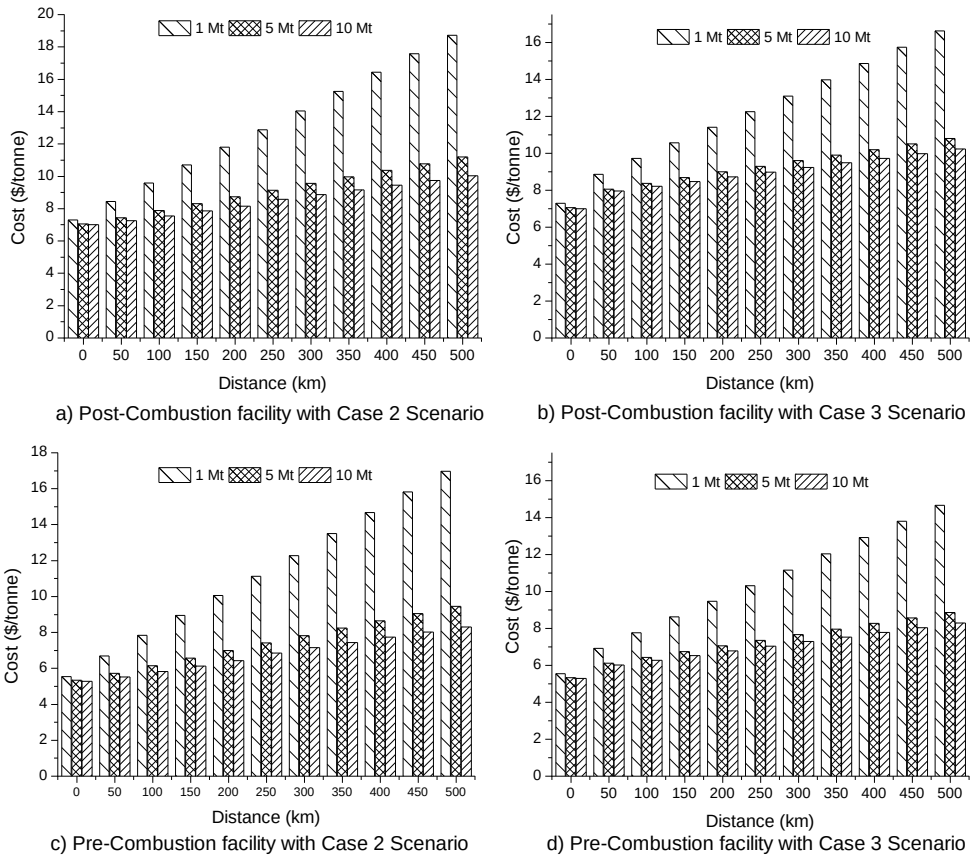

Figure 4-9: Cost Analysis for Various Scenarios

4.7.3. Liquefaction Plant Location Decision

The liquefaction plant can either be located near the capture plant where CO_2 is liquefied and transported in sub-cooled phase to the intermediate storage tank or transported in supercritical phase to intermediate storage site where the liquefaction plant is located and then liquefied. The location of liquefaction plant can be decided on the basis of amount of CO_2 to be transported and distance. Figure 4-10(a) and 4-10(b) show the cost comparison between case 2 and case 3 for post-combustion and pre-combustion capture facilities respectively for different capacities. The CO_2 transportation in liquid phase offers low cost for short distances, however after certain distance supercritical transport may become more economical. In other words, it is better to locate liquefaction plant near capture facility for short distances and small capacities, but locating the liquefaction plant near the intermediate storage and loading terminal is more economical for larger distances and higher capacities.

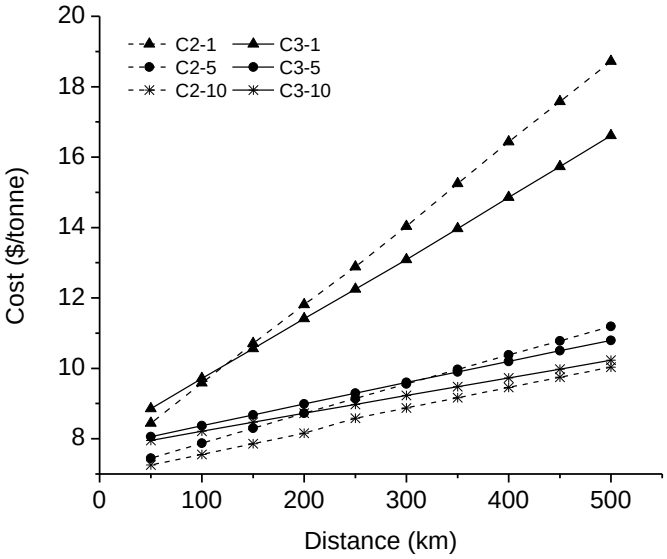

(a) Post-Combustion Source Facility

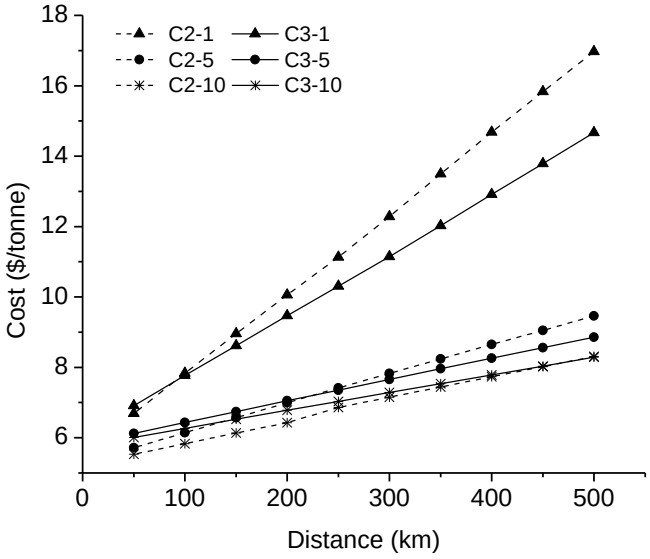

(b) Pre-Combustion Source Facility

(Legend Note: C2=Case 2, C3=Case 3, 1/5/10 represents CO_2 capacity in Mt)

Figure 4-10: Cost Comparison for Deciding Liquefaction Plant Location

4.7.4. Sensitivity of Sea Water Temperature

The liquefaction processes explained earlier employ a number of heat exchangers. There are two type of heat exchangers used in the liquefaction process namely process heat exchangers and sea water heat exchangers. Process heat exchangers are mainly used to recover cold energy from the vapor streams. Whereas, the sea water heat exchangers are employed mainly after the compressor stages to lower the compressed gas temperature. In order to compare the process performance with previous studies, all the process input data were assumed to be the same as in the original work by Aspelund and Jordal [11] and Lee et al [50]. Hence, the sea water temperature for the base case design was assumed as 10 °C. However, sea water temperature can vary depending on the region and the season of the year. Therefore, a sensitivity analysis has been performed for a range of sea water temperatures to investigate its effect on liquefaction energy requirement. Since the compression energy is dependent on the inlet temperature of the gas, an increase in the sea water temperature increases the liquefaction energy requirement. Figure 4-11 shows the effect of sea water temperature on the required liquefaction energy for post-combustion and pre-combustion capture facility processes. The critical temperature of CO_2 is 31.1 °C. The temperature of the compressed CO_2 must be below its critical temperature in order to effectively liquefy it. It means that if the sea water temperature is not low enough to decrease the compressed gas temperature below its critical temperature, then an additional cooling will be required in order to liquefy the compressed CO_2.

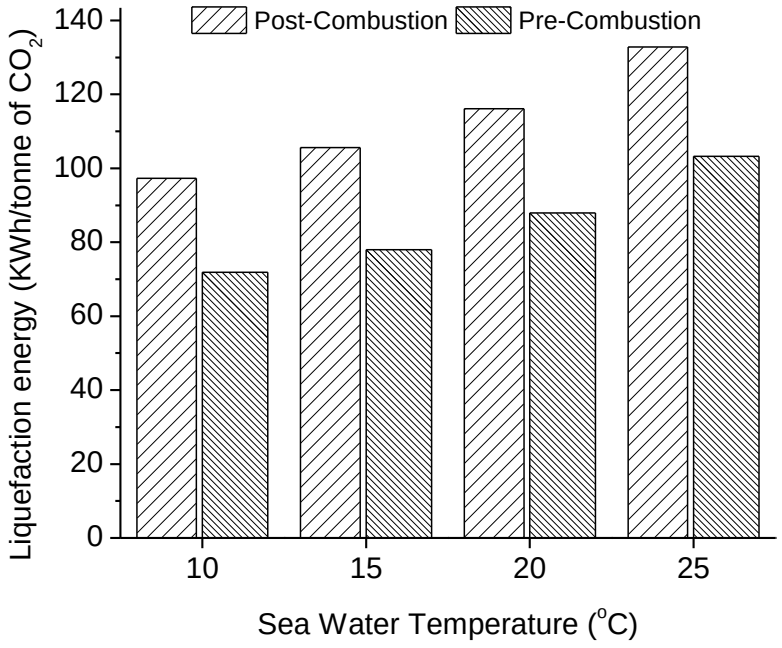

Figure 4-11: Effect of Sea Water Temperature on Liquefaction Energy Requirement

4.8. Summary

CO_2 liquefaction processes are proposed for post-combustion and pre-combustion capture facilities. The liquefaction energy of 97.3 and 71.89 per kWh tonne of CO_2 is required for post-combustion and pre-combustion facilities respectively. The basic liquefaction and intermediate storage cost for post-combustion source varies between 7.00 $ – 7.30 $ per tonne of CO_2 and, a basic cost of 5.28 $ – 5.55 $ per tonne of CO_2 is incurred for pre-combustion source facility. These liquefaction processes are then integrated with various transport scenarios to study the optimum location of liquefaction plant. If the distance between the capture plant and ship loading terminal where the intermediate storage tanks are located is short and CO_2 capacity to be transported in small, then it is better to locate the liquefaction plant near the capture site. On the other hand, if large quantities are to be transported over long distance, locating the liquefaction plant near loading terminal site will be more economical.

CHAPTER 5: Design and Operation Strategy of CO_2 Terminal

5.1. Overview

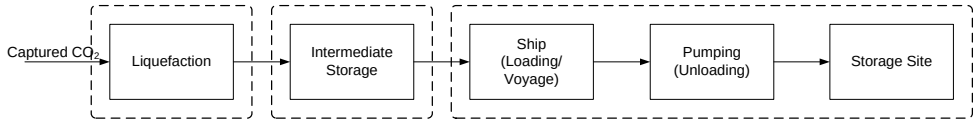

Figure 5-1: CO_2 shipping value chain

Ship transportation itself can be divided into three sub-parts as shown in figure 5-1. First, the captured CO_2 is liquefied through liquefaction plant which is an integral part of ship transportation. The second part is the storage of liquefied CO_2 into intermediate storage tanks until it is loaded on the ships. The third part can be seen as the transport of CO_2 ship from the CO_2 terminal to the storage site. This chapter is mainly dedicated to the design of intermediate storage terminal and operational interaction with other supply chain sections. Chiyoda corporation [12] proposed the concept of shuttle ships which are equipped with injection facilities; hence there is no need for injection platform at the injection site. Alexandrakis and Smart [54] proposed the use of CO_2 ship for multi-product transport. For example, CO_2 ship can be used to transport CO_2 to the storage site and then be used to transport another liquefied gas product available from the storage site or another location and return back to the CO_2 terminal. This concept looks attractive from the supply chain perspective but it will make the system more complicated. Also, vessel cleaning will be required each time before the ship is loaded with a different type of liquefied product. Another study [55] considered insufficient land at the capture site and proposed a floating barge design for CO_2 liquefaction and

intermediate storage. This type of floating barge system can have a single tug and multiple barges, with the tug accompanying one barge at a time.

Most of the studies addressing CO_2 shipping mentioned the need for intermediate CO_2 storage tanks and included it in economic analyses to account for the tank cost. However, shall the CCS technology move further towards commercialization, CO_2 intermediate tank will not be simple buffer storage but rather will develop as a CO_2 terminal with huge volume influxes. Lee et al. [35] presented the conceptual design of a CO_2 terminal with its operating conditions. The scope of the study included the CO_2 storage tank, BOG generation due to heat influx in the system and its re-liquefaction facility. The study also compared the BOG generation under good insulation and bad insulation conditions and consequently the liquefaction energy required to re-liquefy it. Their study was based on the steady-state model built using a commercial simulator. However, the study was not able to explain the behavior of liquid CO_2 and its BOG generation during different stages of terminal operations like CO_2 filling in the tank, holding condition and subsequently CO_2 loading from the tank to the ship. Similar to the assumptions made for LNG terminals, this study assumed that the cryogenic conditions must be maintained within the recirculation line. However, the recirculation flow rate was calculated as 52 % of the input flow which may contribute to an increased pumping energy. A knowledge sharing report for the Rotterdam CCS network [52] also discussed the operating conditions of CO_2 terminal. This study assumed three different pressures of 7, 8 and 9 bara for liquefaction, intermediate storage and shipping. The analysis showed that a storage pressure of 7 bara seems to be the optimum pressure for the overall chain. The study also performed a sensitivity analysis on the tank pressure by varying the heat influx to the storage tank.

Dynamic modeling, which is a collection of time changing patterns to represent a process, is a useful tool for predicting and analyzing the transitions between cases. None of the previous studies investigated the dynamic and reliable operational strategy of CO_2 terminal, its BOG handling system and control philosophy of the tanks. The main objective in this chapter is to explore the operational issues of CO_2 terminal that require attention at the design stage. This chapter is mainly divided in two parts; design and operation of the CO_2 terminal. A dynamic simulation model is made in this study to investigate the various operational modes of CO_2 terminal. Key system parameters, such as storage tank pressure, vessel liquid level, BOG flow rate and recirculation flow rate are tracked during simulation to ensure the safe operation of CO_2 terminal with minimum energy requirement. Essential control schemes have been employed to provide good reliability and keep process variables at their set points. A detailed heat transfer calculation method is followed for the precise quantification of heat flux across the system.

5.2. LNG VS CO_2 Transport

The industry has a long experience operating and managing LNG terminals that may be used as guidance for the development of CO_2 terminals. However, the operating conditions of CO_2 terminal will be quite different than that of the LNG terminal. LNG is stored and transported at atmospheric pressure while CO_2 needs to be stored and transported at a minimum pressure of 6.5 bars. The cargo density of LNG is about 450 kg/m^3 compared to the CO_2 transportation density of 1100 kg/m^3. This means that CO_2 ships can carry more mass than an equivalent LNG ship. Liquid CO_2 in a storage tank or ship is not as cold as LNG, which is usually at – 160 °C. Fire and explosion can result from loss of containment of LNG while high concentration of CO_2 can cause personnel asphyxiation.

5.3. Terminal Design

The CO_2 terminal should be designed in a way such that it can be operated safely while keeping the CO_2 in liquid phase throughout the process. However, due to heat in leaks into the system, the production of BOG is inevitable. Figure 5-2 shows the process diagram for the CO_2 terminal. CO_2 is liquefied at the liquefaction plant and then transported through an insulated pipeline to an intermediate storage tank where it is stored safely. The CO_2 terminal can have a number of storage tanks depending on the liquefaction plant capacity and the shipping schedule. Depending on the specific operation mode, a certain quantity of BOG is continuously produced from the storage tank which is recycled back to the liquefaction plant. Once the ship arrives at the loading port, the liquid CO_2 is pumped from the storage tanks through the forward pipeline to the ship. A small part of the liquid CO_2 is re-circulated through the re-circulation pipeline so that when the CO_2 loading to the ship is started, low temperature can be maintained without vapor flashing in the forward pipeline.

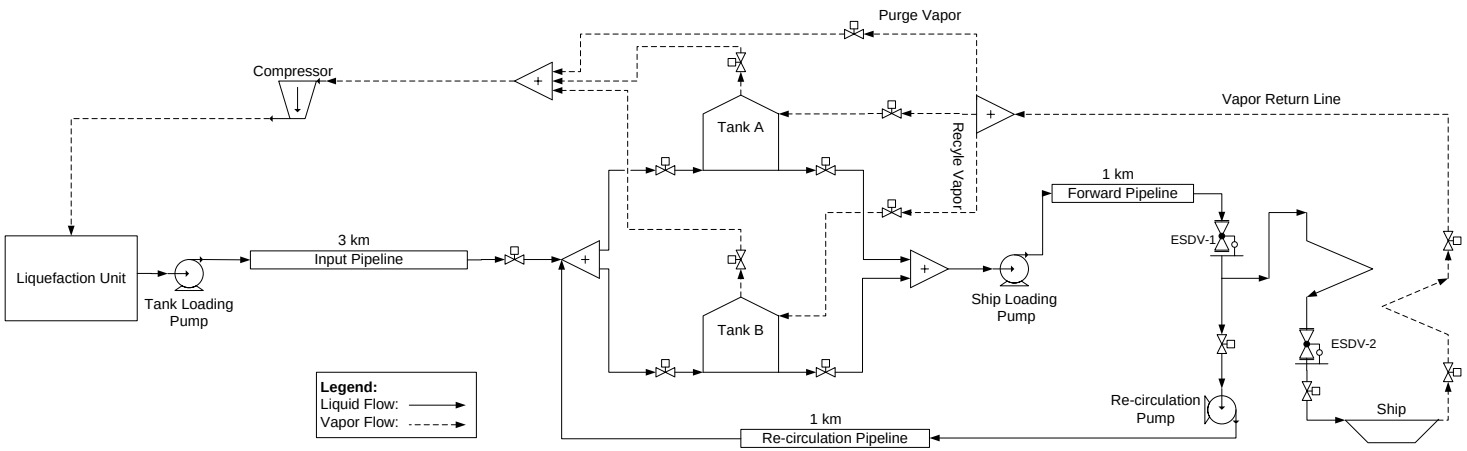

Figure 5-2: Process flow diagram of CO_2 Terminal

The composition of the captured CO_2 stream may vary depending on the source and technology used for CO_2 capture. The variation of impurity content affects the vapor liquid equilibrium (VLE) properties of CO_2 mixtures, mainly boiling and condensing behaviors. The design and operation of the terminal can be influenced by changing the thermodynamic properties of CO_2 mixtures due to presence of impurities. Therefore, non-condensable gases should be removed from the captured CO_2 stream in order to satisfy the requirements of transportation and use the storage reservoir efficiently. Increase of non-condensable gases in the CO_2 stream rise the boiling and condensing pressure compared with the saturated state of pure CO_2. Particularly, the variation of N_2 has the most remarkable impacts on both the dew points and the bubble points of CO_2 mixtures [56]. Different from the behavior of the non-condensable gases, SO_2 has the opposite impact on the VLE properties of CO_2 mixtures. Since SO_2 has a higher critical point than CO_2, the presence of SO_2 in CO_2 mixtures will make the condensing temperature increase at a certain pressure or make the condensing pressure decrease at a certain temperature [56]. In this study, a pure CO_2 stream is assumed in order to have a basic understanding of CO_2 terminal operations.

Based on the storage tank status, this study has divided the operation of CO_2 terminal into three basic modes: loading mode, holding mode and unloading mode. A special case of emergency shutdown (ESD) has been included in the event of an emergency situation. Table 5-1 shows the design parameters for the base case used in this study. This study assumes that liquid CO_2 is available from the liquefaction plant at -52 °C and 6.5 bar. During the loading mode, liquid CO_2 from the liquefaction plant is pumped to the intermediate storage tank where it is kept at a pressure of 7.0 bar. The liquid transferred to the tank results in a level build up in the storage vessel and compression of the vapor phase above the liquid. This vapor has to be removed from the tanks to prevent

excessive pressure build-up in the tanks. A continuous vapor stream is removed from the storage tank and returned to the liquefaction plant during the loading mode. Once the tank is filled with liquid CO_2, it is considered to be in holding mode until the tank is unloaded. The safe liquid CO_2 hold up during holding mode depends on the ambient temperature, tank insulation material, insulation thickness, and filling level of the tank [52]. The tank is under unloading mode when the liquid CO_2 is pumped from the storage tank to the ship. The removal of liquid CO_2 from the storage tank will reduce the pressure which can eventually result in solidification of the tank content. Hence, there is a need to compensate for this pressure drop by feeding CO_2 vapor into the tank. For this purpose, the vapor generated while loading CO_2 into the ship will be returned from the ship back to the storage tanks. This will prevent pressure reduction in the storage tank and pressure build up in the ship. BOG load varies by a large degree between loading mode, holding mode and unloading mode.

Table 5-2 presents a methodology explaining how different design parameters should be selected for the basic design of a CO_2 terminal, what specific design codes should be followed in order to ensure the terminal safety and what process variables should be monitored during different operational modes. The table 5-2 consists of sections including design basis, cryogenic equipment design, layout of the terminal, ship vessel sizing and operational parameters that require attention for the safe operation of the terminal. The details for design and operation of CO_2 terminal are explained further in the following sections.

Table 5-1: CO_2 terminal parameters for the base case design

Terminal annual capacity	5 million ton CO_2
CO_2 specification at liquefaction plant	6.5 bar, - 52.0 °C
CO_2 specification at storage tank	7.0 bar, - 48.8 °C
CO_2 specification at ship	7.1 bar, - 48.6 °C
Storage tank capacity	5000 m^3
Storage tank type	Spherical
Number of tanks	2
Ambient temperature	30 °C
Insulation material	Polyurethane

Table 5-2: Scheme for the basic design of CO_2 terminal

Design Parameter	Description
a. Design Basis	
• Determine the terminal throughput capacity	• Based on the CO_2 demand for the permanent storage or utilization.
• Define operating condition	• Select suitable temperature and pressure based on thermodynamic analysis.
• Number of storage tanks required	• Based on terminal throughput for discrete operation (also involves maximum built-able size based on material selection).
b. Terminal Conceptual Design	
• Determine required equipment	• Must be decided based on required performance while keeping high reliability, operability and maintainability.
• Develop process flow sheet	• Based on the starting and stopping points of the process
1b. Tank design	• ASME Code Section VIII, Division 1 (Pressure Vessels)
• Tank material selection	• ASTM Standards (For cryogenic applications)
• Tank type selection	• Based on previous industry experience
• Maximum design pressure	• 20 %*Maximum operating pressure + Maximum operating pressure
• Tank thickness	• ASME Code Section VIII, Division 1 (Pressure Vessels)
• Storage Tank Sizing	• Based on liquid hold-up requirement
2b. Pipeline Design	• ASME B31.4 (Pipeline transportation systems for liquid hydrocarbons and other liquids)
• Pipeline material selection	• ASTM Standards (For cryogenic applications)
• Pipeline diameter calculation	• Based on optimal pipeline diameter from *Design and Economics for Chemical Engineers*
• Pipeline thickness	• ASME B31.4 (Pipeline transportation systems for liquid hydrocarbons and other liquids)
3b. Insulation Material	
• Selection of suitable insulation material	• Insulation for cryogenic equipment (Refer to reference 13)
• Insulation thickness	• Based on allowable boil-off-rate (BOR) and economic comparison between capital and operating cost.

4b. Heat Flux • Calculate heat flux across storage tanks • Calculate heat flux across pipeline	 • Refer to reference 18. • Refer to equation 7 and 8.
c. Layout of the Terminal • Location of the equipment • Determine pipe lengths based on layout	 • Facilities are laid out according to the sequence of processes at a terminal • Determine process and utilities pipeline lengths based on the equipment placement
d. Ship Vessel Sizing	• Based on transport capacity, transport distance, design speeds of the ship (laden and ballast), loading and unloading time requirement and number of ships used
e. Terminal Operation	
1e. Loading Mode	• Monitor BOG generation in the tank as per design • Pressure controller operation and its tuning for reliable control • Level controller operation and its tuning for reliable control • Calculate minimum re-circulation flow rate during loading mode
2e. Holding Mode	• Ensure proper working of pressure controller
3e. Unloading Mode	• Monitor BOG generation in the ship vessel • Ship vessel pressure controller operation and its tuning for reliable control • Ship vessel level controller operation and its tuning for reliable control • Tank pressure controller operation and its tuning for reliable control • Calculate minimum re-circulation flow rate during unloading mode • Calculate recycle vapor stream flow rate from ship to tank

5.3.1. Tank Design

One of the characteristics of CO_2 is the absence of normal boiling point which means that CO_2 can only exist as gas or solid at an atmospheric pressure. CO_2 in liquid phase can only exist above the triple point pressure of 5.2 bar. However, if the storage pressure is increased significantly, it will cause an increase in CAPEX. Therefore, the operating pressure of the CO_2 terminal is set to be in the range of 6.5 bar to 7.5 bar with the normal operating pressure of 7.0 bar for the storage tank and 7.1 bar for the ship vessel. In this way, a safety margin can be maintained to avoid any dry ice formation below the triple point and the CO_2 tank will cost less compared to current shipping practices at higher pressure. In this study, spherical storage tanks with a maximum design pressure of 9 bar are used. Absence of corners result in the even distribution of stresses on the sphere's surfaces, both internally and externally which adds to its strength. Moreover, a sphere has smaller surface area per unit volume compared to other vessel shapes. This means that the heat flux from the outside environment to the liquid CO_2 will be less than that for cylindrical or other storage vessels. The design and safety control loops for the CO_2 storage tank are shown in figure 5-3. The thickness of the tank material is calculated using the ASME code section VIII (Pressure Vessels) for hemispherical heads as shown in equation 5.1 [57].

$$t = \frac{P\,L}{2\,S\,E - 0.2\,P} \qquad \text{….. Eq. 5.1}$$

Where t is the minimum thickness of the tank, P is the maximum internal design pressure, L is the inside radius, S is the allowable stress in tension and E is the joint quality factor. The allowable stress S value is taken as 129.2 MPa for steel tanks and E is set to 1.0 assuming fully radio-graphed tanks [37]. ASTM A203 has been followed for the compliance of CO_2 tank material. The material used is 3.5 % nickel alloy steel that can be used at temperatures down

to -100 ^{0}C. Safety factor represents the structural capacity of a system beyond the expected load and is a ratio of tensile strength to yield point. The safety factor for 3.5 % Ni-steel used in this study is 1.75 [58].

5.3.2. Pipeline Design

As shown in figure 5-2, four different pipelines are part of the CO_2 terminal. These include the input pipeline from liquefaction plant to storage tank, the forward line, the re-circulation line and the vapor return line. Equation 5.2 proposed by Zhang el al. [26] is used to calculate the optimal diameter of the pipelines.

$$D_{opt} = 0.363 \left(\frac{Q_m}{\rho}\right)^{0.45} \rho^{0.13} \mu^{0.0025} \quad \text{..... Eq. 5.2}$$

Where D_{opt}, Q_m, ρ and μ are the optimal pipe diameter (m), mass flow rate (kg/s), CO_2 density (kg/m^3), and viscosity (Pa-s), respectively. Beggs and Brill [59] method has been used to calculate the pressure drop through the pipelines within the CO_2 terminal. This correlation was the first developed method to apply to all pipe inclination angles and has a good applicability for different pipeline geometries. The total pressure drop through the pipeline is the sum of pressure drops due to potential energy change, kinetic energy change and friction losses as shown in equation 5.3.

$$\left(\frac{\mathrm{d}p}{\mathrm{d}L}\right) = \left(\frac{\mathrm{d}p}{\mathrm{d}L}\right)_{PE} + \left(\frac{\mathrm{d}p}{\mathrm{d}L}\right)_{KE} + \left(\frac{\mathrm{d}p}{\mathrm{d}L}\right)_{fric} \quad \text{..... Eq. 5.3}$$

However, since there is no elevation change involved in this case, the pressure drop due to potential energy can be neglected. The pressure drop caused due to kinetic energy is proportional to the change in the fluid velocity and is given by equation 5.4:

$$\left(\frac{\mathrm{d}p}{\mathrm{d}L}\right)_{KE} = \rho v \left(\frac{\mathrm{d}v}{\mathrm{d}L}\right) \quad \text{..... Eq. 5.4}$$

The pressure drop across the pipeline depends mainly on the frictional pressure gradient and is calculated using equation 5.5 as shown below:

$$\left(\frac{\mathrm{d}p}{\mathrm{d}L}\right)_{fric} = \frac{f\rho v^2}{2g_c D} \qquad \text{..... Eq. 5.5}$$

where f is friction factor, ρ is the fluid density (kg/m^3), v is the in-situ velocity (m/s), L is the length of pipe (m), g_c is the conversion factor (kg-m/N-s^2) and D is the pipeline diameter (m). The fluid velocity (v) is calculated on the basis of volumetric flow rate and calculated pipeline diameter. Whereas, friction factor is calculated based on the Reynolds number and relative roughness of the pipeline. The calculated diameter and pressure drop for different pipelines is presented in table 5-3. The pressure drop across the forward and re-circulation line increases significantly during the unloading mode than that during the loading mode operation.

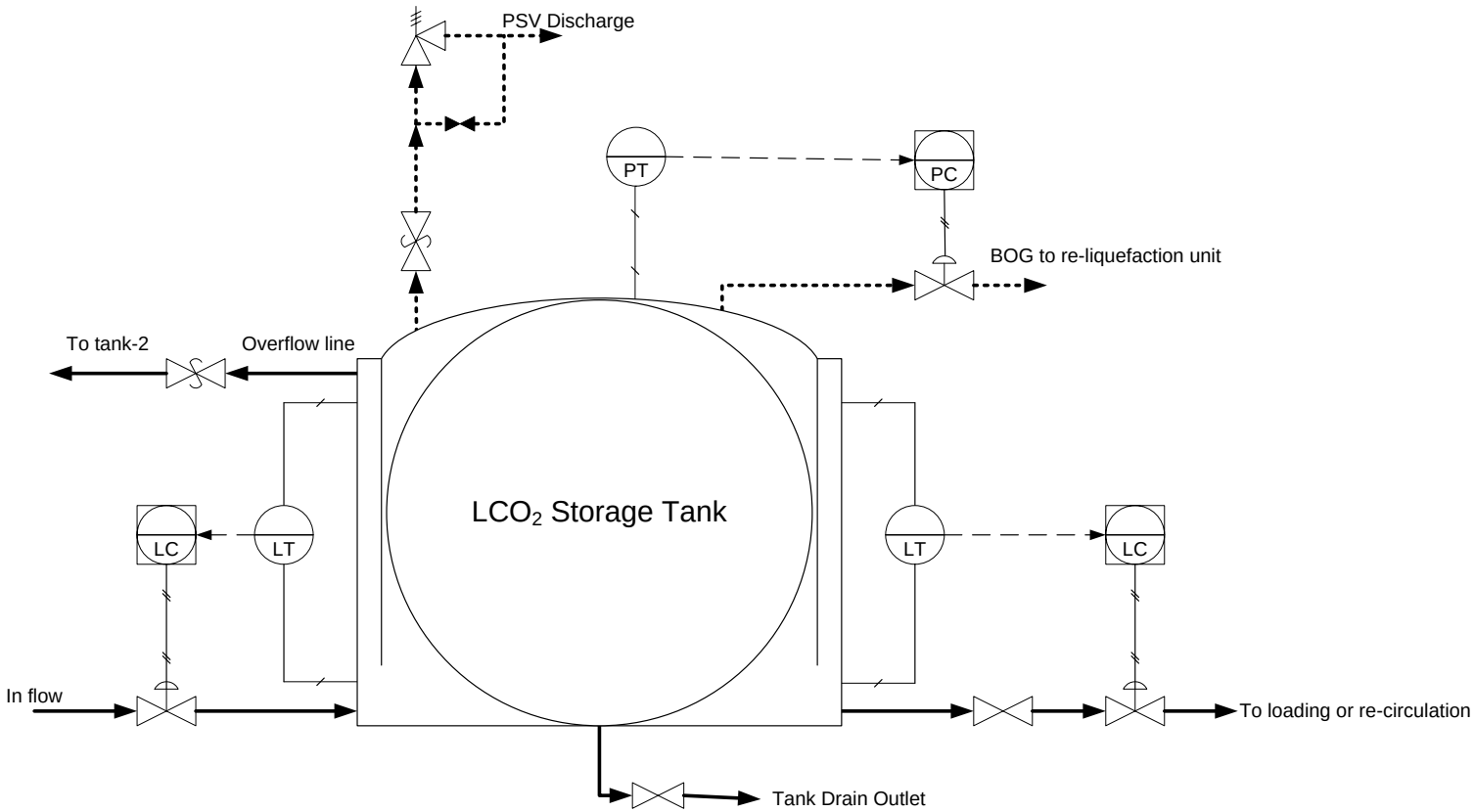

Figure 5-3: Design and control of CO_2 storage tank

Table 5-3: Calculated pipeline diameters

	Nominal pipe size (inches)	Pressure drop (kPa)
Input Pipeline	12	277
Forward pipeline (during loading mode) Forward pipeline (during unloading mode)	14	5.1 150
Re-circulation pipeline (during loading mode) Re-circulation pipeline (during unloading mode)	10	11 44
Vapor return line	3	-

5.3.3. Heat Flux Calculation

The total heat flux is calculated across the pipelines and storage tanks to precisely determine the BOG load which arises from the heat transfer using equation 5.6.

$$dQ = dQ_{pipe} + dQ_{tank} \quad \text{….. Eq. 5.6}$$

Where dQ is the total heat flux across the system, dQ_{pipe} is the heat flux over the pipelines and dQ_{tank} represents the heat transfer across the storage tanks. dQ_{pipe} can be calculated by using equations 5.7 and 5.8.

$$dQ_{pipe} = U_{o,pipe}\,\Delta T\,dA \quad \text{….. Eq. 5.7}$$

$$U_{o,pipe} = \frac{1}{r_o\left(\frac{1}{r_o h_o} + \frac{ln\left(r_1/r_o\right)}{k_{01}} + \frac{ln\left(r_2/r_1\right)}{k_{12}} + \frac{1}{r_2 h_2}\right)} \quad \text{….. Eq. 5.8}$$

Where $U_{o,pipe}$, h, and k represent the overall heat transfer coefficient, convective heat transfer coefficient and thermal conductivity respectively; and r_0, r_1 and r_2 represent the internal radius, external radius and outside radius of insulation for pipeline. The heat flux across the storage tank is calculated using a procedure outlined by Kumana and Kothari [60] in which the heat fluxes are calculated separately for each category of surfaces. In the case of a spherical tank, these surfaces are: wet wall, dry wall and tank bottom. Wet wall refers to the portion of the wall submerged under the liquid surface, whereas dry wall refers to the portion of the wall in the vapor space, above the liquid surface. In this study, heat transfer calculations are based on the maximum tank filling level of 93 % which is a recommended maximum fill level from vendors' data [61]. dQ_{tank} can be calculated using the following equations 5.9 - 5.12.

$$dQ_{tank} = dQ_{wet} + dQ_{dry} + dQ_{bottom} \quad \text{….. Eq. 5.9}$$

$$dQ_{wet} = U_w \Delta T \, dA \quad \text{….. Eq. 5.10}$$

$$dQ_{dry} = U_d \Delta T \, dA \quad \text{….. Eq. 5.11}$$

$$dQ_{bottom} = U_b \Delta T \, dA \quad \text{….. Eq. 5.12}$$

Where dQ_{wet}, dQ_{dry} and dQ_{bottom} represent the heat transfer through wet wall, dry wall and bottom surfaces respectively. U_d, U_w and U_b are the overall heat transfer coefficients for the dry wall, wet wall and bottom surfaces respectively. It may be difficult to estimate the overall heat transfer coefficients U_d, U_w and U_b for the different surfaces of the tank. For the tank geometry chosen in this study, these can fortunately be calculated using the published correlations [62]. The heat transfer coefficient for air is taken as 50 W/m^2-K for wind speeds of up to 15 mph. Table 5-4 shows the calculated heat fluxes for the pipelines and storage tank. The result shows that the heat transfer across the forward line increases during the unloading mode because of much higher flow rate compared to that during loading mode.

Table 5-4: Heat flux across the CO_2 terminal

	Heat influx (kW)
Storage tank	31.7
Ship vessel	48.0
Input pipeline	84.4
Forward pipeline (during loading mode)	28.0
Forward pipeline (during unloading mode)	32.5
Re-circulation pipeline (during loading mode)	27.9
Re-circulation pipeline (during unloading mode)	27.9

5.4. Operational Dynamics

The process performance of CO_2 terminal under different operational modes cannot be described clearly by a static analysis. Therefore, a dynamic simulation has been performed using the commercially available simulation software Aspen HYSYS®. The simulations are done using Soave-Redlich-Kwong (SRK) as the physical property package since it can precisely predict the phase behavior of CO_2. The equipment consists of a tank loading pump, pipeline from liquefaction plant to the CO_2 terminal, storage tanks, a ship loading pump, re-circulation pump, forward pipeline and re-circulation pipeline as shown in figure 5-2. The tank loading pump sends the liquefied CO_2 through a 3 km long pipeline from the liquefaction plant to the CO_2 terminal where intermediate storage tanks are located. The heat leaks from the environment to the system continuously generate BOG. Therefore, in order to reduce BOG, the pipelines and storage tanks are insulated with polyurethane material with a thermal conductivity of 0.018 W/m-K. The minimum recirculation flow of CO_2 required to maintain cryogenic conditions within the pipelines is sent through the forward pipeline back to the storage tank. The forward line and re-circulation line each are assumed to have a length of 1 km.

5.4.1. Loading Mode

Liquid CO_2 available at – 52 °C and 6.5 bar is pumped to the CO_2 terminal where it is stored in a semi-pressurized storage tanks. The tank is operated with a set point pressure of 7.0 bar. The quantity of vapor in the tank outlet increases significantly as soon the CO_2 loading starts in the tank. These vapors are a combination of volume displaced in the tanks by the incoming CO_2, vapor resulting from the pumping energy in the pipeline, and vaporization resulting from heat leaks through the insulated tank and pipelines. The formation of CO_2 vapors results in excessive pressure build up in the tank. Therefore, during the loading mode, a continuous vapor flow is removed from

the storage tank in order to maintain the vessel pressure. While the CO_2 is filling in the tank, a minimum liquid flowrate from the tank is pumped through the forward line and recirculation line to keep the CO_2 terminal within cryogenic operating limits.

In this study, CO_2 loading in the intermediate storage has been performed with a tank capacity of 5,000 m^3. Initially the storage tank is made empty with no liquid CO_2 and BOG in it. Also, before the CO_2 loading starts, the temperature of forward and recirculation pipelines are assumed to be at ambient temperature. Figure 5-4 shows the BOG generation in the 5000 m^3 capacity tank during the loading mode. As soon as the liquid CO_2 enters the tank when starting to fill the tank, it flashes to the vapor phase and a huge amount of CO_2 vapors are generated. As the tank loading continues, the vapor and liquid remain in equilibrium with each other. The liquid CO_2 exists in equilibrium with its vapor inside the tank with the tank pressure being dependent solely on the temperature. The high level switch of storage tank is set at 93 % liquid volume percent of the tank which is controlled by the level controller. The results show that it takes about 9.6 hours to fill 93 % of a 5000 m^3 CO_2 tank. Figure 5-5 shows the pressure control of the tank during the loading mode. As a large quantity of BOG (11,000 kg/hr) is generated in the start of tank filling, the pressure of the tank increases from a set point of 700 kPa to around 707.3 kPa. To keep the tank pressure at its set point, BOG is drawn out from the top of the storage tank. The pressure controller used in this study is a simple PI controller given with a set point of 700 kPa. The tuning parameters for the pressure PI controller are given in table 5-5. The gain (K_c) and integral time (T_i) values are selected using the rules of thumb values with auto-tuning done within the simulator. The valve opening percentage (OP) follows closely with the process variable (PV), which is the tank pressure, to keep it at the set point.

As mentioned previously, a minimum liquid flowrate needs to be re-circulated through the terminal to keep pipelines within the cryogenic limits. During the tank loading mode, the liquid CO_2 re-circulation flowrate depends on the heat flux through the system caused by pumping, turbulent flow and line frictions. Any heat leaking into the system will increase the temperature of the liquid CO_2 and form additional vapors in the tank. The quantity of these additional vapors depends on the length of the pipeline (forward and re-circulation) and the power of the pumps. The vapor formed in the storage tank can be taken out as the BOG stream. However, any significant vapor forming in the pipeline is undesirable as it can lead to safety issues such as pipeline hammering and pump cavitation. The liquid CO_2 recirculation flowrate is calculated based on the presence of any CO_2 vapor in the re-circulation line. Re-circulation flowrate is calculated so that no vapor is formed in the pipeline. This is done by installing a PI controller with a given set point of zero vapor fraction in the re-circulation pipeline. The controller takes the input by measuring vapor fraction in the re-circulation line and manipulates the re-circulation pump power. The tuning parameters for this PI controller are given in table 5-5. The calculated re-circulation flowrate ensuring no vapor formation is around 113,000 kg/hr which is about 19.5 % of the input flowrate. As long as the operating temperature of the terminal remains within the cryogenic limits, the minimum re-circulation flowrate is pumped to keep the operating energy as low as possible.

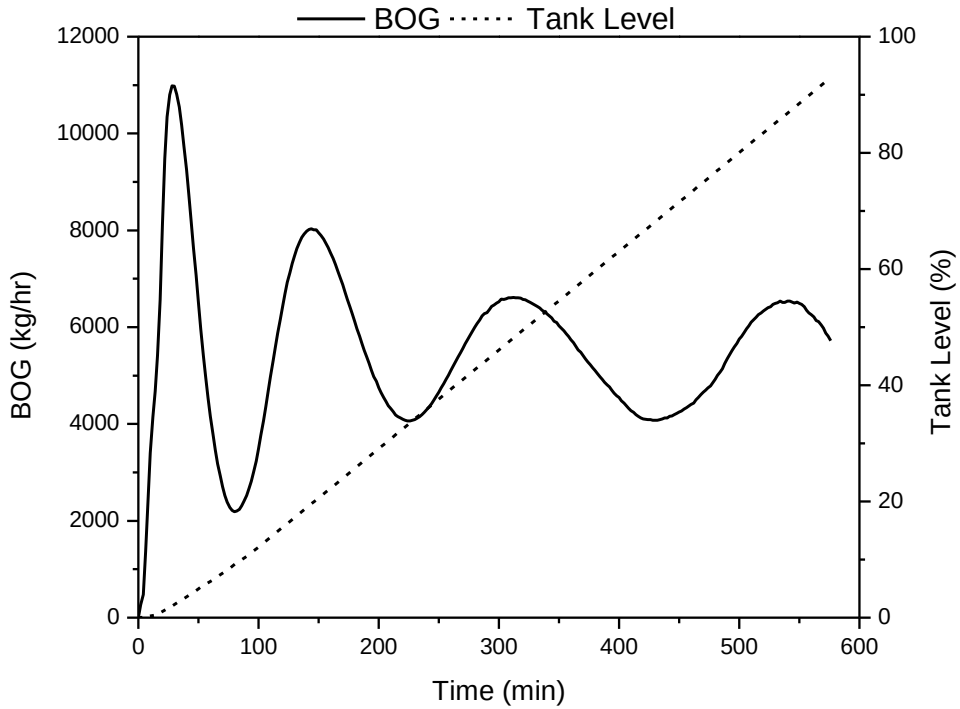

Figure 5-4: BOG generation and tank level during 5000 m^3 tank loading mode

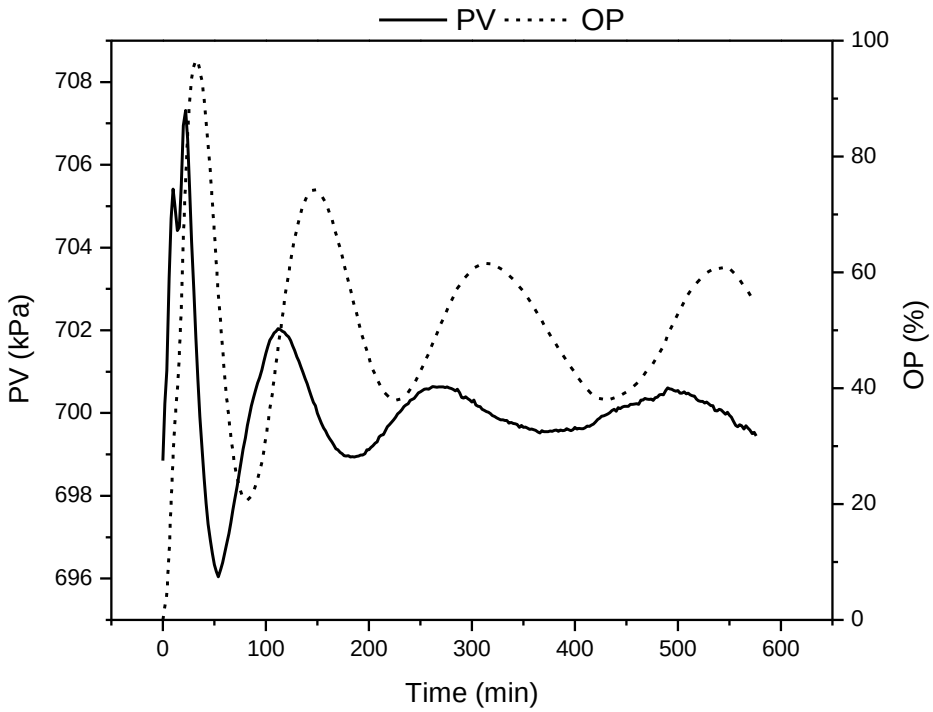

Figure 5-5: Tank pressure control behavior during loading mode

Table 5-5: Tuning parameters for the PI controllers

	Gain (K_c)	Integral time (T_i)
Tank pressure controller	2	3
Ship pressure controller	2	3
Re-circulation flowrate controller	0.5	0.3

5.4.2. Holding Mode

The holding mode refers to a state after liquid CO_2 is filled in the tank and no liquid is being withdrawn from it. The liquid CO_2 can be stored in the tank for long durations as long as heat leaks into the tank are minimized. Decarre et al. [10] studied the CO_2 ship transportation and assumed that the BOG shall neither be released to the atmosphere nor reliquefied during ship transportation. They reported a possible pressure increase in the vessel from 7 bar to 10.4 bar for a transport distance of 100 km. In such a case, when BOG stream is not taken out from the tank, the pressure of the tank rises. The design pressure of the tank limits the amount of BOG that can be handled without releasing or reliquefying it. However, heat flux through the tank depends on many factors like ambient temperature, tank insulation material, insulation thickness, and filling level of the tank. In the case of LNG, BOG generation during the holding mode is 8- 10 times less than during the loading mode [63]. Under specific site conditions and insulation material, CO_2 hold up time in the storage tank can only be increased by using a tank with higher design pressure, which results in an increase in the cost of the vessel. In this study, dynamic simulation studies are done to investigate the effect of ambient temperature, insulation thickness, filling level of the tank and tank capacity on the pressure build up in the tank when BOG is not withdrawn during holding mode.

5.4.2.1. Effect of Ambient Temperature

The ambient temperature is a site specific parameter that can differ significantly from one region to another. Even for one specific location, the ambient temperature may vary throughout the year and an average temperature difference between winter and summer can be as high as 15 °C. Figure 5-6 shows the effect of ambient temperature on the pressure build up in the storage tank. The results show that a high ambient temperature will result in more heat transfer through the tank, which in turn will produce more BOG. Hence, CO_2

terminals located in the cold climate regions will have a natural advantage in terms of operational energy penalty. The storage tank located in colder ambient temperature regions can hold liquid CO_2 for much longer periods of time compared to those located in hotter climate.

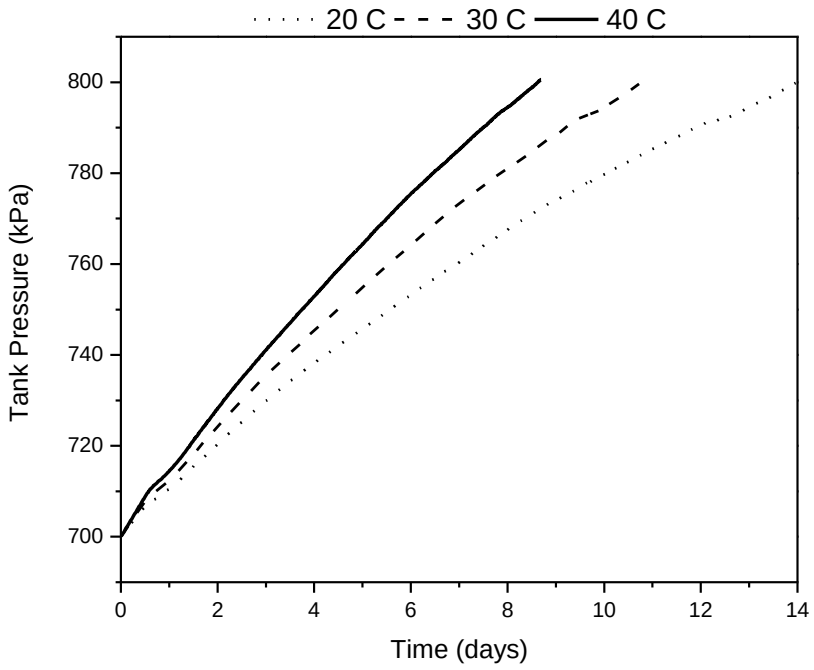

Figure 5-6: Effect of ambient temperature on the tank pressure during holding mode

(Initial filling level = 50 %, Insulation thickness = 0.1, Tank capacity = 5000 m^3)

5.4.2.2. Effect of Insulation Thickness

The heat flux through the system depends on the type of insulation used and its thickness. The higher the thermal resistivity of insulation, the lower the amount of heat that will leak into the system. The thermal resistance of the insulation material can be increased by increasing the insulating layer thickness. In this study, polyurethane foam has been used as an insulation material with thermal conductivity of 0.018 W/m-K. The insulation thickness is a trade-off between insulation costs and energy required to re-liquefy the generated BOG. However, the optimization between insulation thickness and re-liquefaction energy is not in the scope of this study. Throughout this study, an insulation thickness of 0.1 m is used and a sensitivity analysis is done to show the effect of insulation thickness on the pressure build up in the tank. Figure 5-7 shows that increasing the insulation thickness decreases the BOG generation in the tank and, hence, liquid CO_2 can be stored for a longer period of time.

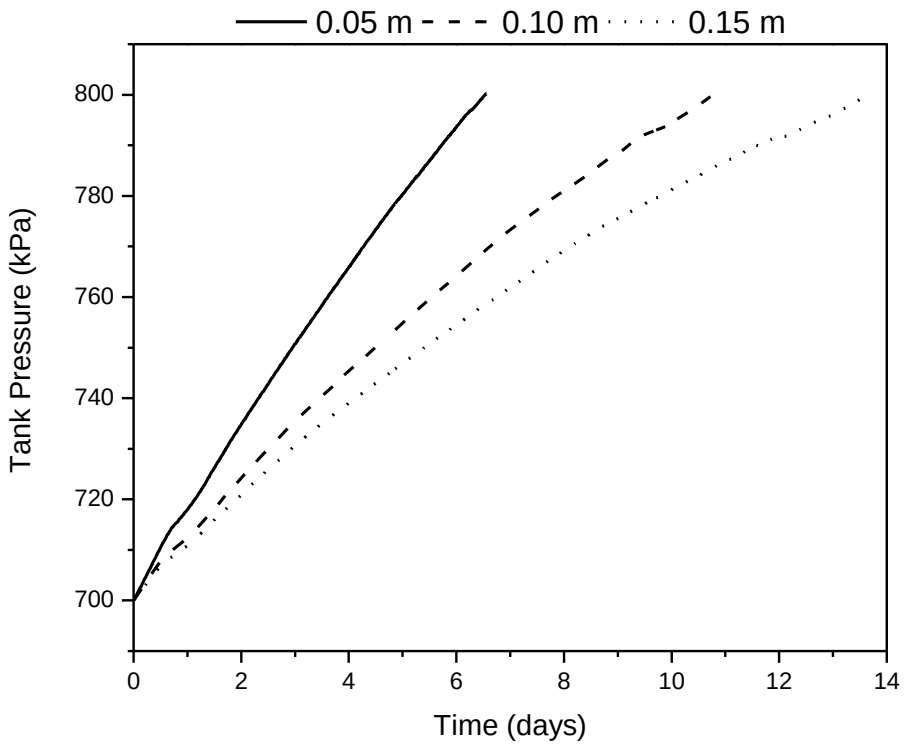

Figure 5-7: Effect of insulation thickness on the tank pressure during holding mode (Initial filling level = 50 %, Ambient temperature = 30 ºC, Tank capacity = 5000 m^3)

5.4.2.3. Effect of Tank Filling Level

Tank filling level is an operational and logistic parameter that is an important factor in the generation of BOG [52]. As described earlier, the maximum filling level of CO_2 tank is set at 93 %. However, depending on the liquefaction plant operation and CO_2 shipping logistics, the available CO_2 level in the tank may vary from day to day operations. For example, depending on the size of ship used for transportation of CO_2, a certain quantity of liquid CO_2 may be left in the tank after loading CO_2 to the ship. It is important from the operational point of view to monitor the CO_2 level remaining in the tank, as it can affect the operational energy requirements. Figure 5-8 shows the pressure build up for various CO_2 filling levels in the tank. Low level of liquid CO_2 in the tank can vaporize faster compared to high filling level. It is thus recommended not to leave small quantities of liquid CO_2 in the tank. Any liquid CO_2 left in the tank due to operational or logistical lags should either be pumped to other tanks with high filling level or new liquid CO_2 production should be filled in that tank.

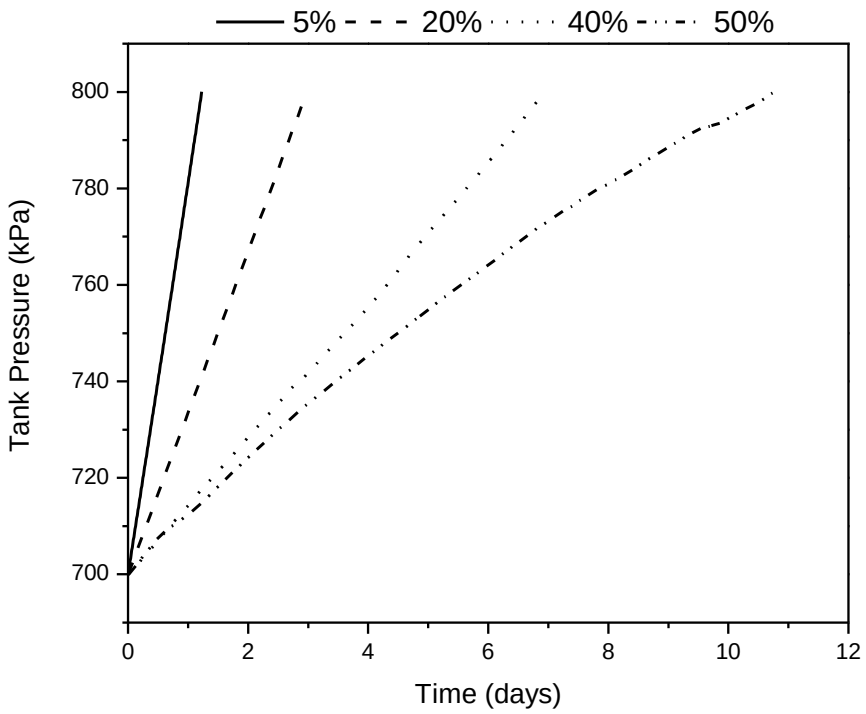

Figure 5-8: Effect of initial filling level on the tank pressure during holding mode

(Ambient temperature = 30 °C, Insulation thickness = 0.1 m, Tank capacity = 5000 m^3)

5.4.2.4. Effect of Storage Tank Capacity

The effect of storage tank's capacity on the pressure build up in the tank is presented in figure 5-9. The results show the same conclusion as discussed in the effect of tank filling level section. A certain quantity of liquid CO_2 present in different capacity tanks can be safely stored for a different period of time. This means that a fixed quantity of CO_2 can be stored longer in a small capacity tank compared to a larger capacity tank.

The results are useful for the careful management of liquid CO_2 supply chain. Also, these results can be used as a guideline to define the maintenance schedule of the liquefaction plant.

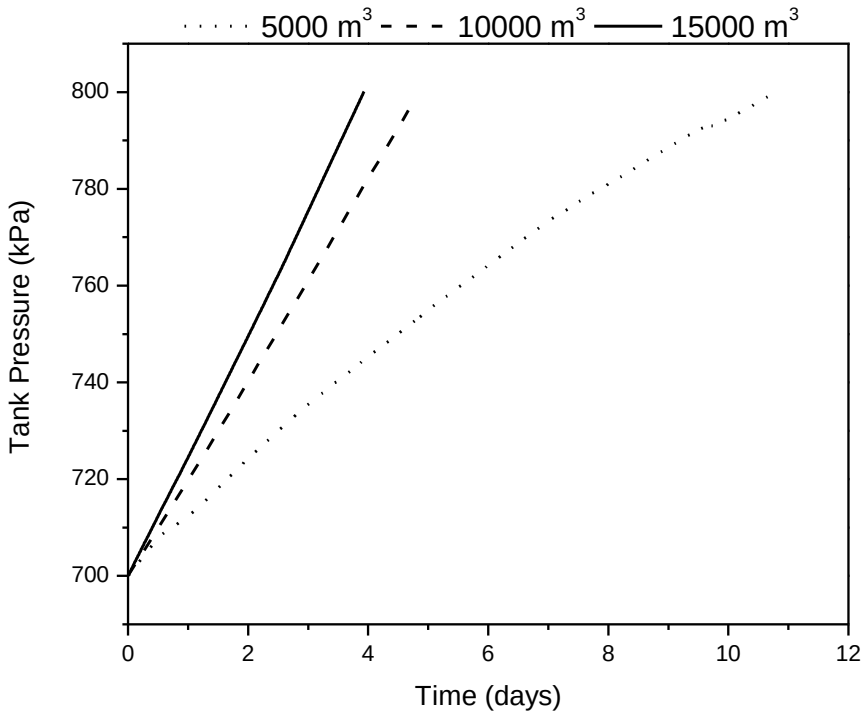

Figure 5-9: Effect of tank capacity on the tank pressure during holding mode

(Ambient temperature = 30 °C, Insulation thickness = 0.1 m, Initial filling level = 2500 m^3)

5.4.3. Unloading Mode

The unloading mode refers to the pumping of liquid CO_2 from the storage tank to the ship. Once the ship arrives at the CO_2 terminal and is ready to be loaded, liquid CO_2 from the storage tank is pumped through the forward pipeline to the ship. The process of ship loading is similar to that of the CO_2 tank loading as discussed previously in loading mode. However, there are some differences in terms of vessel operational conditions. When the ship loading pump starts to send liquid CO_2 to the ship, a large quantity of BOG is produced and taken out from the top of the vessel. The BOG produced during the storage tank filling is sent to the liquefaction plant for re-liquefaction. However, the BOG produced from the ship is recycled back to the storage tank. The removal of the liquid CO_2 from the storage tank decreases the pressure in the tank. Hence there is a need to compensate for the pressure drop in the tank by recycling the BOG produced from the ship. In this way, the recycled BOG keeps the pressure of ship and storage tank within operating limits. In this study, the ship vessel pressure is set at 7.1 bar which is slightly high than that of the storage tank. In the LNG terminals, a vapor return compressor or blower is usually installed to send the BOG from the ship to the storage tank. However, by keeping the ship vessel pressure slightly higher, additional operating and capital cost of such auxiliary equipment can be saved. The re-circulation pipeline is kept within cryogenic conditions by sending a part of the liquid CO_2 flow through the re-circulation pump back to the storage tank. However, the recirculation flowrate during the unloading mode is almost 2.4 times higher than that during the loading mode. Since during the unloading mode, liquid CO_2 is pumped from the storage tank to the ship and the recirculation line, without fresh inflow of CO_2 from the liquefaction plant, the recirculation flowrate is higher to accommodate the same quantity of heat flux as in the loading mode. Figure 5-10 shows the simultaneous emptying and filling of

storage tanks and ship during the unloading mode. The storage tanks are not completely emptied during the unloading mode because the frequent start-up of tanks can decrease the strength of tank material and not recommended from operational perspective. Therefore, the minimum level of liquid CO_2 in the storage tank is set at 2.5 % liquid volume percent of the tank. The actual volumetric flowrate from the storage tank to the ship is set at 750 m^3/hr. The ship capacity is calculated based on the simple shipping schedule. Four ships are assumed for each voyage route of 500 km. The design speed of CO_2 ship is 15.0 knots in the laden voyage and 16.0 knots in the ballast voyage. The voyage time is calculated assuming 12 hours of loading, 12 hours of unloading and 8 hours of harbor/mooring time [55]. Hence, the time required for a single voyage is around 2.75 days for 500 km trip and each ship can make 122 trips per year. The high level switch of ship vessel is set at 95 % liquid volume percent of the vessel. Therefore, the capacity of ship is calculated as 9,500 m^3 for an annual transport capacity of 5 Mton. Figure 5-11 shows the BOG generation in the 9500 m^3 ship along its pressure variation during the unloading mode. As soon as the liquid CO_2 enters the ship vessel, it flashes to vapor phase and a huge amount of CO_2 vapor is generated. The BOG generation from the ship stabilizes after 2 hours of filling and remains constant at flowrate of around 14,000 kg/hr. The ship vessel pressure is maintained within operating limits by using a pressure controller with tuning parameters shown in table 5-5. It is evident from the results that as the ship vessel pressure changes, the corresponding BOG generated also change. BOG produced from the ship vessel is split up into two streams, recycle BOG and purge BOG. Figure 5-12 shows the flowrate of recycle and purge BOG during the unloading mode. The storage tank pressure is maintained at 7.0 bar by using a pressure controller which manipulates the amount of recycle BOG back to the storage tank. The purge BOG stream is sent back to the liquefaction plant for

re-liquefaction. It can be seen from the results that most of the BOG generated from the ship is recycled back to the storage tank.

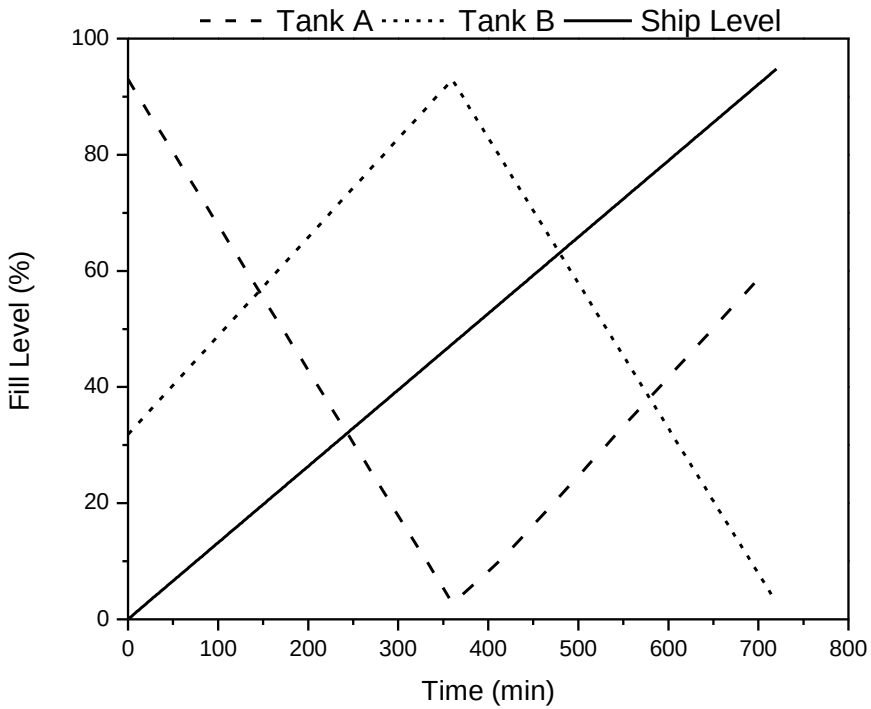

Figure 5-10: Simultaneous filling of ship and emptying of storage tanks

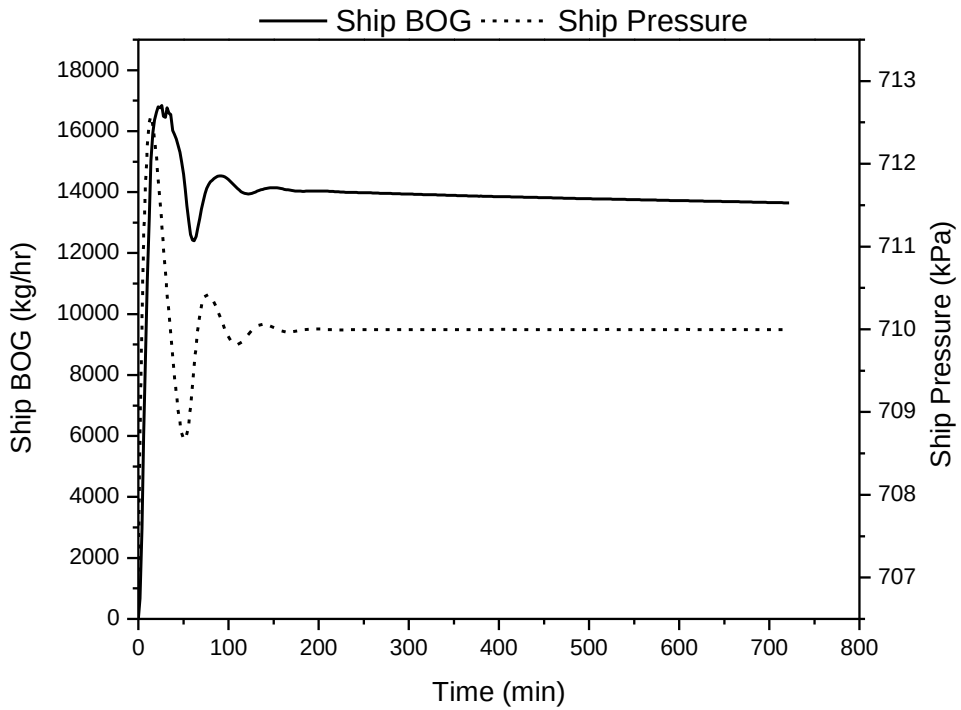

Figure 5-11: BOG generation and pressure variation in ship during unloading mode

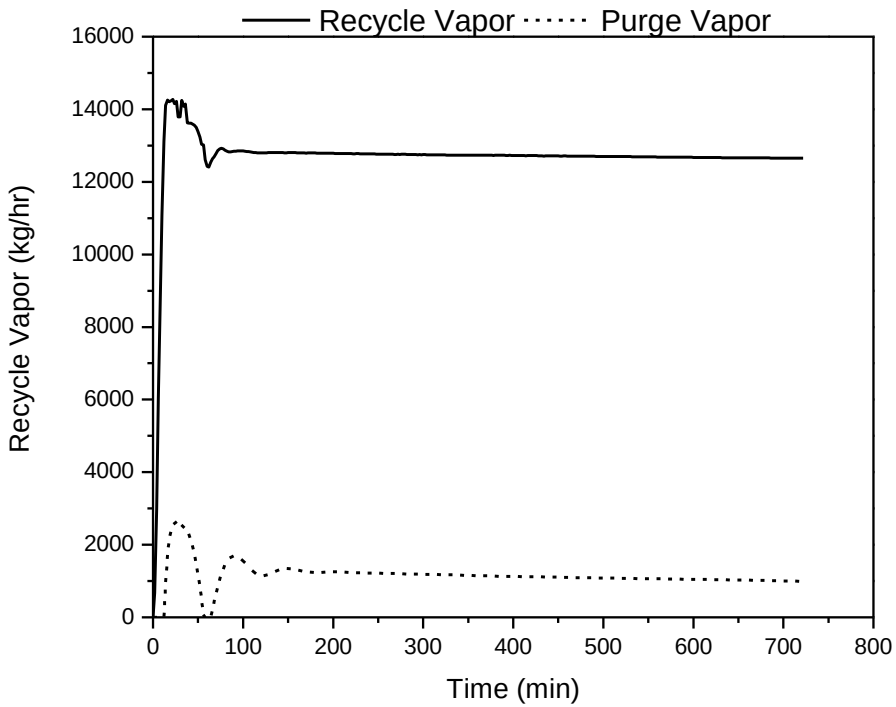

Figure 5-12: Flow rate of recycle and purge vapor from ship during unloading mode

5.5. Emergency Shutdown

Safe operation is the most important factor in the design of the CO_2 terminal. In order to protect personnel and prevent equipment damage, terminals are equipped with an emergency shutdown (ESD) system. The basic purpose of this system is to safely shut flows between ship and terminal in the event of an emergency. ESD system considered for the CO_2 terminal is similar in philosophy to systems applied for LNG terminals. ESD system usually includes fast closing valves, loading arms equipped with emergency release couplers and sometimes, surge protection equipment. ESD system may be activated automatically when pre-defined operational parameters exceed their normal limit or it can be operator initiated. The cause of ESD system initiation can be an abnormal storage tank pressure or tank level, an abnormal ship vessel pressure or level, CO_2 leakage at terminal or ship and loss of electrical power. Depending on the cause of ESD initiation, a hierarchy of actions and timing of valve closures must be developed.

In this study, a logical scheme of ESD system has been developed and its performance is analyzed by using the event scheduler function in the Aspen HYSYS®. Two cases namely, ESD initiation during unloading mode and ESD initiation during loading mode, have been studied to analyze the ESD system response. During the unloading mode, the volume flow rate through the loading arms is quite high. Therefore, the first step in case of ESD initiation is the stoppage of ship loading pump that transfers liquid CO_2 from the tank to the ship along with the tripping of BOG compressor or blower located on the vapor return line. The next step is the closure of terminal and ship ESD valves to shut down the CO_2 flow across the terminal to the ship. This study assumed the closing time of ESD valves to be 30 seconds after the ESD is initiated. The response of ESD system during unloading mode has been studied by activating

the ESD system when CO_2 level in the ship vessel was 40 %. As soon as the ESD system was initiated, ship loading and re-circulation pumps were switched off. ESD valves namely ESDV-1 and ESDV-2 were closed after 30 seconds of ESD initiation. Figure 5-13 shows the mass flow rates across the terminal before and after the ESD initiation. The liquid CO_2 flow rate through forward pipe and re-circulation pipeline was reduced to zero soon after the ESD activation. However, the return vapor flow rate from the ship took little longer to reduce to zero because of the already present CO_2 vapors maintaining the ship vessel pressure. A shutdown time of 30 minutes is assumed in this study. Soon after the shutdown was resolved, the ESD valves were opened along with the pumps start-up. Some quantities of CO_2 vapors were produced in the pipelines during the shutdown time. However, since the liquid re-circulation flow rate is based on the presence of any CO_2 vapor in the re-circulation line, fluctuation can be seen in the flow rates after the start-up time. Once the vapor fraction in the re-circulation line was reduced to zero, the flow rates became steady after 40 minutes of start-up. The analysis shows that the valves and pipelines have been properly sized along with reasonable control loops.

During the loading mode, ESD system may be activated due to a technical problem occurred at the liquefaction unit, storage tank high level or abnormal pressure. The ESD system in response shuts down the tank loading pump, ship loading pump and re-circulation pump along with the closure of ESD valve located at the input pipeline. ESD system during the loading mode showed similar results as discussed above.

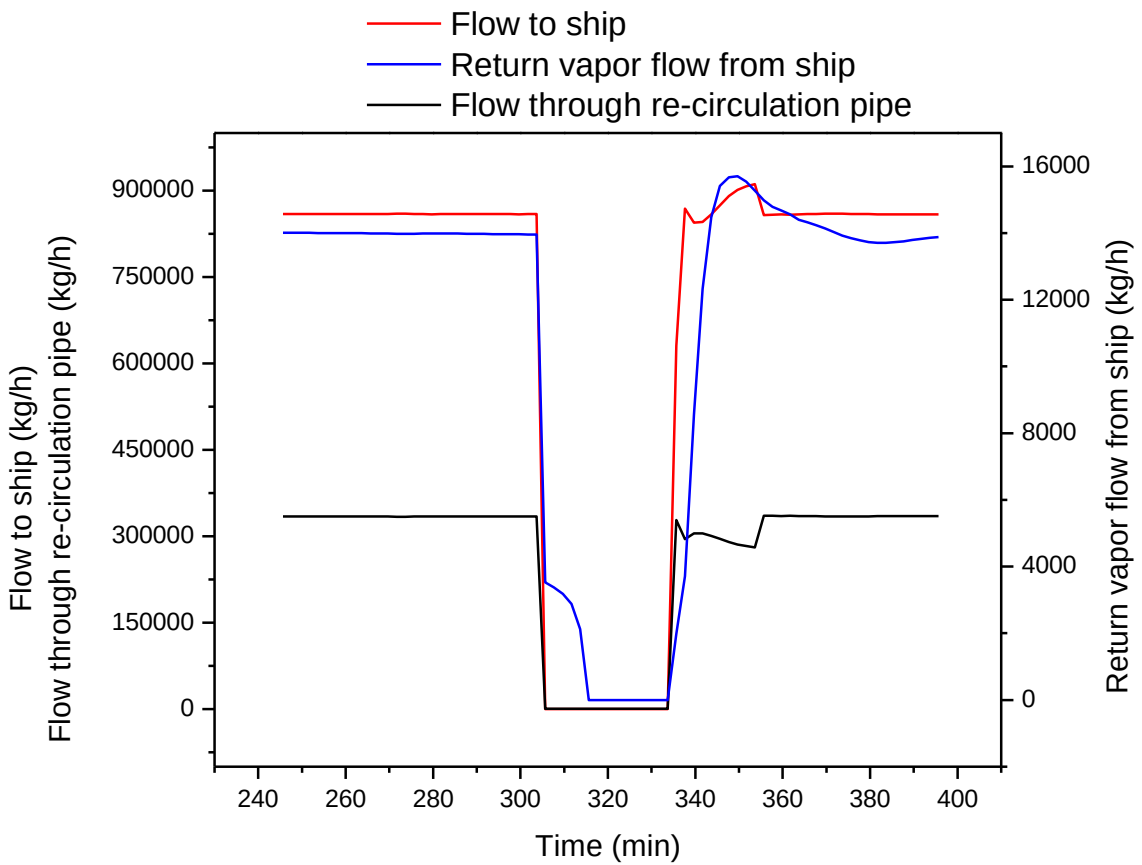

Figure 5-13: Flow rate variation for the period of ESD initiation during unloading mode

5.6. Concept of Dual Terminal Operation

Many studies reported that CO_2 ship transportation should be done near CO_2 triple point as discussed earlier. However, there is currently no commercial scale CO_2 plant operating at -52 °C and 6.5 bar. The existing commercial CO_2 storage and transportation practices are done at – 27 °C and 17 bar. Since there is a need to demonstrate the economic viability of CO_2 ship-based transportation before large-scale implementations, shipping could be done at 17 bar in the initial phase using current ships while new ships are developed to transport CO_2 at 7.1 bar for the larger capacities transportation. Therefore, current small capacity CO_2 ships and LPG ships may be deployed for the early phase demonstration projects. Hence, there is a need to design the CO_2 terminal in such a way that it facilitates the transition from the demonstration phase using current ships to the commercial phase using new ships at 7.1 bar. The CO_2 terminal design presented in this study is based on the concept keeping the initial transition phase requirement in view. A simple process flow diagram of a dual operation terminal is shown in figure 5-14. The liquefaction plant producing the liquid CO_2 operates at 6.5 bar and the liquid CO_2 is pumped to the storage tank for storage at 7.0 bar. Depending on the operational parameters of CO_2 ship vessel, the liquid CO_2 can be pumped to the ship either at 7.1 bar or at 17 bar. In this way, the current design of CO_2 terminal can satisfy CO_2 shipping requirements operating at different thermodynamic conditions.

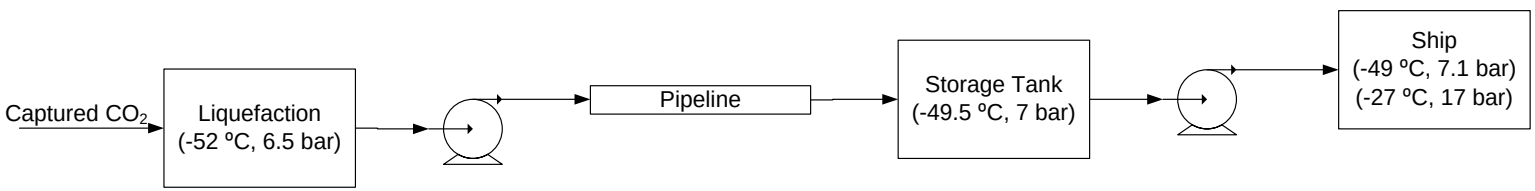

Figure 5-14: Conceptual diagram of dual operational terminal

5.7. Economic Analysis

The CO_2 terminal acts as a connecting link between the CO_2 source and the sink. The objective of designing such a terminal is to ensure a reliable, economical and safe operation while transporting CO_2 in and out of the terminal. Since, the CO_2 transport is always done under pressure, selection of optimum thermodynamic conditions is a key variable in the design of CO_2 terminal. The pressure at which the CO_2 is liquefied, stored and shipped presents the trade-offs between the capital and operating cost of the entire plant. A brief comparison is made to discuss the trade-offs between CAPEX and OPEX for different sections of CO_2 terminal.

5.7.1. Liquefaction Unit

The OPEX slightly increases with an increase in the operating pressure of the liquefaction unit. However, operating the liquefaction unit at a higher pressure will have lower CAPEX compared to that operating it at a lower pressure. This increase in CAPEX at a low liquefier pressure can be explained by the constraint of having a constant CO_2 yield for the liquefaction unit that requires additional pieces of equipment.

5.7.2. Storage Tank

An increase in the storage pressure will lead to a higher thickness of the tank which causes an increase in the CAPEX. However, as will be discussed in the figure 5-16, an increase in the storage tank pressure reduces the amount of BOG generated that can help to decrease the OPEX.

5.7.3. Shipping

Ship vessel pressure has same trade-off between CAPEX and OPEX as for the storage tank. Increasing the ship vessel pressure will increase the vessel thickness causing an increase in the CAPEX. On the other hand, BOG

generation will decrease with a pressure increase, hence a decrease in the BOG handling cost.

Table 5-6 adapted from a knowledge sharing report for the Rotterdam CCS network [52] shows the impact of pressure on the CAPEX, taking 7 bar as a reference case. The analysis clearly shows that a storage pressure of 7 bar seems to be the optimum pressure for the overall chain.

Table 5-6: Cost comparison at different operating pressures

CO_2 Pressure	Liquefaction Additional CAPEX (M€)	Storage Tank Additional CAPEX (M€)	Shipping Additional CAPEX (M€)	Overall Additional CAPEX (M€)
7 bara	Reference Case			
8 bara	- 1.7	+ 5.9	+ 0.8	+ 5.0
9 bara	- 2.3	+ 11.9	+ 1.5	+ 11.1

5.8. Sensitivity Analysis

The design presented in this study explains the operational behavior of a CO_2 terminal under different operational modes. However, a number of assumptions have been made for some of the design parameters which may vary depending on the liquefaction plant design, terminal location and layout, CO_2 transport capacity, equipment design and so on. Therefore, in order to estimate the influence of some of the assumed parameters, a sensitivity analysis has been performed on some of the important design variables.

5.8.1. Effect of Storage Tank Design

The base case assumed a storage tank capacity of 5,000 m^3. Sensitivity has been performed to see the effect of tank size on the BOG generation in the storage tank. Figure 5-15 shows the BOG generation during the tank loading mode of 5,000, 10,000 and 15,000 m^3 storage tank. It can be seen that in case of the larger storage tank capacity, the BOG generation decreases for the same amount of input flow. In case of the 10,000 and 15,000 m^3 tanks, the maximum BOG generated is 8.5 % and 12.2 % lower, respectively, compared to that produced during the loading of the 5,000 m^3 tank. The reason is that as the tank filling starts, a larger vapor space is available that can adjust certain amount of BOG in equilibrium with the liquid CO_2. However, as the tank continues to fill and the process tends to be more stabilized, the large capacity tank produces more BOG compared to the tanks with a smaller capacity because of the larger heat flux for the large capacity tank. Therefore, the recirculation flowrate of liquid CO_2 also increases for the large size tank. The recirculation flowrates after achieving steady state for 5,000, 10,000 and 15,000 m^3 storage tanks are recorded as 113,000, 115,592 and 121,910 kg/h respectively. The cumulative BOG produced to fill 93 % of 5,000, 10,000 and 15,000 m^3 tank capacity is shown in figure 5-16.

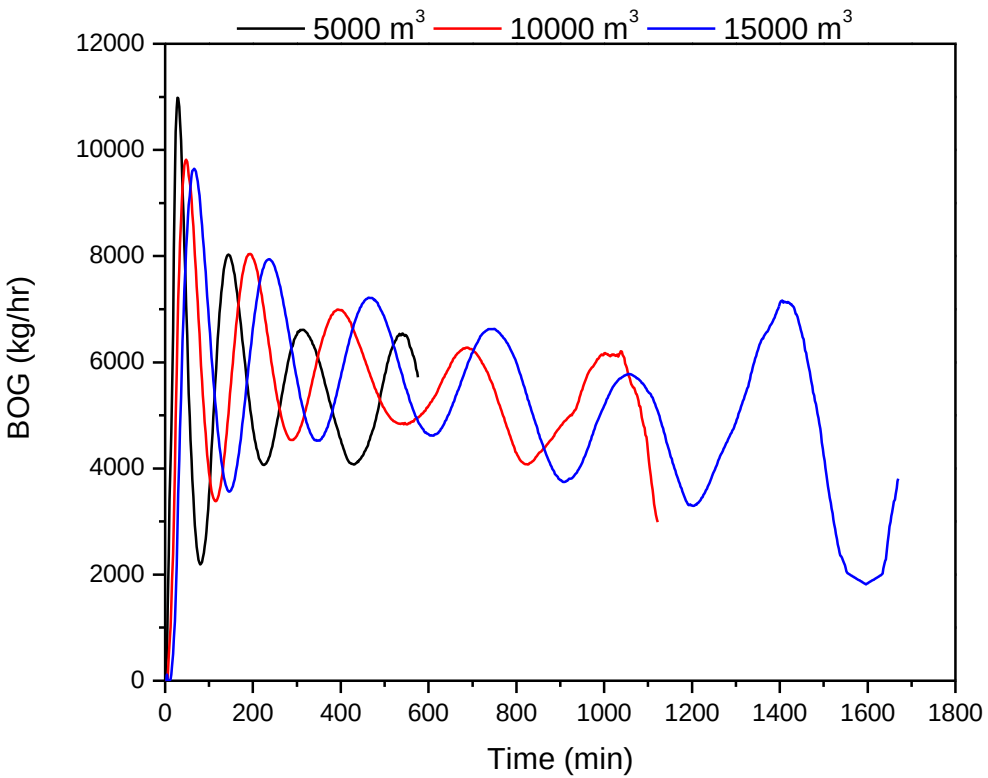

Figure 5-15: Effect of tank size on the BOG generation during loading mode

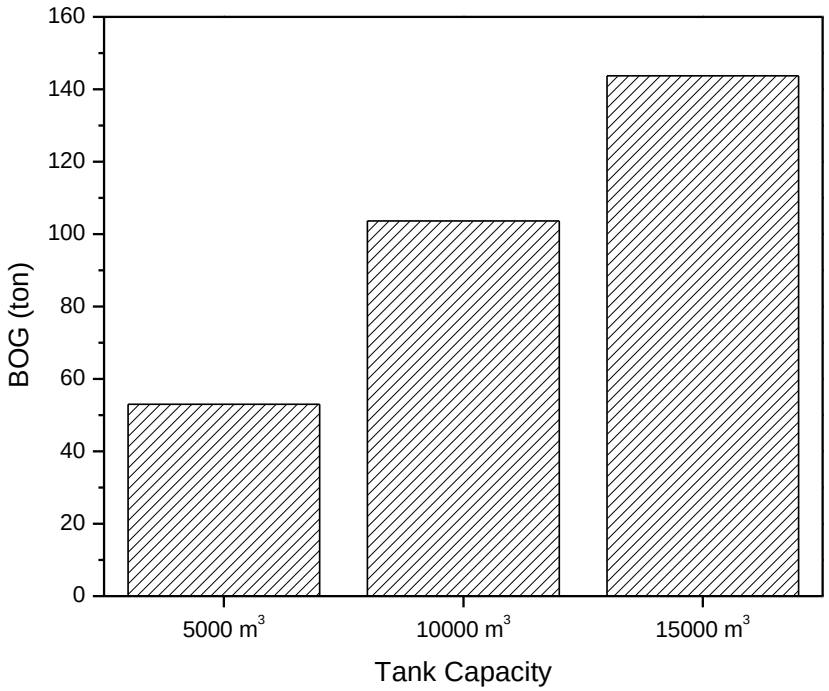

Figure 5-16: Cumulative BOG generation during the loading mode

5.8.2. Effect of Storage Tank Operating Pressure

The previous sections discussed in detail the relation between BOG generation and the tank pressure. This section will look at the effect of storage tank pressure on the BOG generation. A sensitivity analysis has been performed to analyze the effect of tank operating pressure on the generation of BOG. Figure 5-16 shows the BOG generation under tank operating pressures of 700, 725 and 750 kPa. The results show that increasing the tank pressure decreases the BOG generation. However increasing the tank pressure will lead to higher thickness for the tank material, hence causing an increase in the CAPEX. As shown in table 5-6, an increase in tank operating pressure from 7 bar to 8 bar can increase the tank material cost by 5.9 million Euros [52]. Therefore, selection of tank pressure is a trade-off between the operating energy required to handle BOG and the capital cost of the tank.

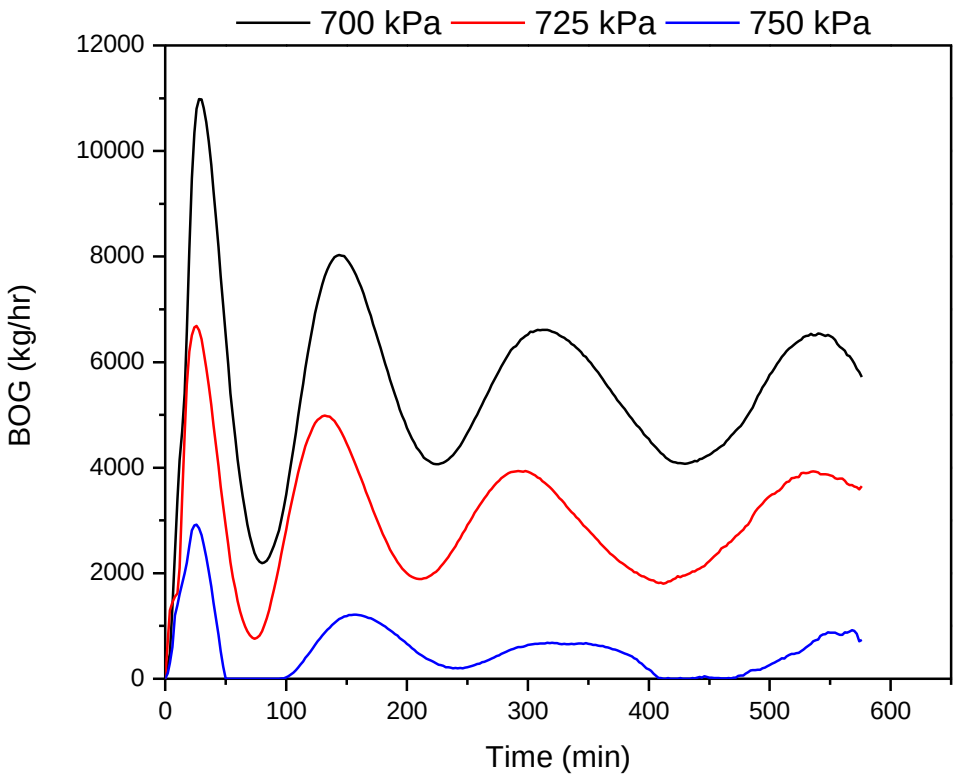

Figure 5-17: Effect of tank pressure on the BOG generation during loading mode

5.8.3. Miscellaneous Factors

A sensitivity analysis is done for some of the other parameters that influence the amount of BOG generation in the CO_2 terminal. First, a sensitivity was performed to see the effect of recirculation flowrate on the BOG generation in the storage tank. In the base case, the recirculation flow rate was calculated so that there is no vapor in the recirculation line going back to the storage tank. The recirculation flow rate can be increased to decrease the BOG generation in the tank. However, an increase in the recirculation flowrate increases the pumping energy requirement. Therefore, any increase in the recirculation flowrate above minimum recirculation flowrate is a trade-off between BOG handling cost and recirculation pumping energy cost.

The length of the pipeline from the liquefaction plant to the CO_2 terminal and the length of the forward and recirculation pipelines can affect the BOG generation within the CO_2 terminal and hence the corresponding costs can vary. In the base case, a pipeline length of 3 km is assumed from the liquefaction plant to the CO_2 terminal, and pipeline lengths of 1 km is assumed for both the forward and recirculation pipeline. However, if any of these pipeline lengths is increased, the BOG generation within the CO_2 terminal will increase causing an increase in operational energy requirements. Since an increase in the pipeline length will increase the heat flux through the terminal, more BOG will be generated.

5.9. Summary

In this chapter, CO_2 terminal design and its operation philosophy has been presented. Based on an assumed terminal annual capacity of 5 Mton, a reasonable equipment sizing and its design has been done. The design is then tested using a dynamic simulation to track the operational performance of the terminal. Under normal operating conditions, three modes namely loading,

holding and unloading have been considered to define the operational characteristics of this pressurized transport chain. In an event of CO_2 leakage or abnormal operational parameters, a logical ESD system has been defined to safely shutdown the terminal operations. Whole terminal operation is kept within an operating pressure range of 6.5 – 7.5 bar with the use of PI controllers. The base case result shows that the maximum BOG rate is 11,000 kg/hr at the beginning of the tank filling operation for a capacity of 5000 m^3 tank. The terminal pipelines are kept under necessary cryogenic conditions by continuous recirculation of liquid CO_2 in order to avoid vapor flashing in the pipelines. The recirculation flowrate during the unloading mode is almost 2.4 times more than during the loading mode. Sensitivity analyses were done for various design parameters and conclude that the BOG rate is a trade-off between the capital cost to reduce BOG generation and the operating cost to handle the generated BOG.

CHAPTER 6: Concluding Remarks

6.1. Conclusion

This thesis addressed the techno-economic analysis of CO_2 transportation through pipeline and ship. The CO_2 transport consists of series of an integral processes that form the CO_2 transport chain. Removing water from the captured CO_2 stream is an essential part of CO_2 transport. Usually the dehydration processes is integrated within the compression section. The level of dehydration required varies depending on the downstream processes and type of CO_2 transportation method. Dehydration using TEG has been simulated in this thesis to see the impact of various factors on the performance of the dehydration process. The results show that TEG absorption process can reduce the water content in the dried CO_2 stream to about 50-60 ppmv. This amount of water content in the dehydrated CO_2 is acceptable for the pipeline transport as experienced from the current projects operational worldwide. However, in case of ship transportation, molecular sieves can be a competitive process choice.

The CO_2 pipeline transport has been studied using three set of thermodynamic conditions. A transport work flow model was defined and then assessed for the Korean case. The defined model provides a quick insight into the important parameters that affect the total transport cost. The offshore pipeline CO_2 transport cost for Korean case varies between $10.90 to $15.45 per tonne of CO_2 transported.

In the case of CO_2 transport by ship, liquefaction is the vital and main cost contributing section. CO_2 liquefaction schemes have been designed in this thesis. The liquefaction energy of 97.3 and 71.89 kWh per tonne of CO_2 is required for post-combustion and pre-combustion capture facilities, respectively. This thesis also explored the optimum location of liquefaction

plant by integrating various transport scenarios with liquefaction processes. The results showed that if the distance between the capture plant and ship loading terminal where the intermediate storage tanks are located is short and CO_2 capacity to be transported in small, then it is better to locate the liquefaction plant near the capture site. On the other hand, if large quantities are to be transported over long distance, locating the liquefaction plant near loading terminal site will be more economical.

Finally, CO_2 terminal design and its operation philosophy has been included in this thesis. CO_2 terminal is a critical section for the ship transportation. If the CO_2 terminal is not well designed, it can pose many safety concerns. Since the operational practices at the CO_2 terminal involve the pressurized tanks at cryogenic conditions, it requires a great deal of dynamic operations understanding. In this thesis, dynamic simulation has been performed to track the operational performance of the terminal. Under normal operating conditions, three modes namely loading, holding and unloading have been considered to define the operational characteristics of this pressurized transport chain. In an event of CO_2 leakage or abnormal operational parameters, a logical ESD system has been defined to safely shutdown the terminal operations. The results show that BOG generation within the CO_2 terminal depends on storage tank size, operating pressure, ambient conditions, insulation thickness, and the filling level of the vessel.

6.2. Future Work

Several topics are suggested for the future work. First, the economic analysis performed for the pipeline and ship transportation is not based on consistent assumptions and the two transportation methods cannot be compared directly. The future work plans to make a direct comparative analysis between the two transportation methods. Secondly, CO_2 transportation using tanker trucks has not been included in this thesis and will be considered in the upcoming study. It appears that many CO_2 transportation projects may use tanker trucks in the early phase before the large scale implementation. This is mainly because of the uncertainties associated with the storage reservoirs, hence, many CCS projects might opt for tanker trucks during the development phase. Thirdly, the future work plans to design and assess the performance of molecular sieves for the dehydration system. For the CO_2 transport by ships at cryogenic conditions, molecular sieves appears to be a competitive dehydration process to achieve the required dried CO_2 composition.

The CO_2 transportation methods and their associated processes analyzed in this study are mainly based on the conceptual design. Consequently, further research should be conducted in order to develop them to the front end engineering design. Control design schemes should be developed and robustness of the process should be carried out. Further, dynamic model construction and simulations are required, especially for the compressor system. Finally, safety analysis is required to identify potential risk and hazards of the processes. Risk and hazard analysis of the processes including HAZOP study should be carried out and the results should be incorporated in the front end engineering design. With the future studies, process flow diagrams and piping and instrumentation diagrams should be obtained, and these processes can then be used for the real world implementation of CO_2 transportation projects.

Nomenclature

D	Pipeline diameter
$D_{in,pipe}$	Inside diameter of pipeline
D_{opt}	Optimal pipeline diameter
E	Longitudinal joint quality factor
f_F	Friction factor
k	Thermal conductivity
L	Total length of pipeline
n	Manning factor (related to roughness of pipe material)
P	Design pressure
p_1	Pressure at inlet of pipeline
p_2	Pressure at outlet of pipeline
P_p	Pipeline internal design pressure
ΔP	Pressure drop across pipeline
Q_m	Mass flow rate
r	Radius of the pipe and tank
S	Allowable stress
t	Minimum tank thickness
t_{pipe}	Pipeline wall thickness
U_0	Overall heat transfer coefficient
v	Velocity of CO_2 in pipeline
Y	Correction factor
z_1	Place height at pipeline inlet
z_2	Place height at pipeline outlet

Greek Letters

ρ	CO_2 density
μ	CO_2 viscosity

Abbreviations and Acronyms

ASME	American Society of Mechanical Engineers
ASTM:	American Society for Testing and Materials
ASU	Air separation unit
BOG	Boil-off gas
BOR	Boil-off rate
CAPEX	Capital expenditures
CCS	Carbon capture and storage
CEPCI	Chemical Engineering's Plant Cost Index
DEG	Diethylene glycol
ECBM	Enhanced coal bed methane
EG	Ethylene glycol

EOR	Enhanced oil recovery
ESD	Emergency shutdown
IEA	International Energy Agency
IEAGHG	International Energy Agency Greenhouse Gas
IGO	International Gas Code industry
IMO	International Maritime Organization
IPCC	Intergovernmental Panel on Climate Change
LNG	Liquefied natural gas
MIT	Massachusetts Institute of Technology
OECD	Organization for Economic Co-operation and Development
OP	Opening percentage
OPEX	Operating expense
PV	Process variable
SRK	Soave Redlich Kwong
TEG	Triethylene glycol
TREG	Tetraethylene glycol
TST	Twu-Sim-Tassone
VLE	Vapor liquid equilibrium
ZEP	Zero emission platform

References

1. Edenhofer, O., R. Pichs-Madruga, Y. Sokona, E. Farahani, S. Kadner, K. Seyboth, A. Adler, I. Baum, S. Brunner, and P. Eickemeier, *Climate change 2014: Mitigation of climate change*, in *Working group III contribution to the fifth assessment report of the Intergovernmental Panel on Climate Change. UK and New York*. 2014.
2. Tanaka, N., *Energy Technology Perspectives 2008–Scenarios and Strategies to 2050.* International Energy Agency (IEA), Paris, 2008.
3. Wong, S., *Module 4–CO_2 Compression & Transportation to Storage Reservoir.* Building Capacity for CO_2 Capture and Storage Project in the APEC Region: A Training Manual for Policy Makers and Practitioners APEC Reference, 2005.
4. Skovholt, O., *CO_2 Transportation System.* Energy Conversion and Management, 1993. 34(9-11): p. 1095-1103.
5. GHG, I., *Pipeline transmission of CO_2 and energy.* Report Number PH, 2002. 4(6).
6. Heddle, G., H. Herzog, and M. Klett, *The economics of CO_2 storage.* Massachusetts Institute of Technology, Laboratory for Energy and the Environment, 2003.
7. Metz, B., O. Davidson, H. De Coninck, M. Loos, and L. Meyer, *Carbon dioxide capture and storage*. 2005: IPCC Geneva, Switzerland.
8. Yoo, B.Y., D.K. Choi, H.J. Kim, Y.S. Moon, H.S. Na, and S.G. Lee, *Development of CO_2 terminal and CO_2 carrier for future commercialized CCS market.* International Journal of Greenhouse Gas Control, 2013. 12: p. 323-332.
9. Wildbolz, C., *Life cycle assessment of selected technologies for CO2 transport and sequestration.* Diplom Thesis. Zurich: Swiss Federal Institute of Technology, 2007.
10. Decarre, S., J. Berthiaud, N. Butin, and J.L. Guillaume-Combecave, *CO_2 maritime transportation.* International Journal of Greenhouse Gas Control, 2010. 4(5): p. 857-864.
11. Aspelund, A. and K. Jordal, *Gas conditioning - The interface between CO_2 capture and transport.* International Journal of Greenhouse Gas Control, 2007. 1(3): p. 343-354.
12. Corporation, C., *Preliminary feasibility study on CO_2 carrier for ship-based CCS* in *Global CCS Institute*. 2011.
13. Platform, Z.E., *The Costs of CO_2 Capture, Transport and Storage.* Post-demonstration CCS in the EU, Technology Platform for Zero Emission Fossil Fuel Power Plants, Brussels, 2011.

14. Seo, Y., D. Chang, J.-Y. Jung, C. Huh, and S.-G. Kang, *Economic evaluation of ship-based CCS with availability.* Energy Procedia, 2013. 37: p. 2511-2518.
15. Roussanaly, S., J.P. Jakobsen, E.H. Hognes, and A.L. Brunsvold, *Benchmarking of CO_2 transport technologies: Part I—Onshore pipeline and shipping between two onshore areas.* International Journal of Greenhouse Gas Control, 2013. 19: p. 584-594.
16. IEAGHG, *CO_2 Pipeline Infrastructure*, in *2013/18*. December 2013.
17. Ø i, L.E. and M. Fazlagic, *Glycol dehydration of captured carbon dioxide using aspen hysys simulation*. 2014: Denmark.
18. Parrish, W., *Fundamentals of Natural Gas Processing. Mechanical Engineering*. 2006: CRC Press.
19. Ø i, L.E. and E.T. Selstø. *Process simulation of glycol regeneration*. in *GPA Europe's meeting in Bergen< www. escet. urjc. es/~ sop/alumnos/proyectos/descargas/propuesta06. pdf>(accessed 06/07/2010)*. 2002.
20. IEAGHG, *Evaluation and analysis of the performance of dehydration units for CO_2 capture*, in *2014/04*. 2014.
21. Zhang, D.J., Z. Wang, J.N. Sun, L.L. Zhang, and Z. Li, *Economic evaluation of CO_2 pipeline transport in China.* Energy Conversion and Management, 2012. 55: p. 127-135.
22. Mazzoldi, A., T. Hill, and J.J. Colls, *CO_2 transportation for carbon capture and storage: sublimation of carbon dioxide from a dry ice bank.* International journal of greenhouse gas control, 2008. 2(2): p. 210-218.
23. Steeneveldt, R., B. Berger, and T.A. Torp, *CO_2 capture and storage - Closing the knowing-doing gap.* Chemical Engineering Research & Design, 2006. 84(A9): p. 739-763.
24. Nimtz, M., M. Klatt, B. Wiese, M. Kuhn, and H.J. Krautz, *Modelling of the CO_2 process- and transport chain in CCS systems-Examination of transport and storage processes.* Chemie Der Erde-Geochemistry, 2010. 70: p. 185-192.
25. McCoy, S.T., *The economics of carbon dioxide transport by pipeline and storage in saline aquifers and oil reservoirs*. 2008: ProQuest.
26. Zhang, Z.X., G.X. Wang, P. Massarotto, and V. Rudolph, *Optimization of pipeline transport for CO_2 sequestration.* Energy Conversion and Management, 2006. 47(6): p. 702-715.
27. Haugen, H.A., N. Eldrup, C. Bernstone, S. Liljemark, H. Pettersson, M. Noer, J. Holland, P.A. Nilsson, G. Hegerland, and J.O. Pande, *Options for transporting CO_2 from coal fired power plants Case Denmark.* Energy Procedia, 2009. 1(1): p. 1665-1672.

28. Barrio, M., A. Aspelund, T. Weydahl, T. Sandvik, L. Wongraven, H. Krogstad, R. Henningsen, M. Mølnvik, and S. Eide. *Ship-based transport of CO_2*. in *7th International Conference on Greenhouse Gas Control Technologies (GHGT-7), Vancouver, Canada*. 2004.
29. Krogh, E. *Liquefied CO_2 Injection Model*. in *6th Trondheim CCS Conference (TCCS-6)*. 2011.
30. Enterprise, S., *Carbon capture and storage- CO_2 transport options for Scotland*. 2011.
31. Jang, H. *Structural Evolution and Its Influence on Sedimentation of the Domi (Fukue) Basin*. in *Offshore Korea Presentation AAPG Annual Convention May*. 2003.
32. GHG, I., *Building the cost curves for CO_2 storage: European sector.* Cheltenham: International Energy Agency Greenhouse Gas R&D Programme, 2005.
33. Hamelinck, C.N., A.P.C. Faaij, W.C. Turkenburg, F. van Bergen, H.J.M. Pagnier, O.H.M. Barzandji, K.H.A.A. Wolf, and G.J. Ruijg, *CO_2 enhanced coalbed methane production in the Netherlands.* Energy, 2002. 27(7): p. 647-674.
34. Vandeginste, V. and K. Piessens, *Pipeline design for a least-cost router application for CO_2 transport in the CO_2 sequestration cycle.* International Journal of Greenhouse Gas Control, 2008. 2(4): p. 571-581.
35. Lee, U., Y. Lim, S. Lee, J. Jung, and C. Han, *CO_2 Storage Terminal for Ship Transportation.* Industrial & Engineering Chemistry Research, 2012. 51(1): p. 389-397.
36. Timmerhaus, K.D., M.S. Peters, and R. West, *Plant design and economics for chemical engineers.* Chemical Engineering Series, 1991.
37. Barron, R., *Cryogenic Systems*. 1985, New York: Oxford University Press.
38. A, C.V., *Overview of Process Plant Piping System Design.* Carmagen Engineering, Inc., ASME International, 2000.
39. Elert, G. *http://hypertextbook.com/facts/2002/EugeneStatnikov.shtml*. (accessed on 16 September 2012).
40. Parker, N., *Using natural gas transmission pipeline costs to estimate hydrogen pipeline costs.* 2004.
41. Pershad, H., K. Harland, A. Stewart, and S. Slater, *CO_2 Pipeline Infrastructure: An Analysis of Global Challenges and Opportunities.* Final Report, 2010.
42. Sinnott, R.K., *Chemical engineering design: SI Edition*. 2009: Elsevier.
43. Erwin, D.L., *Industrial chemical process design*. 2002: McGraw-Hill.

44. Towler, G.P. and R.K. Sinnott, *Chemical engineering design: principles, practice, and economics of plant and process design*. 2013: Elsevier.
45. Serpa, J., J. Morbee, and E. Tzimas, *Technical and economic characteristics of a CO_2 transmission pipeline infrastructure*. 2011: Publications Office.
46. Duan, L., X. Chen, and Y. Yang, *Study on a novel process for CO_2 compression and liquefaction integrated with the refrigeration process.* International Journal of Energy Research, 2013. 37(12): p. 1453-1464.
47. Alabdulkarem, A., Y.H. Hwang, and R. Radermacher, *Development of CO_2 liquefaction cycles for CO_2 sequestration.* Applied Thermal Engineering, 2012. 33-34: p. 144-156.
48. Dopazo, J.A. and J. Fernandez-Seara, *Experimental evaluation of a cascade refrigeration system prototype with CO_2 and NH_3 for freezing process applications.* International Journal of Refrigeration-Revue Internationale Du Froid, 2011. 34(1): p. 257-267.
49. Raja, H., A.K. Anand, V. Muthaiah, J.A. Ferguson, and P.R. Scarboro, *Carbon dioxide liquefaction system*. 2011, Google Patents.
50. Lee, U., S. Yang, Y.S. Jeong, Y. Lim, C.S. Lee, and C. Han, *Carbon Dioxide Liquefaction Process for Ship Transportation.* Industrial & Engineering Chemistry Research, 2012. 51(46): p. 15122-15131.
51. Doctor, R., J. Molburg, and P. Thimmapuram, *Oxygen-blown gasification combined cycle: carbon dioxide recovery, transport, and disposal.* Energy conversion and management, 1997. 38: p. S575-S580.
52. Vermeulen, T., *CO_2 Liquid Logistics Shipping Concept (LLSC) Overall Supply Chain Optimization.* The Hague, 2011.
53. FInkenrath, M., *Cost and performance of carbon dioxide capture from power generation.* 2011.
54. Alexandrakis, M.-I. and B.S. Smart, *Marine transportation for Carbon Capture and Sequestration (CCS)*. 2010, Massachusetts Institute of Technology.
55. Kim, J., *Design and feasibility study of a floating barge for CO_2 liquefaction and storage*. 2011, Korea Advanced Institute of Science and Technology.
56. Li, H., *Thermodynamic properties of CO_2 mixtures and their applications in advanced power cycles with CO_2 capture processes, PhD-thesis.* Royal Institute of Technology, Stockholm, Sweden, 2008.
57. Ellenberger, J.P., R. Chuse, and B.E. Carson, *Pressure vessels: The ASME code simplified*. 2004: McGraw-Hill Professional.

58. Nickel Alloy Steel Plates, T.I.N.C., Inc, One New York Plaza, New York. 1972.
59. Beggs, D.H. and J.P. Brill, *A study of two-phase flow in inclined pipes.* Journal of Petroleum technology, 1973. 25(05): p. 607-617.
60. Kumana, J. and S. Kothari, *Predict Storage-Tank Heat Transfer Precisely.* Chemical Engineer, 1982. 89(6): p. 127-132.
61. The Linde Group, C.s.t. (http://www.linde-engineering.com/internet.global.lindeengineering.global/en/images/P_3_3_e_12_150dpi19_5774.pdf).
62. Green, D.W., *Perry's chemical engineers' handbook.* McGrawHill, New York, 2008. 2.
63. Dobrota, Đ., B. Lalić, and I. Komar, *Problem of boil-off in LNG supply chain.* Transactions on Maritime Science, 2013. 2(02): p. 91-100.

Abstract in Korean (국문초록)

지속적으로 증가하는 이산화탄소 배출은 기후 변화의 주요한 원인으로 지적되고 있다. 이산화탄소 포집 및 저장(CCS) 기술은 이산화탄소 배출을 감소시킬 수 있는 실질적인 기술로 널리 평가되고 있다. 평균 대기 온도 증가를 2°C 이하로 제한하기 위해 CCS는 필수적인 기술이다. CCS 기술은 대규모 점 배출 원으로부터 이산화탄소를 포집하고 안전하게 영구 저장할 저장 지까지 수송하는 두 공정으로 구성되어 있다. 수송은 포집지와 저장소를 연결하는 공정으로 간과해서는 안될 필수적인 요소이다.

본 연구는 full-scale의 이산화탄소 포집 및 저장 기술 적용 시 많은 양의 CO_2를 발생원으로부터 저장소까지 수송시키는 문제에 대해 다룬 것으로 배관 수송과 선박 수송의 기술적, 경제적 분석을 수행하였다. 대규모 CCS의 도입은 다양한 배출 원으로부터 포집된 CO_2를 저장소까지 수송할 수 있는 새로운 기반시설의 개발을 필요로 한다. 지상 소송은 파이프라인, 탱크트럭 및 기차를 이용할 수 있으나, 본 연구는 다양한 열역학적 조건에 따른 파이프라인 및 선박 수송까지만 포함하고 있다; 탈수, CO_2 파이프라인 수송, CO_2 선박수송을 위한 액화 공정, 그리고 CO_2 터미널 설계이다.

A. 탈수 공정

수송에 앞서 포집한 이산화탄소에서 수분을 제거해야 한다. 낮은 수분 함유량은 기기의 부식과 이산화탄소 수화물 생성을 방지하는데 매우 결정적인 요소이다. 탈수 공정을 선택할 시, 운전에서의 문제를 최소화하면서 공정 안전을 확보할 수 있어야 한다. 본 연구에서는 포집한 이산화탄소로부터의 수분 제거에 영향을 줄 수 있는 인자들을 분석하기 위해 glycol을 이용한 탈수 공정의 시뮬레이션을 진행하였다. Glycol 공정을 이용하여 약 50 ppmv까지 수분 함유량을 감소시킬 수 있었다.

B. 파이프라인 수송

초임계 조건에서 대량의 이산화탄소를 가장 경제적으로 수송하는 방법은

파이프라인을 이용하는 것이다. 하지만 다양한 열역학적 조건에서의 수송을 비교할 필요가 있다. 배관 수송 모델링에 있어 입력 변수의 효과를 반영한 현실적인 설계를 수행 하였다. 이 모델은 경제성 분석 및 과제의 실현 가능성을 확인하는데 용이하다. 모델은 화력발전소에서 포집한 이산화탄소를 해상의 저장소까지 수송하는 한국 케이스에 적용하였다. 세 가지의 온도-압력 입력 조건의 파이프라인 수송을 연구하였다.

- Temperature = -20 ℃; Pressure = 6.5 MPa; 액상
- Temperature = 5 ℃; Pressure = 9.3 MPa; 액상
- Temperature = 40 ℃; Pressure = 15.0 MPa; 초임계상

한국에서의 수송 비용은 수송 시나리오에 따라 10.9 - 15.5 USD/tCO_2 였다.

C. 선박 수송을 위한 CO_2 액화 공정

액화 공정은 이산화탄소 선박 수송에 있어 필수적인 요소이다. 최신의 이산화탄소 액화 공정을 포집 공정까지 고려하여 설계하였다. 제안한 공정은 현재까지 연구된 액화 공정 중에서 가장 낮은 에너지를 소비한다. 수송 비용에 대한 열역학적 조건의 영향을 알아보기 위해 여러 시나리오를 분석하였다. 고려된 시나리오는 액화 공정 위치에 근거하여 분류되었다: i) 포집, 액화 및 수송 터미널이 서로 가까운 경우; ii) 포집과 액화 시설이 수송 터미널로부터 멀리 떨어져 있을 경우; iii) 포집 시설이 액화 시설 및 수송 터미널로부터 멀리 떨어져 있을 경우. 액화 에너지는 연소 후 포집과 연소 전 포집이 각각 97.3과 71.89 kWh/tonne of CO_2였다. 연소 후 포집의 기본적인 액화 시설과 중간 저장 비용은 $7.0 – $7.3였으며, 연소 전 포집은 $5.28 - $5.55 였다.

d. CO_2 터미널 설계

CO_2 터미널은 액화 시설과 수송 섹션을 이어주는 역할을 한다. 공정이 비연속적이므로 정상 상태 시뮬레이션으로는 분석할 수 없는 운전 모드가 상당히 많다. 따라서 본 연구는 CO_2 터미널의 다양한 운전 모드를 동적 시뮬레이션을 통해 수행하였다. 네 가지 시나리오가 터미널의 운전 전략을 정의하기 위하여 개발되었다: 적재 모드 (loading mode), 유지 모드 (holding mode), 하역 모드

(unloading mode), 비상정지 모드 (emergency shutdown). 그 결과 CO_2 터미널 내의 BOG (boil-off gas) 발생량은 저장 탱크의 크기, 운전 압력, 대기 온도, 단열 두께 및 저장 탱크의 액위에 주요하게 영향을 받는 것을 확인하였다.

주요어 : 이산화탄소 포집 및 저장 (CCS), CO_2 수송, 경제성 분석, CO_2 액화, CO_2 터미널

학 번 : 2012-31296